A GENERIC SMELL GENERATING

ENZYMATIC BIOSENSOR

A GENERIC SMELL GENERATING ENZYMATIC BIOSENSOR

By

YAQIN XU, B. ENG., M. ENG.

A Thesis

Submitted to the School of Graduate Studies

in Partial Fulfillment of the Requirements

for the Degree

Doctor of Philosophy

McMaster University

DOCTOR OF PHILOSOPHY (2011) McMaster University

(Chemical Engineering) Hamilton, Ontario

TITLE: A Generic Smell Generating Enzymatic Biosensor

AUTHOR: Yaqin Xu

B.ENG. (Tsinghua University)

M.ENG. (Beijing University of Chemical Tech.)

SUPERVISOR: Professor Carlos Filipe

NUMBER OF PAGES: vii, 83

Abstract

This thesis describes a new type of biosensor, which reports the presence of a target by generating a smell that can be easily detected by the human nose. This approach is radically different from, but complementary to, colorimetric based reporting and it paves the way for the development of multi-sensory biosensors that can be used in a variety of fields, such as diagnostic device, food processing and environmental monitoring

Biosensors typically consist of two parts: a bio-recognition element and a signal transducer. The biorecognition element is the component that can specifically interact with its cognate target, while the transducer produces a signal that can be easily identified. The key element of the smell generating biosensor is the enzyme tryptophanase (TPase), which was used as the signal transducer. This enzyme uses either L-tryptophan or S-methyl-L-cysteine as substrates, to produce either indole or methyl mercaptan as final products- both molecules are easily detectable by the human nose. Proof-of-concept for this biosensor was achieved by performing an enzyme-linked immunosorbent assay (ELISA) on magnetic beads with detection of IgG from rabbit serum (the target) in a sample and reporting the presence of the target through the generation of a smell (either indole or methyl mercaptan, depending on the substrate used).

The potential use of TPase for biosensing was further expanded by creating a bienzyme system that allows specifically detecting of adenosine-5'-triphosphate (ATP) and reporting its presence by generating a smell. This bienzyme system is based on the fact that TPase activity is greatly affected by the concentration of pyridoxal phosphate (PLP)- which acts as a cofactor that modulates enzyme activity. The enzyme pyridoxal kinase PKase catalyzes the phosphorylation of pyridoxal to PLP in the presence of ATP. The more ATP presents, the more PLP is produced per unit time. If this occurs in the presence of TPase, larger concentrations of ATP in samples will result in higher amounts and faster rates of PLP formation, leading to increased activity of TPase, hence faster generation of either indole or methyl mercaptan is achieved. This bienzyme was used for the detection of DNA molecules with a specific sequence as well as for the detection of microbial cells through smell generation.

Most widely used biosensors require immobilization of the biologically active elements on a stable surface. Paper, being a cheap and easy accessible substrate, was used for fabrication of the olfactory-based biosensor. Poly(N-isopropylacrylamide-co-vinylacetic acid) (PNIPAM-VAA) microgels with functional groups present on their surface were modified by biotinylation and loaded with streptavidin/avidin (to be prepared as a platform for further biomolecule immobilization). The microgels were then used as a supporter for the bienzyme system on filter paper to construct a paper-based smell-generating biosensor, which opens the way for the creation of printable smell-reporting printable bio-inks.

Acknowledgements

I would like to express my sincere gratitude to my supervisor, Dr. Carlos Filipe, not only for the guidance he gave me on my studies, but also for the countless support, encouragement and help he gave me during my studies at McMaster. He guided me on how to conduct research, and more importantly he showed me how to identify the importance of our research. He always gives me the freedom to work on the project that I was more interested in and encourage me to develop creative ideas and to explore new methods. Moreover, he has been a very generous and helpful friend.

I would also like to thank my co-supervisor, Dr. Robert Pelton for his supervision, guidance on my research and for his invaluable help in teaching me on how to present research results and on how to write scientific papers. He is a true example to me of a hard-working, and successful scientist that has found a true balance in life. I also would like to thank my supervisory committee members, Dr. Yingfu Li, from the Biochemistry Department and Dr. Todd Hoare, from the Chemical Engineering Department, for their suggestions and help on my research work.

I wish to thank SENTINEL Bioactive Paper Network and the Natural Sciences and Engineering Research Council of Canada (NSERC) for their financial support of my research work. Additionally, I would also like to thank many people in the SENTINEL network for their cooperation, help and valuable discussions. Especially, I am grateful to Weian Zhao, Monsur Ali and Sergio Aguirre for their suggestions on my research and for their help on designing the DNA aptamers used in my work. I also wish to thank Ferdinand Gonzaga for his help on coupling chemistry.

I had the privilege of working with three outstanding summer students: Lizanne Pharand, Joanna Sauder and Jackie Obermeyer , all from the Chemical Engineering Department. I thank them for their hard work and creative ideas on the projects. I also had lots of help from members of the McMaster Interfacial Technologies Group. Especially, I want to thank laboratory manager Mr. Doug Keller for all his kind support and assistance, and SENTINEL network secretary Sally Watson, for her help in administrative issues. Dan Zhang, Yuguo Cui, Songtao Yang and Zuohe Wang are also thanked for their help with my work.

I also wish to give my special thanks to the staff in the Chemical Engineering Department: Ms Kathy Goodram, Ms Lynn Falkiner, Ms Nanci Cole, and Ms Andrea Vickers for their administrative assistance, and Dr James Lei, Mr. Paul Gatt, Ms Justyna Derkach and Mr. Dan Wright for their technical support.

Finally, I wish to thank my husband, Hang Li, for loving me and supporting me, and my parents and my sister for their love and support. I would also like to thank Luying Wang, Quan Wen, Junlei Qu and other friends for their friendship.

TABLE OF CONTENTS

Abbreviation

DNA	deoxyribonucleic acid
MG	microgel
IgG	immunoglobulin G
DLS	dynamic light scattering
EDC	N-(3-Dimethylaminopropyl)-N'-ethylcarbodiimide hydrochloride
DMSO	dimethyl sulfoxide
APT	aptamer
RNA	ribonucleic acid
TPase	tryptophanase
PLP	pyridoxal phosphate
PKase	pyridoxal kinase
ATP	adenosine 5′-triphosphate
PL	pyridoxal
SMLC	S-methyl-L-cysteine
ELISA	enzyme-linked immuosorbent assay
PNIPAM	Poly(N-isopropylacrylamide)
VAA	vinylacetic acid
IPTG	Isopropyl β-D-1-thiogalactopyranoside
PEG	polyethylene glycol
HABA	2-(4-hydroxyazobenzene) benzoic acid
NHS	N-hydroxysulfosuccinimide
LB	Lysogeny broth

Chapter 1 Introduction

Biosensor technology has been fast gaining popularity in various areas, including medical diagnostics [1], food safety evaluation [2], and environmental monitoring. [3] A biosensor was first described in 1962 by Clark for the detection of glucose.[4] Shortly thereafter, glucose, lactate and alcohol biosensors were commercialized in the 1970s.[5] The total biosensor market was estimated to be $10.8 billion by 2007. [6] Compared to traditional analysis methods, biosensors provide rapid, simple, sensitive, selective and low cost detection.

A biosensor is defined as an analytical device that consists of a biorecognition element and a transducer. It is a special form of chemical sensor. If an analyte is present, the bioelement will interact with the analyte and trigger signal generation or amplification through the transducer. The mechanism for a biosensor is shown in Figure 1.

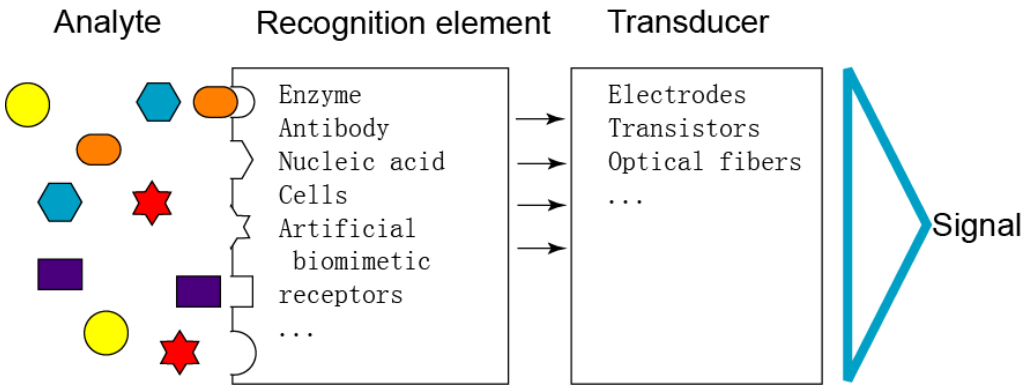

Figure 1 Principle and mechanism of a biosensor

The bioelement in a biosensor has the ability to recognize an analyte and interact with it. A biosensor obtains specificity from the specific recognition ability of the bioelement, which could be an enzyme [1], antibody [7], nucleic acid [8], cell [9], or tissue [10], among which enzymes and antibodies are the most commonly used. For example, the glucose sensor which possesses a large percent of the biosensor market uses glucose oxidase and horseradish peroxidase as its bioelement, [1] and most pregnancy test kits on the market use antibodies to bind the target protein, human chorionic gonadotropin hormone, in urine. [11]

A transducer is defined as that part of a device that converts an observed physical or

chemical change into a measurable signal. [12] An electrode [13], piezoelectric crystal [14], oxygen optrode [15], microthermopile [16], polymer [17] , or enzyme [7] could be employed as a transducer in the biosensor. Depending on the transducer used, a biosensor can be classified as a piezoelectric biosensor [14], electrochemical biosensor [13], calorimetric biosensor [16], ion-sensitive (pH sensitive) biosensor [17], acoustic biosensor [18], colorimetric biosensor [19], and so on.

In a biosensor, the bioelement is usually immobilized on the sensor support or sensor surface using different kinds of methods, such as entrapment, covalent bonding, adsorption, and encapsulation. Immobilized recognition units usually provide accurate measurement and easier manipulation. The support surface could be made of metal, crystal, polymer, paper and so on.

1.1 Paper-based Biosensor

Being used as a support surface, paper is inexpensive, easily accessible, easily printed or coated, and porous.[20] Paper-based biosensors (bioactive paper) are defined by VTT, a Finnish research organization, as "paper-like products, cardboard, fabrics and their combinations, etc., with active recognition and/or functional material capabilities". [21] Researchers have been making efforts to utilize paper-based biosensors in diagnostic applications, food safety control, water treatment and virus detections.[20]

There are several advantages in utilizing paper as a support: 1) paper is easily accessible and cheap, 2) paper has a porous structure for easy capture and chromatographic separation, 3) paper can be easily printed and patterned, 4) paper is biodegradable and environmentally friendly. Existing commercialized bioactive paper products include dipstick test kits, viruses-killing tissue and antibacterial non-woven fabric. [20] For research purpose, efforts have been made to produce bioactive paper for detection of various analytes, such as toxins [22], pathogens [23], bacteria [24] and DNA [25].

For example, Zhao et al utilized DNA aptamer modified nano gold particles on paper to detect target DNase I, as shown in Figure 2. The presence of the target decomposes the DNA structure between nano gold particles, causing aggregation and color change.

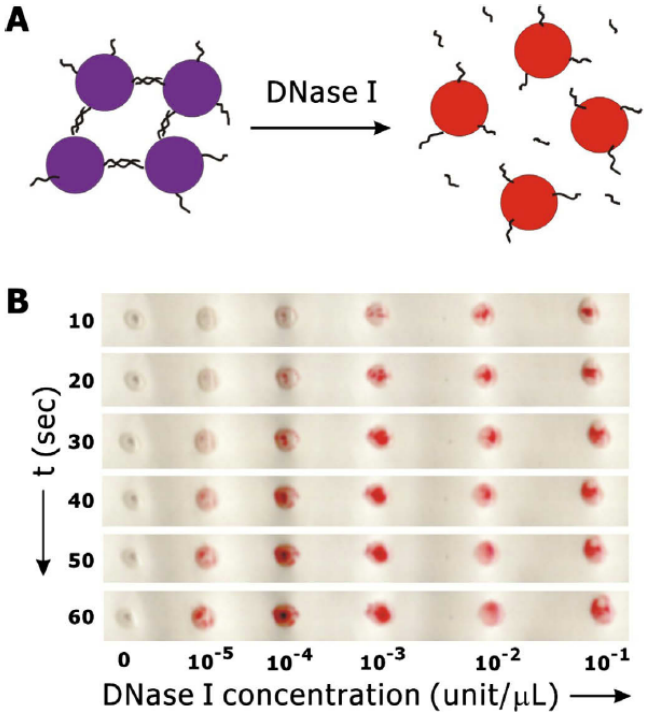

Figure 2 A paper-supported biosensor measuring the presence of DNase. Decomposition of the stabilizing chains on the nanoparticles causes them to aggregate and give a color change. [20]

Because of the structure of paper, immobilization strategies for biosensors on paper include physical adherence, chemical or biochemical coupling and bioactive pigment. [20] Physical adherence is attaching biosensors to the pores or surface of paper cellulose by Van der Waals and electrostatic forces. Chemical or biochemical immobilization of biosensors is achieved through chemical modification and covalent bonding to link the biosensor to paper cellulose, cellulose binding modules or other biochemical binding agents.

The immobilization methods also rely on material science progress. The development of polymer science and nano material technology has enhanced immobilization efficiency and biological activity. Paper has a complicated chemistry on its surface, so polymers and nano particles are usually used as supporters for biomolecules to separate them and stabilize their activity. Nano-materials, such as carbon nano-tubes and gold nano-particles, possess special physical and chemical properties, including a high surface to volume ratio, electron transfer particularity, self-assemble ability, and good interaction with biomolecules. Microgels [26], silica [27], sol-gel particles [28] and microcapsules [29] have

been used as supporters and carriers for biomolecules on bioactive paper. For example, previous research in our group used carboxylated microgels as a supporter for antibodies and DNA aptamers on paper, as shown in Figure 3.

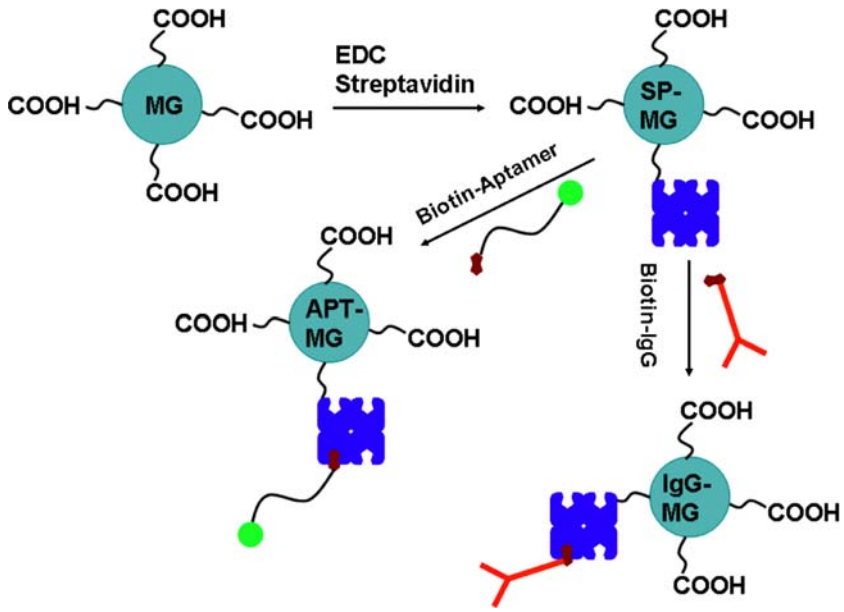

Figure 3 Immobilization of antibody and DNA aptamer on carboxylated microgels. [30]

Paper-based biosensors are usually designed to provide a direct color, fluorescence or illuminance signal for the human eye. Various bio-recognition elements, such as antibodies [30], enzymes [31] and DNA molecules [32], have been immobilized on paper for the capture of the target analyte. Visual signals could be produced by enzymes [33], aggregation of nano particles [32] or the match of fluorophore and quencher [34]. Figure 2 above also gives an example of a biosensor that provides a color signal called a colorimetric biosensor. This type of biosensor has been gaining a great deal of interest, because it is easily manipulated, quick, usually cheap, and provides a direct signal.

1.2 Smell-generating Biosensor

Similar to a colorimetric biosensor, we consider a smell-generating biosensor, another type of device that provides a direct signal. The human nose is sensitive enough to recognize thousands of odors, even when the person is not paying attention to the smells. [35] This property of the nose provides the suitability of applying smell-generating biosensors in the efficient detection and timely warning of the presence of targets.

To our knowledge, smell-generating biosensors have not been explored enough, as only two patents have been reported. In 2007, Nicklin et al used recombinant cells to release a volatile substance as a reporter for biodetection. [36] The other patent, invented by Melker et al, utilized an RNA aptamer and nano tube complex to detect analytes/biomarkers and release a smell. The smell compound is capped inside nano tubes and the caps are linked to RNA aptamers. When the analyte is present, the aptamer will interact with the analyte and result in the uncapping of the nano tube so that the smell compound is released to signal the biodetection. This invention was believed to provide a method for screening an analyte/biomarker present in exhaled breath. [37]

1.2.1 Smell signal

Regarding smell signals the definition of "detectable smell" is that the concentration of the volatile chemical in the gas phase is higher than its odor threshold for the human nose or an electronic nose, so as to give a sensible smell or reading. For example, ammonia has an olfactory threshold of 5 ppm, which means the ammonia concentration must be above 5 ppm for the human nose to sense it. [38] Table 1 gives odor thresholds for some chemical compounds. Generally, the theory for the working mechanism of the human nose to sense odor is that an odorant molecule stimulates cells in the nose and the stimulus is then transmitted by nerves to the brain, giving the odor sensation. [39]

Table 1 Olfactory threshold of some chemical compounds for the human nose

Chemical	Olfactory threshold *	Henry's law constant (Kcc)*
Ammonia [38]	5 ppm	3.15×10^{3}
Hydrogen Sulfide[40]	10ppb 5.0×10^{-10} mol/dm^3	≈ 17
Indole [40]	0.02 ppb 1.0×10^{-12} mol/dm^3	4.08×10^{5}
Methanethiol[40]	0.2 ppb 1.0×10^{-11} mol/dm^3	≈ 17

* Kcc: The dimensionless ratio between the aqueous concentration and its gas concentration at equilibrium; ppm: part per million; ppb: part per billion

Besides the human nose, digital electronic noses have been developed rapidly in recent

decades to give quantitative measurements of chemical compounds in the gas phase and to be used in some cases to warn of the presence of dangerous gases. [41] Depending on the odor threshold of a compound, an electronic nose could be more sensitive, or less sensitive, than the human nose. Commercial electronic noses from Interscan Corporation are able to detect gaseous compounds, including hydrogen, hydrogen sulfide, hydrogen chloride, carbon monoxide, nitric oxide, nitrogen dioxide, ozone, sulfur dioxide, chlorine, ethylene, hydrazine, ammonia, etc. An electronic electrode from YSI can detect various volatile compounds, such as formaldehyde, propylene oxide, and ammonia. The ToxiRAE PID gas detector from RAE Systems is a photoionization detector for instantaneous monitoring of volatile organic compounds and the warning of excessive exposure through sound alarms.

1.2.2 Smell signal produced by tryptophanase

In our research, we found that a special enzyme, tryptophanase (TPase), could produce several types of smell compounds by catalyzing a series of β-elimination reactions and β-replacement reactions involved in the metabolism of amino acids, including L-serine, L-cysteine, S-alkyl-L-cysteine, S-(o-nitro-phenyl)-L-cysteine, β-chloroalanine, and 2,3-diaminopropionate. [42] Figure 4 shows that the hydrolysis of L-tryptophan and S-methyl-L-cysteine, catalyzed by tryptophanase, produces indole and methyl mercaptan (methanethiol). [42a]

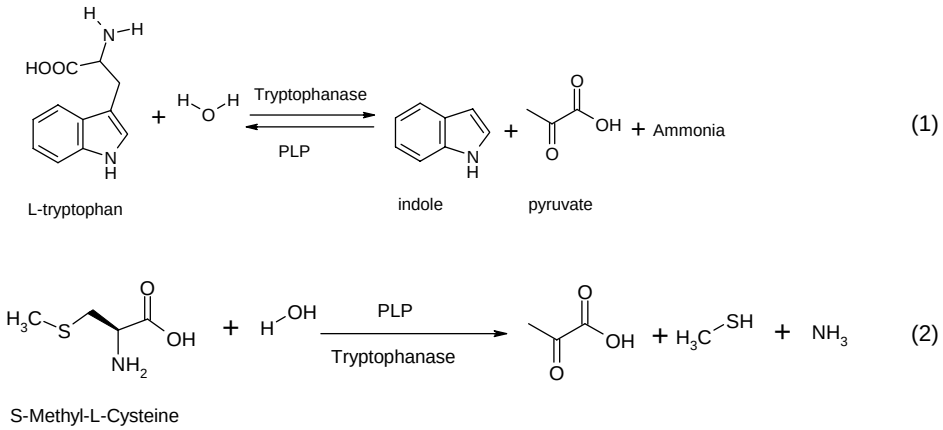

Figure 4 β-elimination of L-tryptophan and S-methyl-L-cysteine by TPase.

Indole (C_8H_7N) contributes to oral malodor (bad breath) and the peculiar odor of feces. However, at a very low concentration, indole has a flowery smell and is a component of many perfumes. Indole has a very low threshold, around 0.02 ppb . [40] The

toxicological properties of indole have not been studied and the United States OSHA does not list indole as a carcinogen. At a room temperature of 20 °C, indole is a white solid and has a solubility of 0.19 g/100 ml water.

Methanethiol (CH_3SH), also known as methyl mercaptan, is a colorless, flammable gas with an extremely strong and repulsive odor. At very high concentrations it is highly toxic and affects the central nervous system. Its penetrating odor provides a warning at dangerous concentrations. It has been used as an additive in natural gas to provide warnings of natural gas leaks. The odor threshold of methyl mercaptan is reported as 0.2 ppb. [40] The United States OSHA Permissible Exposure Limit is listed as 10 ppm. [43]

1.2.3 Tryptophanase

Tryptophanase (TPase) is a tetrameric protein in which four subunits are held together by surface hydrophobic interactions and by the cofactor pyridoxal phosphate (PLP). [44] TPase has been purified from *E. coli* [45], *P. vulgaris* [44], *B. alvei* [46], and *S. thermophilum* [47], and requires PLP and some cationic ions to have catalytic activity. [48] Figure 5 (a) shows the typical crystal structure of TPase. [44] Figure 5 (b) shows a TPase dimer that binds a potassium ion and PLP in each subunit. [49] The binding of PLP involves lysine on the TPase surface. [50] PLP is not the only cofactor for TPase; ions such as K^+, NH_4^+ or Rb^+ need to be present at the same time to activate TPase. [51] It has been reported that the cationic ions bring about an increase in affinity of the enzyme for PLP. [48] Research has also shown that temperature affects the affinity of the apoenzyme for PLP and that high concentrations of PLP may inhibit enzyme activity. [52] The kinetic study of tryptophanase showed that the K_m value for L-tryptophan in reaction (1) in Figure 4 was measured to be 4 s^{-1} and 5 s^{-1}. [53] The K_m value for S-methyl-L-cysteine in reaction (2) was measured to be 10 mM. [42a]

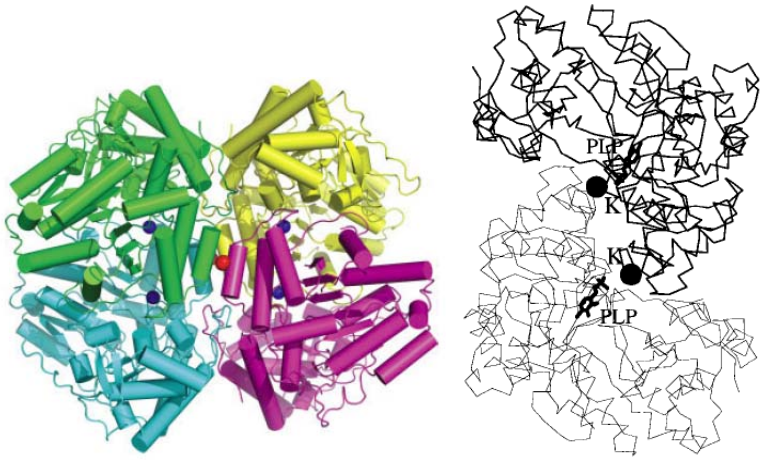

Figure 5 (a) Crystal structure of tetrameric *E. coli* TPase, each chain is colored differently by Almog et al; [44] (b) Stereo diagram of catalytic dimer of two TPase subunits which are bound with PLP and potassium ions by Isupov et al. [49]

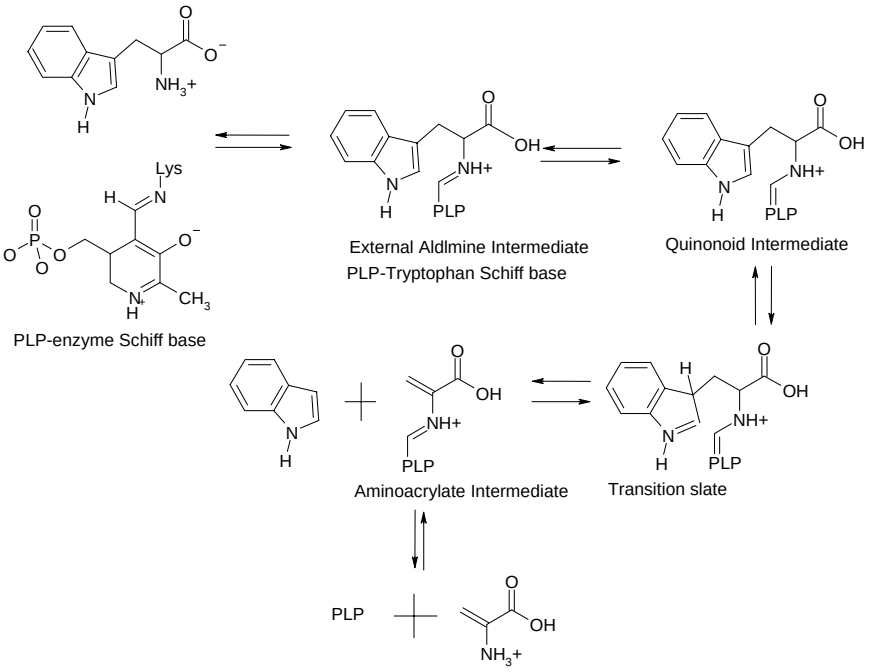

Figure 6 PLP functions in the decomposition of tryptophan by tryptophanase [54]

The kinetics for the β-elimination reaction of L-tryptophan and the functions of PLP during the reaction are shown in Figure 6. First, PLP binds covalently to an amino group of a lysine residue in the active site of tryptophanase. This PLP-tryptophanase binding forms a Schiff base linkage which is a functional group containing a

carbon-nitrogen double bond with a nitrogen atom that connects to an alkyl group. Secondly, an amino group in the substrate, such as tryptophan, reacts with the imine carbon. This causes the release of the amino group Lysine. Simultaneously, a new PLP-tryptophan Schiff base is formed . Finally, indole, ammonia and pyruvate are produced after the conversion of several intermediates. Then PLP is released and a new PLP-tryptophanase Schiff base can form again. Theoretically, one PLP molecule can help tryptophanase produce many indole molecules in a given time period.

TPase activity is usually measured by two strategies. One strategy is to measure the amount of pyruvate or indole produced by TPase. The pyruvate formed from various substrates can be measured by the method of Friedemann and Haugen. [47, 55] Indole was measured through colorimetric methods where indole reacts with p-dimethylaminobenzaldehyde to form a reddish color that has a maximum absorbance at 570 nm. [56] This method was first developed by Scott[56a] and later modified. [56b, c] Figure 7 shows the mechanism of the colorimetric method. The other enzyme assay utilizes a synthetic substrate, S-(o-nitro-phenyl)-L-cysteine (SOPC), to directly monitor the consumption of the substrate via a spectrometer. [57]

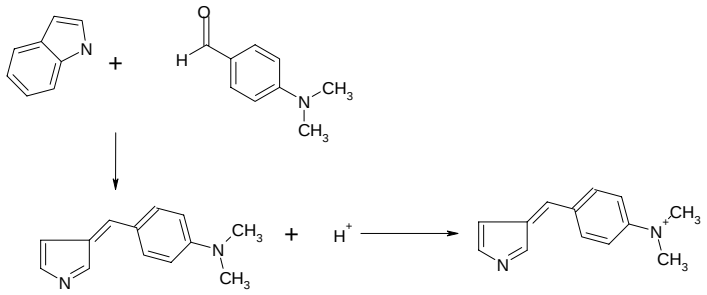

Figure 7 Colorimetric mechanism of quantifying indole by p-dimethylaminobenzaldehyde. [56b]

1.2.4 Pyridoxal kinase

The important cofactor for tryptophanase, pyridoxal phosphate, plays a very important role in organism metabolism. It is produced by pyridoxal kinase in vivo. Pyridoxal kinase (PKase, EC 2.7.1.35) catalyzes the phosphorylation of three forms of vitamin B6 in the presence of adenosine 5′-triphosphate (ATP) and zincum cations, as shown in Figure 8. [58] Then the pyridoxine phosphate and pyridoxamine phosphate can be converted to pyridoxal phosphate by oxidase. [58]

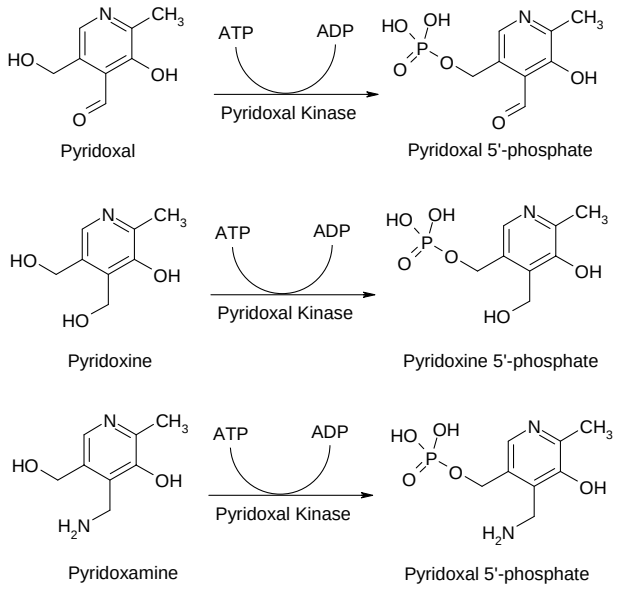

Figure 8 Pyridoxal Kinase catalyzes phosphorylation of pyridoxal, pyridoxine and pyridoxamine.[58]

Pyridoxal kinase was originally purified from sheep liver[59], sheep brain[60] and bovine brain[61]. More recently the gene for pyridoxal kinase from human cells [62] and microorganisms such as *E. coli* [63] and *B. subtilis* [64] was cloned and expressed in *E. coli*. The crystal structure of PKase derived from sheep and *E. coli* has been studied. [58, 63] PKase is a dimeric protein with a molecular weight of 60 kDa, containing two subunits. [65] Each subunit binds with ATP and pyridoxal molecules, and functions independently during catalysis. [66] Figure 9 shows the crystal structure of PKase expressed from recombinant *E. coli* and its binding sites for ATP and pyridoxal.

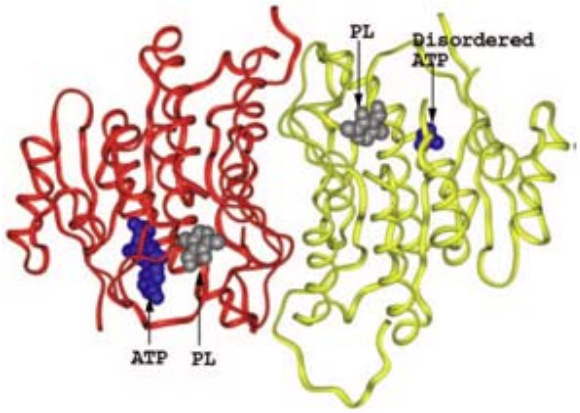

Figure 9 The dimeric structure of the MgATP and pyridoxal (PL) bound PKase by Safo et al. [63] ATP and PL are shown as blue and gray spheres, respectively.

It has been reported that metal ions are essential for the conversion of pyridoxal into PLP.[67] The order of activation for PKase from bovine brain was Zn^{2+} > Co^{2+}>Mn^{2+}>Mg^{2+}>Fe^{2+}. [61] These ions in a complex with ATP become substrates for PKase. [61, 67] However, a study on the kinetic constants of PKase from human cells and *E. coli* has shown that MgATP is a preferred substrate over ZnATP. [62] Under 37 ºC and pH 7.3, the K_m for MgATP was determined to be 420 µM when ATP concentration varies from 50 µM to 1 mM with pyridoxal held constant at 1 mM by using 100 µg human PKase. [62] Another study has shown that at pH 6.5, steady state constants for the substrate MgATP were K_{cat}=0.1 s^{-1} and K_m=100 µM under room temperature, in the presence of 1mM ATP, 0.2 mM pyridoxal and increasing concentrations of magnesium. [67]

The enzymatic activity of PKase is usually measured through the production of PLP. The rate of formation of PLP can be measured by following the increase in absorbance at 388 nm, at which PLP is known to have a molar absorption coefficient of 4900 $M^{-1}cm^{-1}$ at pH 7. [61, 66] Because PLP is a cofactor of some enzymes, incubating PLP with excess apoenzyme and quantifying the product could be applied to develop methods for measuring PLP. [68] Moreover, PLP and pyridoxal can be oxidized by phenylhydrazine, and then, by controlling temperature and pH, the PLP generated by PKase can be quantified without the interference of pyridoxal. [69] Also some radioactive assays have used radioactive substrate to monitor the consumption of substrate or the generation of products to calculate PKase activity. [59, 70]

1.3 ATP Detection

ATP is an important biological compound involved in various vital biological processes. Intracellular ATP has been recognized as an energy source for many important reactions.[71] Intracellular ATP concentration is often higher than 5 mM, and part of this can be released outside the cells. [71]

Several strategies have been developed for the detection of ATP, including a bioluminescence ATP assay [72], an electrochemical method [73], a fluorescence resonance energy transfer method [74] and a DNA aptamer switching method [75]. Other than these, atomic force microscopy has been reported to be able to detect and locate extracellular ATP on living cells.[76] The bioluminescence assay utilizes the enzyme luciferase to convert the substrate ATP to generate light. [72] This can detect ATP at 0.002 μmol/L. This assay is widely used in rapid detection of microorganisms in the food industry, such as *Staphylococcus aureus*, *Escherichia coli*, *Listeria monocytogenes*, and *Sacharomyces cereviciae*. [77]

1.4 Objectives

The overall objective of my work in this thesis is to develop a generic smell-generating enzymatic biosensor for biodetection. The specific objectives of this research are:

1. *Application of tryptophanase as a reporter providing smell signals in biodetection.* The goal was to modify tryptophanase and apply the biotinylated enzyme as a reporter in a magnetic beads based enzyme linked immunosorbent assay (ELISA) to generate a smell signal upon detection of the analyte.

2. *Smell generating enzymatic system for detection of ATP, microorganism cells and DNA.* The goal was to combine the enzyme tryptophanase with the enzyme pyridoxal kinase to act as a bienzyme detector for ATP. Conditions for the bienzyme system are optimized. The biosensor is expected to be applied in cells and DNA detection.

3. *Biotinylation of PNIPAM-VAA microgel and controlled streptavidin uptake.* The goal was to modify the microgel surface with biotin molecules which can take up streptavidin to provide a platform for subsequent biomolecule immobilization.

4. *Paper-based smell-generating biosensor.* The goal was to immobilize the bienzyme on paper, using microgel as the supporter for the construction of paper-based smell-generating detection.

1.5 Thesis Outline

Chapter 1: The present chapter presents the research background of this thesis, including the mechanism of biosensors, the components of biosensors, and an introduction to smell signals, tryptophanase and pyridoxal kinase. The specific objectives and an outline of the thesis are also presented here.

Chapter 2: This chapter describes the modification of the enzyme tryptophanase by biotinylation and its application as a reporter in a classic bioassay, ELISA. The experimental methods for measuring smell were set up and optimized reaction conditions for tryptophanase were obtained. Smell signals generated in ELISA upon detection of the analyte were characterized.

Chapter 3: This chapter describes the combination of tryptophanase with pyridoxal kinase as a biosensor for ATP. Optimized conditions for this bienzyme system were obtained. Using ATP as a bridge, the bienzyme biosensor was able to detect microorganism cells and target DNA through the production of smell signals. The reaction conditions for this bienzyme system were optimized. Activation effect, specificity and sensitivity of ATP to the system were investigated.

Chapter 4: This chapter describes the biotinylation and the streptavidin uploading on poly (N-isopropylacrylamide-co-vinylacetic acid) microgels. The optimized biotin density for maximum streptavidin uploading was investigated. This provides a platform for the subsequent biomolecule immobilization on microgels.

Chapter 5: This chapter describes the immobilization of tryptophanase and pyridoxal kinase on a paper strip to provide bi-signal biodetections. The paper-based smell generating biosensor provides a convenient and easily manipulated assay.

Chapter 6 This chapter summarizes the main conclusions and contributions of this project, and gives suggestions for future researches.

1.6 References

1. Wang, J., Glucose biosensors: 40 years of advances and challenges. *Electroanalysis* **2001,** *13* (12), 983.

2. (a) Velasco-Garcia, M.; Mottram, T., Biosensor technology addressing agricultural problems. *Biosystems engineering* **2003,** *84* (1), 1-12; (b) Hall, R., Biosensor technologies for detecting microbiological foodborne hazards. *Microbes and Infection* **2002,** *4* (4), 425-432.

3. Weetall, H., Biosensor technology What? Where? When? and Why? *Biosensors and Bioelectronics* **1996,** *11* (1-2).

4. Clark Jr, L. C.; Lyons, C., Electrode systems for continuous monitoring in cardiovascular surgery. *Annals of the New York Academy of Sciences* **1962,** *102* (1), 29-45.

5. Malhotra, B. D.; Chaubey, A., Biosensors for clinical diagnostics industry. *Sensors and Actuators B: Chemical* **2003,** *91* (1-3), 117-127.

6. Lin, C.; Wang, S. M., BIOSENSOR COMMERCIALIZATION STRATEGY- A THEORETICAL APPROACH. *Frontiers in Bioscience* **2005,** *10*, 99-106.

7. Perlmann, P.; Perlmann, H., Enzyme Linked Immunosorbent Assay. **1994**.

8. Zhao, W.; Chiuman, W.; Lam, J. C. F.; McManus, S. A.; Chen, W.; Cui, Y.; Pelton, R.; Brook, M. A.; Li, Y., DNA aptamer folding on gold nanoparticles: from colloid chemistry to biosensors. *Journal of the American Chemical Society* **2008,** *130* (11), 3610-3618.

9. Bousse, L., Whole cell biosensors. *Sensors and Actuators B: Chemical* **1996,** *34* (1-3), 270-275.

10. Oungpipat, W.; Alexander, P.; Southwell-Keely, P., A reagentless amperometric biosensor for hydrogen peroxide determination based on asparagus tissue and ferrocene mediation. *Analytica chimica acta* **1995,** *309* (1-3), 35-45.

11. Kerman, K.; Nagatani, N.; Chikae, M.; Yuhi, T.; Takamura, Y.; Tamiya, E., Label-free electrochemical immunoassay for the detection of human chorionic gonadotropin hormone. *Analytical Chemistry* **2006,** *78* (15), 5612-5616.

12. Wolfbeis, O. S., Fiber-optic chemical sensors and biosensors. *Analytical Chemistry* **2008,** *80* (12),

4269-4283.

13. Xia, W.; Li, Y.; Wan, Y.; Chen, T.; Wei, J.; Lin, Y.; Xu, S., Electrochemical biosensor for estrogenic substance using lipid bilayers modified by Au nanoparticles. *Biosensors and Bioelectronics* **2010,** *25* (10), 2253-2258.

14. Bizet, K.; Gabrielli, C.; Perrot, H.; Therasse, J., Validation of antibody-based recognition by piezoelectric transducers through electroacoustic admittance analysis. *Biosensors and Bioelectronics* **1998,** *13* (3-4), 259-269.

15. Schaffar Otto, S.; Bernhard, P., A fast responding fibre optic glucose biosensor based on an oxygen optrode. *Biosensors and Bioelectronics* **1990,** *5* (2), 137-148.

16. Zhang, Y.; Tadigadapa, S., Calorimetric biosensors with integrated microfluidic channels. *Biosensors and Bioelectronics* **2004,** *19* (12), 1733-1743.

17. Cai, Q.; Zeng, K.; Ruan, C.; Desai, T. A.; Grimes, C. A., A wireless, remote query glucose biosensor based on a pH-sensitive polymer. *Analytical Chemistry* **2004,** *76* (14), 4038-4043.

18. Ellis, J.; Thompson, M., Viscoelastic Modeling with Interfacial slip of a Protein Monolayer Electrode-Adsorbed on an Acoustic Wave Biosensor. *Langmuir* **2010**, 369-395.

19. Liu, J.; Lu, Y., A colorimetric lead biosensor using DNAzyme-directed assembly of gold nanoparticles. *J. Am. Chem. Soc* **2003,** *125* (22), 6642-6643.

20. Pelton, R., Bioactive paper provides a low-cost platform for diagnostics. *TrAC Trends in Analytical Chemistry* **2009,** *28* (8), 925-942.

21. Aikio, S.; Gronqvist, S.; Hakola, L.; Hurme, E.; Jussila, S., Bioactive Paper and Fibre Products: Patent and Literary Survey. **2007**.

22. Hossain, S. M. Z.; Luckham, R. E.; Smith, A. M.; Lebert, J. M.; Davies, L. M.; Pelton, R. H.; Filipe, C. D. M.; Brennan, J. D., Development of a Bioactive Paper Sensor for Detection of Neurotoxins Using Piezoelectric Inkjet Printing of Sol- Gel-Derived Bioinks. *Analytical Chemistry* **2009,** *81* (13), 5474-5483.

23. Bodenhamer, W. T., Displacement assay for selective biological material detection. Google Patents: 2007.

24. Minikh, O.; Tolba, M.; Brovko, L.; Griffiths, M., Bacteriophage-based biosorbents coupled with

bioluminescent ATP assay for rapid concentration and detection of Escherichia coli. *Journal of microbiological methods* **2010,** *82* (2), 177-183.

25. Ali, M. M.; Aguirre, S. D.; Xu, Y.; Filipe, C. D. M.; Pelton, R.; Li, Y., Detection of DNA using bioactive paper strips. *Chem. Commun.* **2009,** (43), 6640-6642.

26. Su, S.; Ali, M. M.; Filipe, C. D. M.; Li, Y.; Pelton, R., Microgel-based inks for paper-supported biosensing applications. *Biomacromolecules* **2008,** *9* (3), 935-941.

27. Voss, R.; Brook, M. A.; Thompson, J.; Chen, Y.; Pelton, R. H.; Brennan, J. D., Non-destructive horseradish peroxidase immobilization in porous silica nanoparticles. *J. Mater. Chem.* **2007,** *17* (46), 4854-4863.

28. Bang, J. H.; Lim, S. H.; Park, E.; Suslick, K. S., Chemically responsive nanoporous pigments: colorimetric sensor arrays and the identification of aliphatic amines. *Langmuir* **2008,** *24* (22), 13168-13172.

29. Kouisni, L.; Rochefort, D., Confocal microscopy study of polymer microcapsules for enzyme immobilisation in paper substrates. *Journal of Applied Polymer Science* **2009,** *111* (1), 1-10.

30. Su, S.; Ali, M.; Filipe, C.; Li, Y.; Pelton, R., Microgel-Based Inks for Paper-Supported Biosensing Applications. *Biomacromolecules* **2008,** *9* (3), 935-941.

31. (a) Di Risio, S.; Yan, N., Piezoelectric Ink Jet Printing of Horseradish Peroxidase: Effect of Ink Viscosity Modifiers on Activity. *Macromolecular Rapid Communications* **2007,** *28* (18 19), 1934-1940; (b) Di Risio, S.; Yan, N., Adsorption and inactivation behavior of horseradish peroxidase on cellulosic fiber surfaces. *Journal of colloid and interface science* **2009,** *338* (2), 410-419.

32. Zhao, W.; Brook, M. A.; Li, Y., Design of Gold Nanoparticle Based Colorimetric Biosensing Assays. *ChemBioChem* **2008,** *9* (15), 2363-2371.

33. Wang, J.; Pelton, R.; Veldhuis, L. J.; MacKenzie, C. R.; Hall, J. C.; Filipe, C. D. M., Wet-strength resins and surface properties affect paper-based antibody assays. *Appita Journal: Journal of the Technical Association of the Australian and New Zealand Pulp and Paper Industry* **2010,** *63* (1), 32.

34. Ali, M.; Aguirre, S.; Xu, Y.; Filipe, C.; Pelton, R.; Li, Y., Detection of DNA using bioactive paper strips. *Chemical communications (Cambridge, England)* **2009,** (43), 6640.

35. Dickinson, T. A.; White, J.; Kauer, J. S.; Walt, D. R., Current trends in [] artificial-nose'technology. *Trends in Biotechnology* **1998,** *16* (6), 250-258.

36. Nicklin, S. C., Megan Louise; D'souza, Natasha Joanna WHOLE CELL BIOSENSOR USING THE RELEASE OF A VOLATILE SUBSTANCE AS REPORTER. 2007.

37. Melker, R. J. D., Donn Michael Application of biosensors for diagnosis and treatment of disease 2005.

38. Tepper, J. S.; Weiss, B.; Wood, R. W., Alterations in behavior produced by inhaled ozone or ammonia* 1. *Fundamental and Applied Toxicology* **1985,** *5* (6), 1110-1118.

39. Schild, D., Principles of odor coding and a neural network for odor discrimination. *Biophysical journal* **1988,** *54* (6), 1001-1011.

40. Greenman, J.; EL-Maaytah, M.; Duffield, J.; Spencer, P.; Rosenberg, M.; Corry, D.; Saad, S.; Lenton, P.; Majerus, G.; Nachnani, S., Assessing the relationship between concentrations of malodor compounds and odor scores from judges. *The Journal of the American Dental Association* **2005,** *136* (6), 749.

41. Arnold, J. W.; Senter, S. D., Use of digital aroma technology and SPME GC MS to compare volatile compounds produced by bacteria isolated from processed poultry. *Journal of the Science of Food and Agriculture* **1998,** *78* (3), 343-348.

42. (a) Newton, W.; Morino, Y.; Snell, E., Properties of crystalline tryptophanase. *Journal of Biological Chemistry* **1965,** *240* (3), 1211; (b) Phillips, R.; Sundararaju, B.; Faleev, N., Proton Transfer and Carbon-Carbon Bond Cleavage in the Elimination of Indole Catalyzed by Escherichia coli Tryptophan Indole-Lyase. *J. Am. Chem. Soc* **2000,** *122* (6), 1008-1014.

43. Rappaport, S., Threshold limit values, permissible exposure limits, and feasibility: the bases for exposure limits in the United States. *American journal of industrial medicine* **1993,** *23* (5), 683-694.

44. Almog, O.; Kogan, A.; Leeuw, M.; Gdalevsky, G.; Cohen Luria, R.; Parola, A., Structural insights into cold inactivation of tryptophanase and cold adaptation of subtilisin S41. *Biopolymers* **2008,** *89* (5), 354-359.

45. Ku, S.; Yip, P.; Howell, P., Structure of Escherichia coli tryptophanase. *Acta Crystallographica Section D: Biological Crystallography* **2006,** *62* (7), 814-823.

46. Hoch, J.; Simpson, F.; DeMoss, R., Purification and Some Properties of Tryptophanase from Bacillus alvei*. *Biochemistry* **1966,** *5* (7), 2229-2237.

47. Suzuki, S.; Hirahara, T.; Horinouchi, S.; Beppu, T., Purification and properties of thermostable tryptophanase from an obligately symbiotic thermophile, Symbiobacterium thermophilum. *Agricultural and biological chemistry* **1991,** *55* (12), 3059-3066.

48. Suelter, C.; Snell, E., Monovalent cation activation of tryptophanase. *Journal of Biological Chemistry* **1977,** *252* (6), 1852.

49. Isupov, M.; Antson, A.; Dodson, E.; Dodson, G.; Dementieva, I.; Zakomirdina, L.; Wilson, K.; Dauter, Z.; Lebedev, A.; Harutyunyan, E., Crystal structure of tryptophanase1. *Journal of molecular biology* **1998,** *276* (3), 603-623.

50. Metzler, C.; Viswanath, R.; Metzler, D., Equilibria and absorption spectra of tryptophanase. *Journal of Biological Chemistry* **1991,** *266* (15), 9374.

51. Happold, F.; Struyvenberg, A., The activation of tryptophanase apo-enzyme by potassium, ammonium and rubidium ions. *Biochemical Journal* **1954,** *58* (3), 379.

52. Honda, T.; Tokushige, M., Effects of temperature and monovalent cations on activity and quaternary structure of tryptophanase. *Journal of biochemistry* **1986,** *100* (3), 679.

53. Sloan, M.; Phillips, R., Effects of [alpha]-Deuteration and of Aza and Thia Analogs of l-Tryptophan on Formation of Intermediates in the Reaction of Escherichia coli Tryptophan Indole-lyase†. *Biochemistry* **1996,** *35* (50), 16165-16173.

54. Salvà, A.; Donoso, J.; Frau, J.; Muñoz, F., Theoretical studies on transimination of vitamin B6 analogs. *International Journal of Quantum Chemistry* **2002,** *89* (1), 48-56.

55. (a) Friedemann, T.; Haugen, G., Pyruvic acid. II. The determination of keto acids in blood and urine. *J. biol. Chem* **1943,** *147*, 415-442; (b) Koepsell, H.; Sharpe, E., Microdetermination of pyruvic and [alpha]-ketoglutaric acids. *Archives of Biochemistry and Biophysics* **1952,** *38* (1), 443-449.

56. (a) Scott, T., An enzymic method for the estimation of L-tryptophan. *Biochemical Journal* **1961,** *80* (3), 462; (b) McEvoy-Bowe, E., Modification of the Scott method for the determination of indole. *The Analyst* **1963,** *88*, 893; (c) Shimada, A.; Shishido, H.; Nakamura, I., Tryptophanase-catalysed degradation of D-tryptophan in highly concentrated diammonium hydrogen phosphate solution. *Amino Acids* **1996,** *11* (1), 83-89.

57. Suelter, C.; Wang, J.; Snell, E., Direct spectrophotometric assay of tryptophanase. *FEBS letters* **1976,** *66* (2), 230.

58. Li, M.; Kwok, F.; Chang, W.; Lau, C.; Zhang, J.; Lo, S.; Jiang, T.; Liang, D., Crystal structure of brain pyridoxal kinase, a novel member of the ribokinase superfamily. *Journal of Biological Chemistry* **2002,** *277* (48), 46385.

59. Karawya, E.; Fonda, M., Purification, assay, and kinetic properties of sheep liver pyridoxal kinase. *Analytical biochemistry* **1978,** *90* (2), 525-533.

60. Kerry, J.; Rohde, M.; Kwok, F., Brain pyridoxal kinase. *European Journal of Biochemistry* **1986,** *158* (3), 581-585.

61. Neary, J.; Diven, W., Purification, properties, and a possible mechanism for pyridoxal kinase from bovine brain. *Journal of Biological Chemistry* **1970,** *245* (21), 5585.

62. di Salvo, M.; Hunt, S.; Schirch, V., Expression, purification, and kinetic constants for human and Escherichia coli pyridoxal kinases. *Protein expression and purification* **2004,** *36* (2), 300-306.

63. Safo, M.; Musayev, F.; Di Salvo, M.; Hunt, S.; Claude, J.; Schirch, V., Crystal structure of pyridoxal kinase from the Escherichia coli pdxK gene: Implications for the classification of pyridoxal kinases. *Journal of bacteriology* **2006,** *188* (12), 4542.

64. Newman, J.; Das, S.; Sedelnikova, S.; Rice, D., Cloning, purification and preliminary crystallographic analysis of a putative pyridoxal kinase from Bacillus subtilis. *Acta Crystallographica Section F: Structural Biology and Crystallization Communications* **2006,** *62* (10), 1006-1009.

65. Kwok, F.; Churchich, J., Interaction between pyridoxal kinase and pyridoxine-5-P oxidase, two enzymes involved in the metabolism of vitamin B6. *Journal of Biological Chemistry* **1980,** *255* (3), 882.

66. Kwok, F.; Scholz, G.; Churchich, J., Brain pyridoxal kinase dissociation of the dimeric structure and catalytic activity of the monomeric species. *European Journal of Biochemistry* **1987,** *168* (3), 577-583.

67. Churchich, J.; Scholz, G.; Kwok, F., Activation of pyridoxal kinase by metallothionein. *Biochimica et Biophysica Acta (BBA)-Protein Structure and Molecular Enzymology* **1989,** *996* (3), 181-186.

68. (a) Chabner, B.; Livingston, D., A simple enzymic assay for pyridoxal phosphate. *Analytical biochemistry* **1970,** *34* (2), 413-423; (b) Suelter, C.; Wang, J.; Snell, E., Application of a direct spectrophotometric assay employing a chromogenic substrate for tryptophanase to the determination of pyridoxal and pyridoxamine 5'-phosphates. *Analytical biochemistry* **1976,** *76* (1), 221-232.

69. Wada, H.; Snell, E., The enzymatic oxidation of pyridoxine and pyridoxamine phosphates. *Journal of Biological Chemistry* **1961,** *236* (7), 2089.

70. Camp, V.; Chipponi, J.; Faraj, B., Radioenzymatic assay for direct measurement of plasma pyridoxal 5'-phosphate. *Clinical chemistry* **1983,** *29* (4), 642.

71. Gordon, J., Extracellular ATP: effects, sources and fate. *Biochemical Journal* **1986,** *233* (2), 309.

72. Chen, J., ATP bioluminescence: a rapid indicator for environmental hygiene and microbial quality of meats. *Dairy Food and Environmental Sanitation* **2000,** *20* (8), 617-620.

73. Kueng, A.; Kranz, C.; Mizaikoff, B., Amperometric ATP biosensor based on polymer entrapped enzymes. *Biosensors and Bioelectronics* **2004,** *19* (10), 1301-1307.

74. Chen, Z.; Li, G.; Zhang, L.; Jiang, J.; Li, Z.; Peng, Z.; Deng, L., A new method for the detection of ATP using a quantum-dot-tagged aptamer. *Analytical and Bioanalytical Chemistry* **2008,** *392* (6), 1185-1188.

75. Wang, J.; Jiang, Y.; Zhou, C.; Fang, X., Aptamer-based ATP assay using a luminescent light switching complex. *Analytical Chemistry* **2005,** *77* (11), 3542-3546.

76. Schneider, S.; Egan, M.; Jena, B.; Guggino, W.; Oberleithner, H.; Geibel, J., Continuous detection of extracellular ATP on living cells by using atomic force microscopy. *Proceedings of the National Academy of Sciences of the United States of America* **1999,** *96* (21), 12180.

77. Trudil, D.; Loomis, L.; Pabon, R.; Hasan, J.; Trudil, C., Rapid ATP method for the screening and identification of bacteria in food and water samples. *Moscow University Chemistry Bulletin,(Vestnik Moskovskogo Universiteta. Serie 2. Khimiya.)* **2000**, 27-29.

Chapter 2 Tryptophanase: A Smell Generating Transducer for Biosensors

In Chapter 2, all the experiments were conducted by myself and Joanna Sauder who worked as a summer student. I wrote the first drafts. Dr. Filipe and M. Monsur Ali edited sections for the final version. Dr. Filipe, Dr. Pelton and Dr. Li contributed many helpful suggestions on my experiments and paper writing.

Tryptophanase: A Smell Generating Transducer for Biosensors

Yaqin Xu[†], M. Monsur Ali[‡], Joanna Sauder[†], Yingfu Li[‡], Robert Pelton[†]* and Carlos D. M. Filipe[†]*

† Department of Chemical Engineering, McMaster University, Hamilton, Ontario, Canada, L8S 4L7

‡ Department of Biochemistry and Biomedical Sciences, McMaster University, Hamilton, Ontario, Canada L8N 3Z5

ABSTRACT: Herein we report an enzyme-based biosensor that signals binding of a specific target molecule by producing a smell that can be easily detected by the human nose. The key component of this biosensor is the enzyme tryptophanase (TPase), which uses either L-tryptophan or S-methyl-L-cysteine as substrates, with production of either indole or methyl mercaptan as final products (both easily detectable by the human nose). To assemble a working biosensor, TPase (the signal transducer component of the biosensor) was first biotinylated and linked to a biotinylated antibody (the biorecognition component of the biosensor) using avidin. Proof-of-concept for this biosensor was achieved by performing an enzyme-linked immunosorbent assay (ELISA) on magnetic beads with detection of IgG from rabbit serum (the target) in a sample and reporting its presence through the generation of a smell (either indole or methyl mercaptan, depending of the substrate used). The approach described herein is modular and is readily applicable for a variety of biorecognition elements, such as antibodies, proteins and aptamers as part of a new generation of smell generating biosensors.

Biosensors are widely used in clinical, food, environmental and agricultural areas for monitoring and detecting target analytes and reporting their presence through the generation of a variety of signals.[1-3] In general, biosensors consist of two parts: a biorecognition element and a signal transducer. The biorecognition element is the component that can specifically interact with its cognate target, while the transducer produces a signal that may be either electrochemical[4], piezoelectrical[5], calorimetric[6], colorimetric[7] or acoustic[8] to indicate the presence of the target analyte. Colorimetric sensors, which rely on the use of the sense of sight, are widely used in a large variety of applications. [9,10]

The human nose is a remarkable "analytical instrument". A notable example of how this has been exploited to improve safety of the general public is the use of mercaptans as additives to natural gas, which serve as odorants that provide an easily detectable smell to signal a gas leak. It is therefore somewhat surprising that only a small number of detection systems have been developed that make use of the sense of smell, or in other words, biosensor that use a smell generating transducer as a part of the biosensor. To our knowledge, only two odor-generating biosensors have been reported in the literature: the first is based on the use of whole cells to generate a smell of either acyl esters, hydrogen sulphide or methanethiol; [11] the second is based on the use of nanotubes filled with volatile organic compound, such as acetone, ammonia, and methyl mercaptan, and capped with aptamer – in the presence of the target, prostate specific antigen that is produced by prostate cancers, the cap is opened and the volatile compound is released resulting the generation of a noticeable smell. [12] Exploiting the sense of smell has part of detection systems has some attractive features: detection is independent of the subject paying constant attention to a display or waiting for a colour change to take place and detection can be easily done in poorly illuminated spaces where colour based signals are hard to be read; these biosensors could be part of facemasks that would report the presence of an agent by generating a noticeable smell.

We provide proof-of-concept of the use of the enzyme tryptophanase (TPase, EC 4.1.99.1) as a transducer for smell-generating biosensors. A simple diagram of this type of biosensor is presented in Figure 1a, showing its use in an enzyme-linked immunosorbent assay (ELISA) where smell generation signals the presence of a specific target, such as is demonstrated later on this paper.

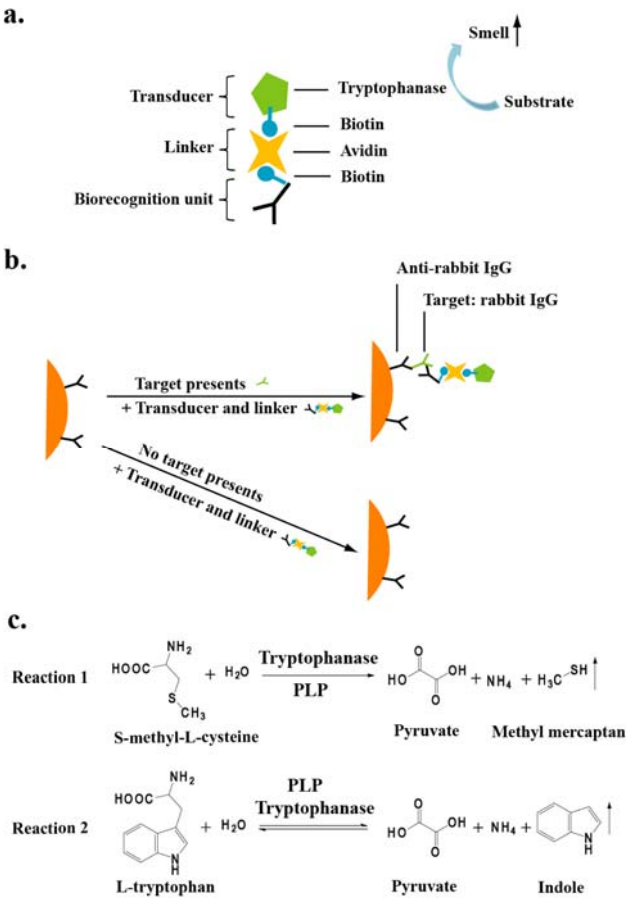

Figure 1. The components for a smell generating biosensor and the key reactions. (a) a biorecognition component linked to a transducer that generates smell, and the biorecognition leads to smell.; (b) Reactions catalyzed by TPase, using L-tryptophan and S-methyl-L-cysteine as substrates to produce indole and methyl mercaptan, as

products easily detectable by the human nose. Pyridoxal phosphate (PLP) is a cofactor required for TPase.

Tryptophanase is a pyridoxal phosphate-dependent enzyme that catalyzes a series of β-elimination and β-replacement reactions. The enzyme catalyzes the hydrolysis of L-tryptophan and S-methyl-L-cysteine to indole and methyl mercaptan, respectively (reaction 1 and 2 in Figure 1b). [13] Both these products are easily detectable by the human nose. The threshold concentration for indole (C_8H_7N) is 0.02 ppb (1.0×10^{-12} mol/dm^3),[14] with a noticeable floral odor associated with low concentrations and an unpleasant odor which comtributes to mouth malodor and the smell of toilet associated with higher concentrations. Methyl mercaptan, is a colorless, flammable gas with a very strong and unpleasant smell and with an odor threshold level of 0.2 ppb (1.0×10^{-11} mol/dm^3). [14] The United States OSHA Permissible Exposure Limit for methyl mercaptan is listed as 10 ppm. [15] Mercaptans are used as an additive to natural gas in order to provide warning of natural gas leaks. [16]

The biosensor developed in this work consisted of a biorecognition element and a signal transducer. The biorecognition element in the smell-generating reported herein was anti-rabbit IgG- which is able to specifically recognize rabbit IgG (the target). The transducer responsible for signal generation was TPase. We wished to obtain a general and modular method for assembling a potentially large number of smell-generating biosensors, *i.e.* being able to couple a variety of biorecognition elements to TPase. To this end, we prepared biotinylated TPase using N-Hydroxysulfosuccinimide (sulfo-NHS) biotin and TPase. The biotinilyated TPase can then be linked to any biotinylated biorecognition element (in our case, biotinylated anti-rabbit IgG) through the use of avidin.

In our first attempts to biotinylate TPase, a large loss of catalytic activity of the enzyme was observed (almost 93% of the initial activity lost – see Table S1 in supplementary information), which is consistent with other reports. [17] We hypothesized that this was due to reaction of lysine residues in the catalytic site of the enzyme[18,19] with the coupling agent (sulfo-NHS biotin). To minimize this effect, we performed the conjugation in the presence of 10 mM L-tryptophan, in an attempt to occupy and protect the catalytic site using the substrate. Using this approach, more than 60% of the initial catalytic activity was maintained (Table S1 in the supplementary information), with an average of 4.264±0.198 biotin molecules being incorporated per TPase molecule. This provides an adequate balance between the level of biotinylation required for linkage to avidin and the catalytic activity required for signal generation. Since biotin-avidin interactions are widely used in bioassays and biodetection, the biotinylated TPase provides a general platform for subsequent applications of TPase as a transducer in a variety of biosensors.

The smell-generating biosensor was assembled by mixing biotinylated TPase (the transducer), avidin (the linker) and the biotin labeled anti-rabbit IgG (the biorecognition element) in a molar ratio of 1:2:2.5 respectively. This biosensor was used in an ELISA-like manner as shown in Figure 2 (we refer to it as a smell-reporting-ELISA). The presence of the target molecule in the sample, in our case rabbit IgG, is signaled through the generation of a smell- indole or methyl mercaptan, depending on which substrate was used in the procedure.

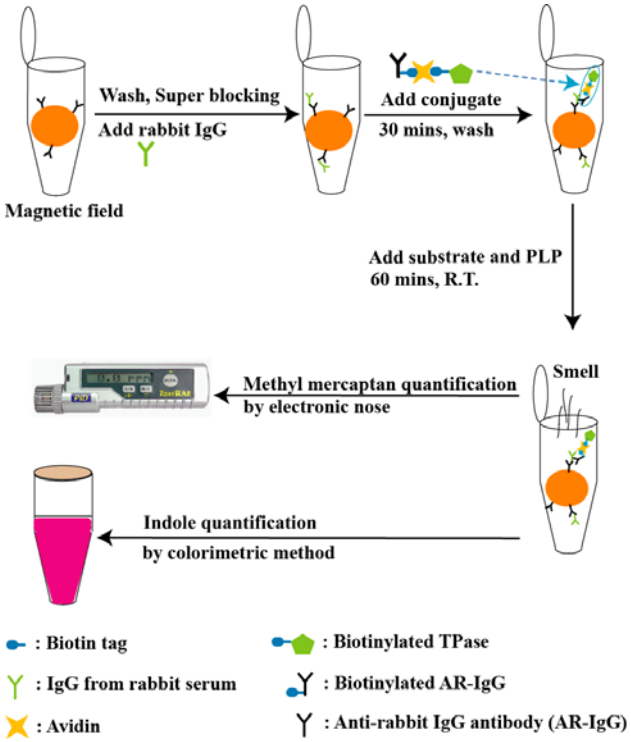

Figure 2. Schematic of the steps associated with the smell-reporting-ELISA on magnetic beads for detecting IgG from rabbit serum in a sample and reporting its presence through smell generation using biotinylated tryptophanase (TPase). The biosensor was assembled by combining biotinylated TPase, avidin and biotinylated anti-rabbit IgG. When S-methyl-L-cysteine was used as the substrate for TPase, the final product methyl mercaptan was detected in the gas phase using a photoionization detector. When the substrate was tryptophan, the indole concentration in the liquid phase was measured using Kovac's reagent[20-22].

To perform a smell-reporting-ELISA, 2 mL of 2.5 g/mL MagnaBind magnetic beads functionalized with anti-rabbit IgG (AR-IgG) were washed and blocked using SuperBlock T20 (PBS) buffer from Pierce. The beads were resuspended in 300 µL PBS buffer (10 mM, pH 7.4) and 200 µL of 2.2 mg/mL IgG from rabbit serum (RIgG) were added to the test sample, while 200 µL of 2 mg/mL BSA and 200 µL of 10 mM PBS buffer were added to control sample I and control sample II respectively (Figure 2). The samples were incubated under room temperature for 30 mins and the beads were washed and resuspended in PBS buffer. The AR-IgG-Avidin-biotinylated TPase complex (150µL containing 75 µg TPase) was then added to all three samples and incubated under room temperature for 30 mins. The beads were then washed by 500 µL PBS buffer (10mM, pH 7.4) for three times and resuspended in 200 µL KDP buffer. Then the beads were added to a 700 µL reaction mixture containing 15 mM tryptophan (the substrate for the reaction), and 0.1 mM of pyridoxal phosphate (a cofactor required by TPase. [13] In the sample containing rabbit IgG (the target molecule), the indole concentration in the liquid phase was found to be 2.2 µg/mL, while the control samples showed no production of indole (Figure 3a).

Assuming that equilibrium is reached between the gas and liquid phases, Henry's law and the ideal gas law can be used to calculate the indole concentration in the gas phase (detailed calculations are shown in supplementary information). For an headspace volume of 39.3 ml the indole concentration in the gas

phase was 1.1 ppb, 0.013 ppb and 0.025 ppb for the test sample, control sample I and control sample II respectively (Figure 3b). The presence of the target in the test sample resulted in a much higher production of indole as compared to the control samples (no target was present). The indole concentration in the gas phase of the test sample was 55 times higher than the threshold level for detection with the human nose, which shows that the biosensor produces a strong signal. It is apparent that the estimated levels of indole in the gas phase for the control samples are in the vicinity of the threshold level for the human nose. It is important to point out that gas phase concentrations were estimated based on the concentrations of indole measured in the liquid phase, which were very low for these samples (measured absorbances less than 0.006 units – Figure 3a) and statistically indistinguishable from zero. This implies that the estimated indole concentration in the gas phase is not statistically different than zero and during the experiments, no noticeable smell was detected.

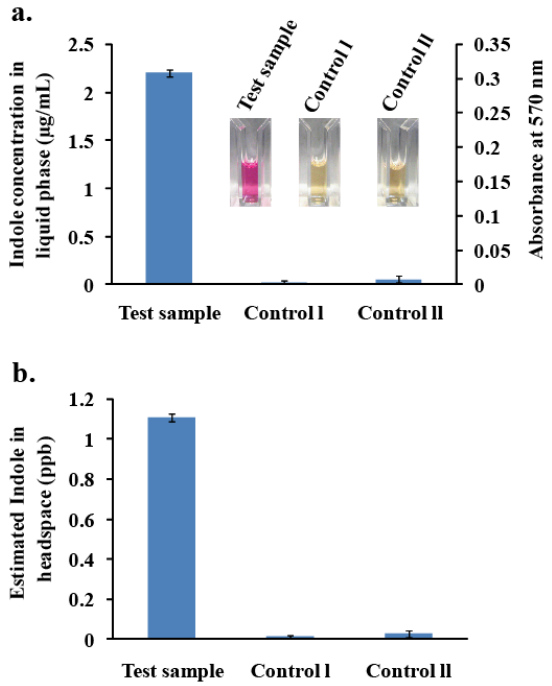

Figure 3. Indole generation in the smell-reporting-ELISA for a test sample containing 44 µg of the target, and two control samples (BSA was added to Control I but not to Control II): (a) Indole concentration in solution (primary Y axis is concentration in µg/ml and the secondary Y axis shows the absorbance of the samples at 570 nm - after adding Kovac's reagent).[20-22] (b) Estimated concentration of indole in the headspace of a 40ml glass vial. Each experiment was done in triplicate and the standard error is reported

When S-methyl-L-cysteine is used as the substrate for TPase in the smell-reporting-ELISA, the signaling molecule generated is methyl mercaptan. The concentration of methyl mercaptan on the gas phase was measured using a ToxiRAE Plus PID, which is a photoionization detector for monitoring volatile organic compounds (VOC). Because ammonia has a much higher solubility in water and is much less volatile than methyl mercaptan, the PID reading gives directly the concentration of methyl mercaptan in the gas phase. The smell-reporting-ELISA with S-methyl-L-cysteine as the substrate was done using 700 µL of a reaction mixture containing magnetic beads (2 mg), PLP(0.1 mM) and S-methyl-L-cysteine (15mM), and the mixture was added to a glass vial (with a total volume of 40 mL), which was capped and let sit on the bench under room temperature for one hour. The methyl mercaptan concentration in the headspace of the vial was measured by connecting vial directly to the PID (inset in Figure 4a). For the test sample, which contained 44 µg of the target molecule (rabbit IgG), the methyl mercaptan concentration in the headspace was 1.3 ppm after one hour of incubation (Figure 4a). This concentration is 6,500 times higher than the threshold level for the human nose. Using S-methyl-L-cysteine as the substrate, rather than L-tryptophan, results in a much stronger smell signal. For the control experiment, where BSA was added to further block the surface of the particles from non-specific binding of the assembled biosensor, the concentration in the headspace was found to be equal to zero (Control I in Figure 4a). When BSA was not used in the control sample (Control II in Figure 4a), there was a residual amount of assembled biosensor that was non-specifically adsorbed in the particles, leading to a very small, albeit measurable level of methyl mercaptan in the gas phase. The results in Figure 4a clearly show a very large increase in the level of methyl mercaptan formation associated with the presence of the target, and they also show that blocking of the surfaces is important to prevent false positives, like in any other ELISA.

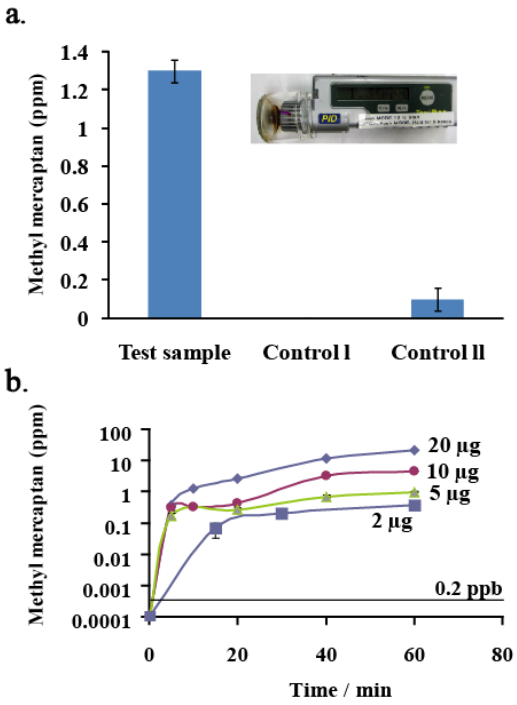

Figure 4. Using S-methyl-L-cysteine as the substrate for TPase and methyl mercaptan as the signaling molecule: (a) Methyl mercaptan concentration in the headspace of generated in the smell-reporting-ELISA for a test sample containing 44 µg of the target, and two control samples (BSA was added to Control I but not to Control II). Each experiment was done in triplicate and the standard error is reported; (b) concentration of methyl mercaptan in the headspace as a function of time for samples containing different amounts of TPase. Each data point is the average of three measurements and the standard error is reported. The straight line represents the threshold level for the human nose, which is 0.2ppb.

The ideal biosensor should generate a signal as quickly as possible; ideally signal generation should be instantaneous. For

TPase, the kinetics of enzymatic catalysis dictate the rate at which the signal is generated. To get a sense of how long it takes to generate a measurable signal, we performed a series of experiments using different amount of TPase in solution. These experiments were done using S-methyl-L-cysteine as the substrate and monitoring the concentration of methyl mercaptan in the headspace as a function of time. As expected, higher amounts of TPase present in the mixture resulted in faster rates of methyl mercaptan generation as shown in Figure 4b. A line for a methyl mercaptan concentration in the headspace equal to 0.2 ppb (threshold level for the human nose) is shown for reference, and it shows that even 2 µg of TPase are able to generate a signal above this line in less than 5 mins. These result that a signal is generated rapidly, which is critical for practical applications.

In summary, we developed a system that is able to link a binding event with the generation of a smell that can be easily detected by the human nose. The biosensor developed uses TPase as the signal transducer. This enzyme catalyzes the conversion of either L-tryptophan or S-methyl-L-cysteine to generate indole and methyl mercaptan, respectively. This transducer was linked to a biorecognition element (anti-rabbit IgG) using a biotin-avidin interaction, which makes the system modular and easy to use in conjuction with a variety of biorecognition elements, such as aptamers, proteins and other biotin labeled biomolecules. We demonstrated the use of this biosensor in a smell-reporting-ELISA, where the presence of a target (rabbit IgG), resulted in the formation of indole and methyl mercaptan at concentrations that can be easily detected by the human nose. Signal generation is fast. The use of TPase has a large potential for the creation of a new generation of biosensors that make use of the sense of smell. These could be done in combination with colorimetric based sensors, which would provide multi-sensory reporting of a binding event, or the presence of a target.

Supporting Information Available: Description of the material included. This material is available free of charge via the Internet at http://pubs.acs.org.

Corresponding Author

peltonrh@mcmaster.ca and filipec@mcmaster.ca

ACKNOWLEDGMENT

We thank Dr. Weian Zhao for critical reading and valuable comments on this manuscript. This research was supported by research grants from the Natural Sciences and Engineering Research Coundcil of Canada (NSERC) through the network grant SENTINEL (Bioactive Paper Network). YL and RP are Canada research chairs.

REFERENCES

(1) Velasco-Garcia, M. N.; Mottram, T. Biosystems Engineering 2003, 84, 1.
(2) H all, R. H. Microbes and Infection 2002, 4, 425.
(3) Weetall, H. H. Biosensors and Bioelectronics 1996, 11, i.
(4) Xia, W.; Li, Y.; Wan, Y.; Chen, T.; Wei, J.; Lin, Y.; Xu, S. Biosensors and Bioelectronics 2010, 25, 2253.
(5) Bizet, K.; Gabrielli, C.; Perrot, H.; Therasse, J. Biosensors and Bioelectronics 1998, 13, 259.
(6) Zhang, Y.; Tadigadapa, S. Biosensors and Bioelectronics 2004, 19, 1733.
(7) Liu, J.; Lu, Y. Journal of the American Chemical Society 2003, 125, 6642.
(8) Ellis, J. S.; Thompson, M. Langmuir 2010, 26, 11558.
(9) Liu, J.; Lu, Y. J. Am. Chem. Soc 2003, 125, 6642
(10) Ou, L. J.; Jin, P. Y.; Chu, X.; Jiang, J. H.; Yu, R. Q. Analytical Chemistry 2010, 2306.
(11) Nicklin, S.; Cooper, M.L.; D'souza, N. J. WO 2007/083137 A1, 2007
(12) Melker, R. J., Dennis, D. M. U.S. Patent 6 974 706 B1, 2005.
(13) Newton, W.; Morino, Y.; Snell, E. Journal of Biological Chemistry 1965, 240, 1211.
(14) Greenman, J.; EL-Maaytah, M.; Duffield, J.; Spencer, P.; Rosenberg, M.; Corry, D.; Saad, S.; Lenton, P.; Majerus, G.; Nachnani, S. The Journal of the American Dental Association 2005, 136, 749.
(15) Rappaport, S. American journal of industrial medicine 1993, 23, 683.
(16) Crouch, W.; Williams, R.; Bartlesville, O.; U.S. Patent 3 752 659, 1973.
(17) Huang, X.; Catignani, G.; Swaisgood, H. Journal of Agricultural and Food Chemistry 1995, 43, 895.
(18) Salvà, A.; Donoso, J.; Frau, J.; Muñoz, F. International Journal of Quantum Chemistry 2002, 89, 48.
(19) Metzler, C.; Viswanath, R.; Metzler, D. Journal of Biological Chemistry 1991, 266, 9374.
(20) McEvoy-Bowe, E. The Analyst 1963, 88, 893.
(21) Scott, T. Biochemical Journal 1961, 80, 462.
(22) Shimada, A.; Shishido, H.; Nakamura, I. Amino Acids 1996, 11, 83.

Supporting Information

Tryptophanase: A Smell Generating Transducer for Biosensors

Yaqin Xu[†], M. Monsur Ali[‡], Joanna Sauder[†], Yingfu Li[‡], Robert Pelton[†]* and Carlos D. M. Filipe[†]*

† Department of Chemical Engineering, McMaster University, Hamilton, Ontario, Canada, L8S 4L7

‡ Department of Biochemistry and Biomedical Sciences, McMaster University, Hamilton, Ontario, Canada L8N 3Z5

Materials and Apparatus

Apotryptophanase from *Escherichia coli* (TPase), DL-Dithiothreitol solution, Kovac's reagent (containing p-dimethylaminobenzaldehyde) for indole determination, IgG from rabbit serum, L-Tryptophan, Pyridoxal 5'-phosphate hydrate, n-butanol, HABA/Avidin reagent and biotin-labeled anti-rabbit IgG (whole molecule) produced in goat were purchased from Sigma-Aldrich. EZ-link Sulfo-NHS-Biotin (SNB), magnetic beads covered with anti-rabbit IgG (produced in goat), Ellman's reagent and super block T20 buffer were purchased from Pierce. A cylinder of 20 ppm methyl mercaptan in nitrogen was purchased from Linde Canada Limited. A tube rotator with adjustable rotisserie assemblies was purchased from VWR. KDP buffer was prepared according to previous report[1] that it consisted of 0.2 M potassium phosphate (pH 7.8), 2mM dithiothreitol and 6.7 mM ammonium sulfate. The ToxiRAE Plus PID gas detector was purchased from RAE systems and UV-VIS measurements were done using a Beckman Coulter DU800

spectrophotometer.

Experimental Section

Quantification of indole in solution. Briefly, *p*-dimethylaminobenzaldehyde was added to indole containing solutions and the absorbanse of the sample was measured at 570 nm. [2] Standard solutions, with a volume of 700 µL and containing from 0 to 9 µg/mL of indole were prepared and 700 µL of water saturated n-butanol was vigorously mixed with the standard solutions. These samples were then centrifuged at 1,000g for 1min, and 500 µL of the supernatant was collected and mixed with an equal volume of Kovac's reagent containing *p*-dimethylaminobenzaldehyde. After a five min incubation period, the absorbance of the samples was measured at 570 nm and a standard curve of absorbance vs. indole concentration could be generated (Figure S1). The test samples (700 µL) were carried through the same procedure as for the standards and the indole concentration was determined by measuring the absorbance of the reaction at 570 nm reaction mixture and using the calibration curve.

Quantification of Methyl mercaptan in solution. The standard curve for quantification of methyl mercaptan in solution was prepared by using cysteine as the standard solution. The thermo scientific procedure was followed and the standards were prepared according to Table S1. The Reaction Buffer prepared consisted of 0.1 M sodium phosphate buffer at pH 8.0 and 1mM EDTA. Ellman's reagent was prepared by dissolving 4 mg of Ellman's Reagent (Thermo Scientific) in 1 mL of Reaction Buffer. 250 uL of each standard solutions in Table S1 was then added to a separate vial containing 2.5 mL of

reaction buffer and 4 mg of Ellman's Reagent. The vials were mixed and then incubated at room temperature for 15 minutes. The absorbance was then measured in the UV Spec at 412 nm using visible light only. The standard curve created using cysteine as the standard was used to measure the concentration of methanethiol in solution as shown in Figure S2. Methanethiol was produced by incubating 40 ug of Tpase with 15mM of S-methyl-L-cysteine and 0.1mM PLP for 1 hour (Note all dissolved in KDP Buffer). Following the incubation 250 uL of the sample were added to 2.5 mL of Reaction Buffer and 50 uL of Ellman's Reagent and allowed to incubate at room temperature for 15 min. The absorbance was then read on the UV Spec using the Cysteine standard curve.

Biotinylation of TPase Using Sulfo-NHS-Biotin (SNB). Our initial attempts at TPase biotinylation involved the SNB reaction with the amino groups on the surface of TPase in KDP buffer either with the presence of L-tryptophan or without the presence of L-tryptophan as shown in Table S1. In sample I, to 0.5 mL of 4 mg/mL TPase in KDP buffer L-tryptophan was added to a concentration of 10 mM. Five minutes later, 200 μg SNB was added and the mixture were left under room temperature for 2 hours. The sample II without the presence of L-tryptophan was prepared without adding L-tryptophan. The control sample III was prepared by adding KDP buffer only. Each sample was prepared with triplicates. After 2 hours, an additional 200 μg SNB was added to samples I and II. Then all three samples were placed on ice for four hours. Following this an additional 200 μg SNB was added to sample I and II and samples were then placed in the 4^{o}C fridge overnight. In the following day, the samples were put into dialysis tube and underwent dialysis in ten times diluted KDP buffer for 8 hours on ice.

The dialysis buffer was changed after 3 hours and 6 hours. The samples were then transferred into glass vials and stored in the 4ºC fridge. The protein concentrations in the samples were quantified by using the Bradford method. The quantity of biotin present on the enzyme was determined based on the HABA/Avidin test in which the dye 4'-hydroxyazobenzene-2-carboxylic acid (HABA) binds with avidin and can be replaced by biotin. The enzyme activity of the biotinylated Tpase (BTPase) was measured based on the amount of indole generated by 50 µg of BTPase in 1 hour as shown in Table S2.

Optimization of conditions for TPase. We performed a series of experiments to determine the optimal conditions for TPace activity, where the following conditions were varied one at a time: pH, temperature, substrate concentration (L-tryptophan or S-methyl-L-cysteine), PLP concentration and the concentration of TPase. For all the tests, the samples had a total volume of 700 µL and the product concentration (indole or methyl mercaptan) was measured after one hour of incubation.

Indole generated was quantified by adding *p*-dimethylaminobenzaldehyde and reading absorbance via UV-Vis spectrometer. Methyl mercaptan generated was quantified by using Ellman's reagent

The results are shown in Figure S3. The optimized conditions are 15 mM L-tryptophan or S-methyl-L-cysteine, 0.2 mM PLP, 50 µg TPase in buffer with a total volume of 700 µL under pH 9 and 37 ºC for one hour. Since room temperature and mild pH conditions are optimal for ELISA tests, in the following text, other than specified, smell generation by TPase are carried out under these conditions: 15 mM L-tryptophan or S-methyl-L-cysteine, 0.2 mM PLP, 50 µg TPase in KDP buffer with a total volume of 700 µL under

pH 7.8 and room temperature (20 ºC) for one hour.

Measurement of methyl mercaptan in headspace. ToxiRAE PID gas detector measures the volatile organic chemicals in the gas phase. It is calibrated firstly by using 20 ppm methyl mercaptan in nitrogen then it is connected to a glass bottle where ELISA reaction was happening as shown in Figure S 4. Wait for 15 seconds to record the peak reading. The reaction mixture in the bottle contains 15 mM S-methyl-L-cysteine, 50 µg TPase and 0.2 mMPLP.

ELISA on magnetic beads. The ELISA on magnetic beads followed the procedure in the paper. 0.8 mL of 1 mg/mL BTPase solution, 0.5 mL 1 mg/mL Avidin and 0.3 mL 2 mg/mL anti-rabbit IgG biotin were mixed together and sit on a tube rotator with rotating speed of 18 rpm under room temperature for two hours then sit in the 4 ºC fridge overnight. 2 mL of magnetic beads covered with anti-rabbit IgG produced in goat was washed with 10 mM PBS buffer (pH 7.4) and blocked with 500 µL superblocking buffer for 30 mins. Then the beads were washed and redispersed in 300 µL PBS buffer. Then 200 µL of 2.2 mg/mL IgG from rabbit serum in PBS buffer was added to the test sample. To the control sample I 200 µL of 2 mg/mL BSA in PBS buffer was added. To the control sample II, 200 µL of 10 mM PBS buffer was added. Each sample has triplicates. The samples were on a rotator with rotating speed of 18 rpm under room temperature for 30 mins. The samples were washed by PBS buffer again for three times and redispersed in 420 µL PBS buffer. 80 µL of anti-rabbit IgG biotin was added to each sample. The samples were on a rotator under room temperature for 30 mins. The beads were washed by 500 µL of 10 mM PBS buffer for three times and redispersed in 350 µL of PBS buffer.

Then 150 µL of BTPase-avidin-B-anti rabbit IgG solution prepared above was added to each sample. The samples then sat on a rotator under room temperature for 30 mins. After that, the beads were washed by 500µL of 10 mM PBS buffer for three times. 15 mM L-tryptophan or S-methyl-L-cysteine, 0.1 mM PLP were then added to the cleaned beads and the volume was made up to 700 µL by adding KDP buffer. The samples sat on a rotator under room temperature for 60 mins and the supernatant was taken for quantification of indole or methyl mercaptan. To measure the production of methyl mercaptan by using ToxiRAE PID gas detector, the 700 µL reaction mixture containing beads were transferred to a 40mL glass bottle with a cap. One hour later, the cap is opened and connected to the ToxiRAE PID gas detector as shown in Figure S4.

Theoretical calculation of Indole in the headspace. For an indole solution of X µg/mL, if assume that Henry's law and Ideal gas law are obeyed and indole has Henry's law constant of 4.08×10^5, Indole in the head space of a 40 mL glass bottle is calculated to be 0.503X ppb (part per billion) as shown below. [3] The concentration of indole in the gas phase directly relates to the intensity of smell as we know that the threshold of indole for human nose is 0.02 ppb.

Calculation:

Henry's law constant for indole under 20 °C at 1 atmosphere pressure is
KHi= 4.08×10^{5}
Indole has a molecular weight Mi= 117.15 g/mol
In a 40 mL bottle filled with 700 μL liquid reaction mixture, if assume that X μg/mL indole was produced in the liquid phase quantified by colorimetric method. Then the mole concentration of indole (C) in the solution is :

$$C=\frac{\frac{X}{Mi}}{KHi}=2.092\times10^{-8}\ \text{mol}/m^{3} \qquad \textbf{Equation 1}$$

The mole concentration of air under 20 °C at 1 atmosphere pressure is:

$$Cair=\frac{P}{RT}=\frac{1.01325\times10^{5}}{8.314\times293}=41.595\ \text{mol}/m^{3} \qquad \textbf{Equation 2}$$

Estimated indole concentration (ppb) in the headspace could be calculated as:

$$C_{EI}=\frac{C}{Cair}\times10^{6}=\frac{2.092\times10^{-8}}{41.595}\times10^{6}=0.503\,\text{ppb}$$

Ammonia production is negligible for the electronic nose. ToxiRAE PID gas detector measures the volatile organic chemicals in the gas phase. Although ammonia was also produced by TPase, the following calculation shows that ammonia does not contribute to the reading of the PID gas detector. If 0.5 mM of L-tryptophan is hydrolyzed, then in the headspace of a 40 mL glass vial there is 164.3 ppm of methyl mercaptan and 3.7 ppm of ammonia. Compared with methyl mercaptan, the concentration of ammonia is almost negligible.

If assume that in 700 μL reaction solution, 0.5 mM L-tryptophan is hydrolyzed, the amount of ammonia and methyl mercaptan or indole produced would be:
$M = 0.7\times10^{-3}\times0.5\times10^{-3} = 3.5\times10^{-7}$ mole

Henry's law constant for each chemical is: (directionless)

Ammonia KHa=3150

Indole KHi=408000

Methyl mercaptan KHm=17

In a glass vial of 40 mL containing liquid reaction mixture of 0.7 mL, the gas volume is 39.3 mL.

The mole concentration of indole (Ci) , methyl mercaptan (Cm) and ammonia (Ca) in the gas phase would be:

The mole concentration of indole (Ci) , methyl mercaptan (Cm) and ammonia (Ca) in the gas phase would be:

Ci= $\frac{1000M}{0.7\times KHi + 39.3} = 1.225\times10^{-9}$ mol/L

Cm= $\frac{1000M}{0.7\times KHm + 39.3} = 6.836\times10^{-6}$ mol/L

Ca= $\frac{1000M}{0.7\times KHa + 39.3} = 1.56\times10^{-7}$ mol/L

Equition 2 gives the air concentration under under 20 °C at 1 atmosphere pressure is Cair=0.0416 mol/L
Thus, the concentrations of these three volatile chemicals in the unit of ppm are written as:

Indole: $\frac{Ci}{Cair}\times10^{6} = 0.029\,\text{ppm}$ **Equation 3**

Methyl mercaptan: $\frac{Cm}{Cair}\times10^{6} = 164.346\,\text{ppm}$ **Equation 4**

Ammonia: $\frac{Ca}{Cair}\times10^{6} = 3.749\,\text{ppm}$ **Equation 5**

Supplementary References:

(1) Metzler, C.; Viswanath, R.; Metzler, D. *Journal of Biological Chemistry* **1991**, *266*, 9374.

(2) Scott, T. *Biochemical Journal* **1961**, *80*, 462.

(3) Greenman, J.; Duffield, J.; Spencer, P.; Rosenberg, M.; Corry, D.; Saad, S.; Lenton, P.; Majerus, G.; Nachnani, S.; El-Maaytah, M. *Journal of dental research* **2004**, *83*, 81.

Table S 1 – Cysteine Standards for Standard Curve

Standard	Volume Reaction Buffer (mL)	Amount of Cysteine (MW 121.16)	Final Concentration (mM)
A	100	18.174 mg	1.5
B	5	25 mL A	1.25
C	10	20 mL A	1.0
D	15	15 mL A	0.75
E	20	10mL A	0.5
F	25	5 mL A	0.25
G	30	0 mL	0.0 Blank

Table S2. Biotinylation of TPase

Experimental Condition	TPase 4mg/mL	L-tryptophan	SNB µg	Biotin/Enzyme	Indole* µg/mL
I (conjugation in the presence of L-tryptophan)	0.5 mL	10 mM	200	4.264±0.198	8.281±1.112
II (conjugation in the absence of L-tryptophan)	0.5 mL	0	200	3.443±0.243	1.021±0.013
III Non-conjugated TPase	0.5 mL	0	0	0	13.602±0.962

* Indole was generated by 50 µg BTPase under room temperature for 1 hour and quantified using the colorimetric method described before.

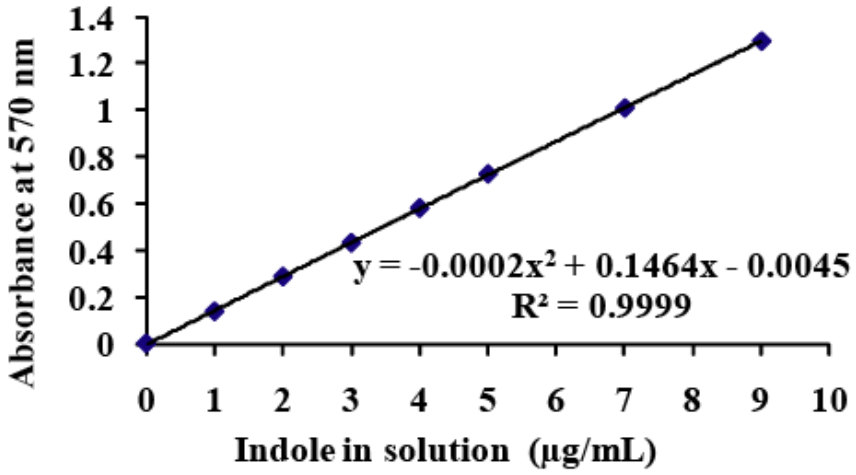

Figure S1. Standard curve for indole concentration: absorbance at 570 nm as a function of the indole concentration in standard samples**.**

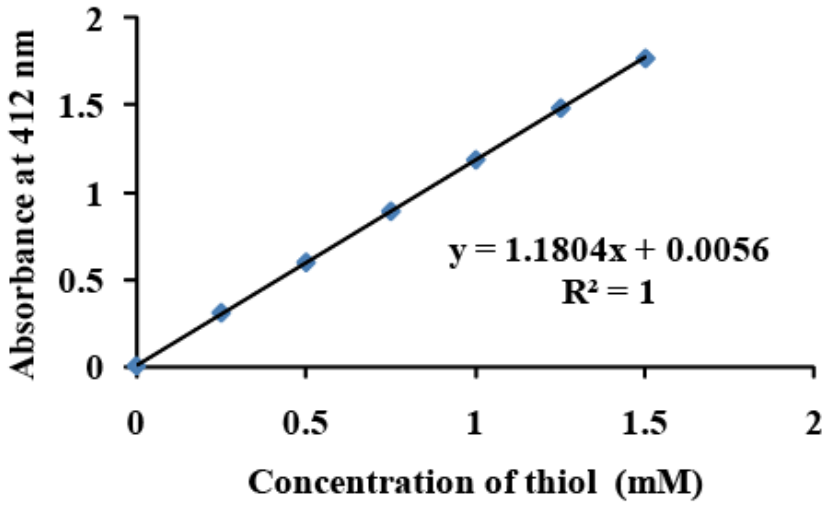

Figure S2. Standard curve for thiol concentration: absorbance at 412 nm as a function of the thiol concentration in standard samples.

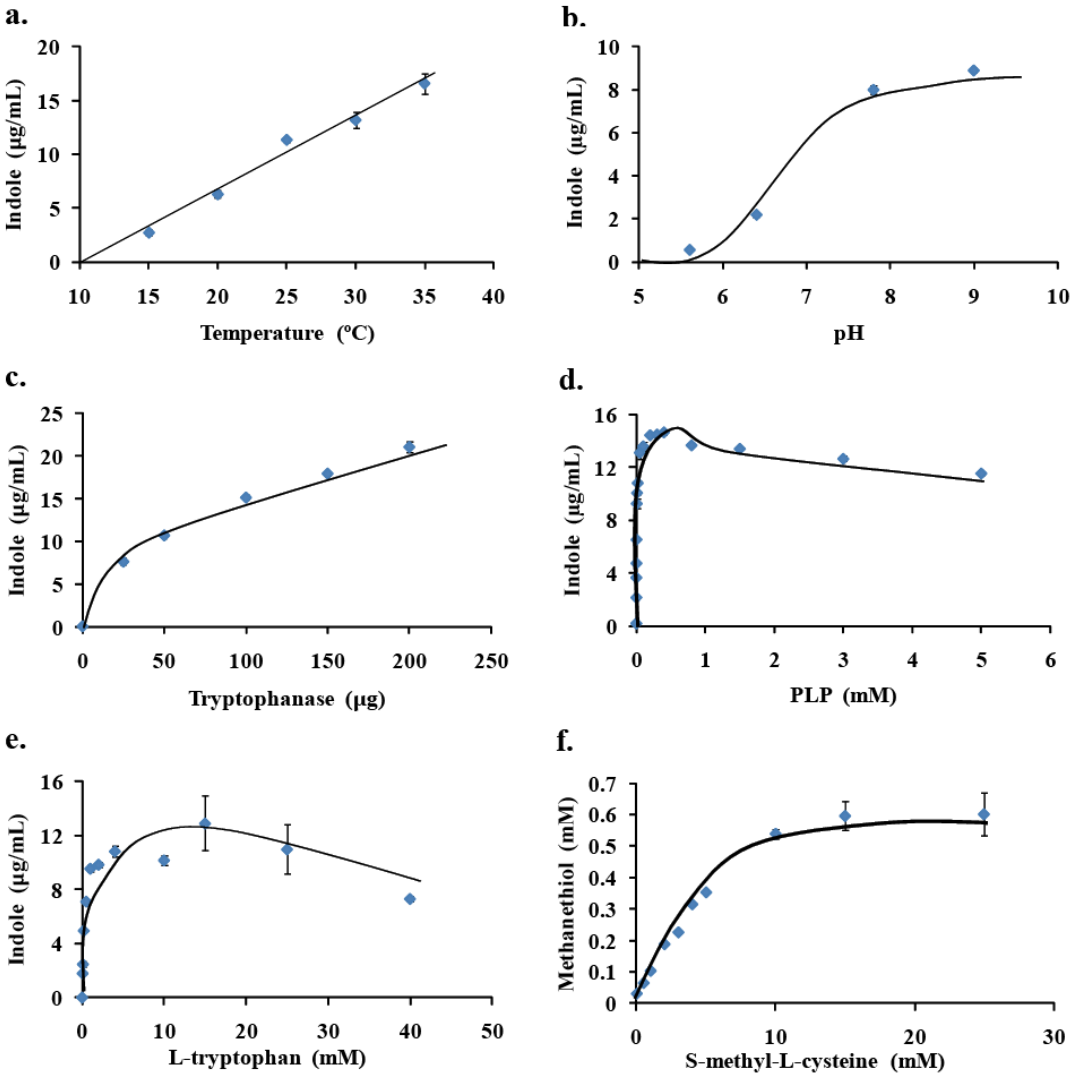

Figure S3. Optimization of conditions for TPase. a) Effect of Temperature on TPase activity; b) Effect of pH on indole production; c) Different amount of TPase result in different indole production; d) Effect of coffactor concentration on indole production; e) Effect of substrate L-tryptophan concentration on indole production; f) Effect of substrate S-methyl-L-cysteine on methyl mercaptan production. Each sample was prepared in 700 µL reaction mixture for 1hour with three replicates. Other than the changing condition, 50µg TPase, 15 mM L-tryptophan and 0.1 mM PLP, pH 7.8 and 20 ºC were used.

Figure S4. ToxiRAE Plus PID gas detector is connected to a 40 mL glass bottle where 700 µL of reaction mixture produces methyl mercaptan.

Chapter 3 A Generic Smell Generating Biosensor Using a Bienzyme System

All the bienzyme reaction and smell quantification experiments were conducted by me and Joanna Sauder who worked as a summer student. The DNA detection system was designed by M. Monsur Ali and Sergio D. Aguirre. After I wrote the draft, Dr. Filipe and Dr. Pelton revise it. Also, Dr. Filipe, Dr. Pelton and Dr. Li contributed many helpful suggestions on my experiments and paper writing.

((Catch Phrase))

DOI: 10.1002/anie.200((will be filled in by the editorial staff))

A Generic Smell-generating Biosensor Using a Bienzyme System

*Yaqin Xu, Joanna Sauder, M. Monsur Ali, Sergio D. Aguirre, Robert Pelton, Yingfu Li, Carlos D. M. Filipe**

Biosensor technology can provide specific real time or near real time detection of target analytes, such as bacteria, protein and small molecules. [1] Recently, user-friendly biosensing platforms producing signal outputs that can be assessed by the human senses, such as sight or smell, are of significant interest. Such technology is well suited for use in the field where analytical instrumentation is unavailable. For example, colorimetric biosensors for protein and ions have found widespread use due to their simplicity and convenience. [1c, 2] They commonly require minimal handling and provide a visual signal read by the naked eye. Although explored to a less extent, smell is another easy and convenient signaling method that can be used to engineer sensitive and easy-to-use biosensors. [3] There are only two patents that describe smell-generating biosensors for diagnosis[4] or underwater detection. [5] One is based on the use of whole cells to generate a smell of volatile organic compound [5], while the other one is based on the use of nanotubes filled with volatile organic compound, such as methyl mercaptan, and capped with aptamer which will interact with target analyte and uncap the nanotube in the presence of the target. [4] The smell-generating biosensor could provide a new approach for biosensing even for individuals that suffers from optical complications, such as color-blindness or trauma. Additionally, a smell-generating reporter can be used with an off-the-shelf electronic nose to quantify smell or even trigger an alarm signal if excessive smell is produced. An electronic nose provides the possibility for a smell-generating biosensor to have multi-signals. [6]

Our group recently reported that tryptophanase (TPase, EC 4.1.99.1) can be used as a smell-generating reporter. We observed that TPase could be modified and applied in biodetections to generate detectable smell in a reasonable time period of less than one hour. Herein, we take advantage of that observation by combining another enzyme pyridoxal kinase (PKase, EC 2.7.1.35) with TPase to form a robust bienzyme system as a detector for adenosine-5_-triphosphate (ATP). As the first enzymatic smell-generating detecting system, this detector is applied in detection of microorganism cells and target DNA through utilization of DNA aptamer, which is functionalized nucleic acid for the recognition of targets. [7]

TPase is a tetrameric protein that requires the cofactor pyridoxal phosphate (PLP) and cations to be biologically active. [8] It catalyzes a series of β-elimination reactions and β-replacement reactions to produce volatile chemicals, such as indole, methyl mercaptan and hydrogen sulphide, which can be detected by smell. [9] PKase catalyzes the phosphorylation of pyridoxal, one form of vitamin B6, into pyridoxal phosphate (PLP) by utilizing the phosphate on adenosine 5′-triphosphate (ATP).

The bienzyme system which combines TPase and PKase together is illustrated in Figure 1. We hypothesized that the presence of ATP would trigger the bienzyme system to produce an indole or methyl mercaptan smell signal through the following three-step mechanisms: 1) PKase catalyzes the phosphorylation of pyridoxal to PLP ; 2) PLP activates TPase 3) Activated TPase catalyzes the hydrolysis of L-tryptophan or S-methyl-L-cysteine to produce the smell of indole or methyl mercaptan.

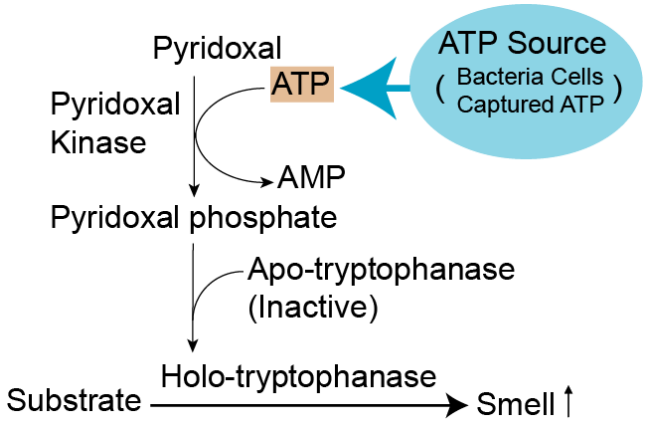

Figure 1. Pyridoxal kinase converts pyridoxal into PLP, which serves as a cofactor to activate tryptophanase to produce indole or methyl mercaptan .

First, we examined the smell generation of the bienzyme system by measuring the production of indole or methyl mercaptan as triggered by ATP. In the case of indole, we compared two samples containing all components with the L-tryptophan substrate in the absence or presence of ATP, under room temperature. At the time of 1 hour, ATP was added to one sample to a final concentration of 2 mM. The indole production in the solution was measured by

[*] Y. Xu, J. Sauder, Prof. R. Pelton, Prof. C. D. M. Filipe
Department of Chemical Engineering
McMaster University
Hamilton, Ontario, Canada, L8S 4L8
Fax: (+1) 9055285114
E-mail: filipec@mcmaster.ca

M. M. Ali, S. D. Aguirre, Prof. Y. Li
Department of Biochemistry and Biomedical Sciences
McMaster University
Hamilton, Ontario, Canada, L8S 4L8

[**] This work was supported by research grants from the Natural Sciences and Engineering Research Council of Canada (NSERC) through the network grant SENTINEL (Bioactive Paper Network). We thank professor Martin Safo at Virginia Commonwealth University for providing enzyme pyridoxal kinase. We also thank Dr. Weian Zhao for critical reading of the manuscript.

Supporting information for this article is available on the WWW under http://www.angewandte.org or from the author.

adding *p*-dimethylaminobenzaldehyde and measuring the absorbance at 570 nm using a UV-VIS spectrometer hourly. [10] Figure 2a shows the indole concentration in the headspace of these samples calculated by Henry's law and Ideal gas law (see Supporting Information for the calculation). More than 5 ppb indole was generated in one hour after adding ATP, whereas the control sample with the absence of ATP showed minimal signal. Similarly, samples prepared with the S-methyl-L-cysteine substrate demonstrated the same trend that more than 10 ppm of methyl mercaptan was produced within 30 mins (Figure 2b). These observations confirm that ATP activates the bienzyme system to produce smell within minutes of exposure to ATP.

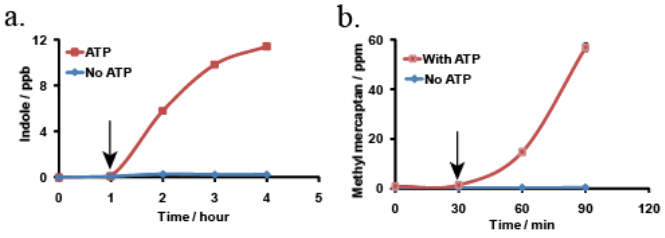

Figure 2. Detection of ATP by the bienzyme system. The detection solution contains: 50 µg PKase, 40 µg TPase, 0.1 mg/mL pyridoxal, 0.1 mM Mg^{2+}, and 15 mM L-tryptophan. Arrows indicates the time point where ATP was added. Each dot was produced in three replicates.

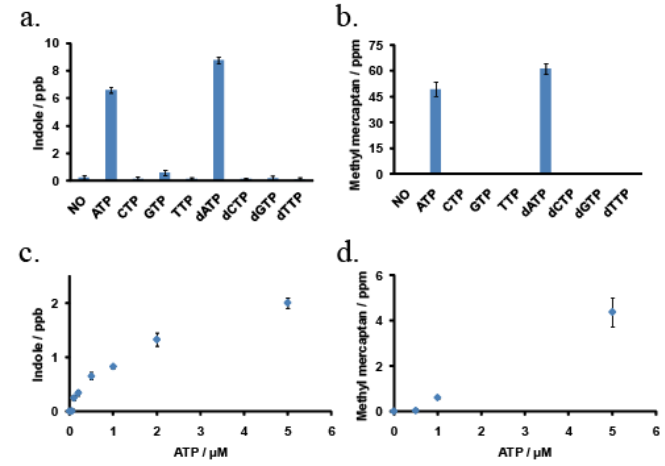

Figure 3. Specificity and sensitivity of the ATP detector by the bienzyme system. 0.2 mM NTP or dNTP.

To demonstrate the specificity of ATP detection for the bienzyme system, we compared the smell generation triggered by the addition of guanosine triphosphate (GTP), cytidine triphosphate (CTP), thymidine triphosphate (TTP), deoxyadenosine triphosphate (dATP), deoxyguanosine triphosphate (dGTP), deoxycytidine triphosphate (dCTP), and deoxythymidine triphosphate (dTTP). Figure 3 a shows that the addition of either ATP or dATP resulted in significant indole production, 6.6 ppb and 8.8 ppb respectively while other dNTPs and NTPs showed minimal signal. If change the substrate to S-methyl-L-cysteine, ATP and dATP triggered 49.1 ppm and 61.4 ppm methyl mercaptan production while other dNTPs and NTPs didn't activate smell production (Figure 3 b).

In order to determine the sensitivity of this bienzyme system for ATP, the optimized reaction conditions were obtained first for a bienzyme system of 700 µL containing 40 µg tryptophanase and 50 µg pyridoxal kinase: 15 mM of L-tryptophan or S-methyl-L-cysteine, 1mM zinc or 0.6mM magnesium, 0.1 to 5 mg/mL pyridoxal, pH 7.8 and room temperature of 20 °C as shown in Supporting Information online. ATP was titrated to the bienzyme mixtures to a concentration ranging from 0.01 µM to 8 mM and indole or methyl mercaptan generated in the headspace of a 40 mL bottle was measured after one hour. As expected, indole production was positively correlated to ATP concentrations, as shown in Figure 3. For instance, 0.1 µM ATP triggered 0.25 ppb indole production in one hour (Figure 3c). The detection limit for ATP through indole production is 0.1 µM ATP. According to International Union of Pure and Applied Chemistry (IUPAC), the detection limit is defined as the minimum single result that can be distinguished from a suitable blank value. [11] Samples prepared with the S-methy-L-cysteine substrate showed that 1 µM ATP triggered 0.6 ppm methyl mercaptan production (Figure 3d). Thus the detection limit for ATP through methyl mercaptan production is 1 µM.

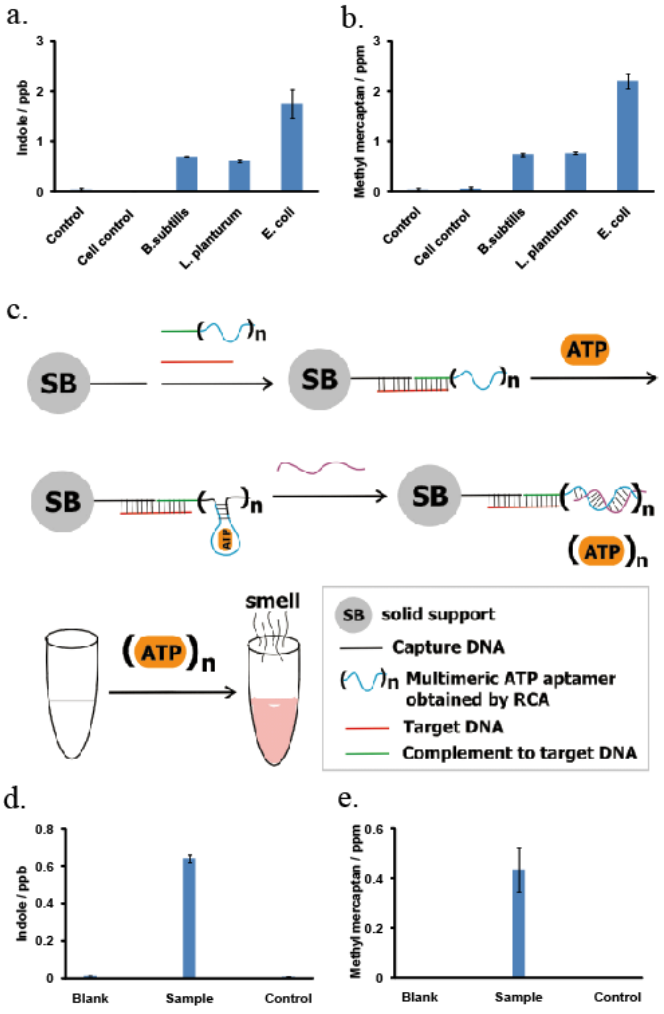

Figure 4. Detection of bacteria cells and target DNA by using the bienzyme system and producing smell signal.

Since ATP is a vital component of biological organisms, it was expected that our smell-generating biosensor for ATP could be used for the detection of bacteria, *Escherichia coli*, *Bacilus subtilis* and *Lactobacilus planturum*, which were used as model organisms. These three bacteria were cultured in growth media to a

concentration of OD_{600}≈1, washed with sodium phosphate buffer (PBS, pH 7.4, 50 mM) to remove any indole generated during cell growth and resuspended in PBS buffer to the original volume.

Controls include PBS only and the mixture of cell and PBS did not show detectable smell, while cell samples showed strong indole and methyl mercaptan production as shown in Figure 4 a & b (For the detailed procedure, see Supporting Information online). This is due to the existence of intracellular and extracellular ATP in bacteria cells culture. The *E. coli* sample showed much stronger smell production, compare with the other two types of cells. This may because that *E.coli* cells contain higher amount of tryptophanase since tryptophanase is often purified from *E.coli*. [12] Generally, this bienzyme system is expected to detect all kinds of bacteria cells.

To extend the application of this ATP-triggered smell-generating system to DNA detection, a DNA aptamer-based capturing system was designed as shown in Figure 4 c. Capture DNA was first immobilized on a solid supporting beads. Then one part of the multimeric ATP aptamer which was prepared by rolling circle amplification (RCA) [13] and one part of the capture DNA were designed to be complementary to the target DNA. If target DNA presents, it would be captured and then ATP was added and retained in the multimeric aptamer "pockets". At last, after washing and adding complementary DNA the ATP would be replaced from the RCA and released into the solution. The collected solution is added to bienzyme mixture to trigger smell generation. After one hour, the indole and methyl mercaptan generated were quantified as shown in Figure 4 d & e. Control sample was prepared by adding PBS buffer instead of target DNA and each sample had triplicates. The sample showed around 0.3 ppb indole or 0.3 ppm methyl mercaptan smell signal, while the control sample showed minimal signal. It is illustrated that the combination of bienzyme system with the DNA detection system successfully detected the target DNA and released detectable smell signal.

In summary, we demonstrated an enzymatic smell-generating biosensor for detection of ATP, microorganism cells and DNA. The bienzyme system is capable of producing smell of indole or methyl mercaptan upon the presence of targets. The sensitivity for detecting ATP was determined to be 0.1 μM ATP through producing indole and 1 μM ATP through producing methyl mercaptan. Both gram-positive cell (*E. coli*) and gram-negative cells (*Bacilus subtills* and *Lactobacilus planturum*), trigered bienzyme system to produce smell. Moreover, the DNA detection system designed by using DNA aptamer showed capability of catching target DNA and releasing ATP to trigger the production of smell signal.

This work serves as the first step toward understanding the nature of the bienzyme system on smell production. The discoveries in this exploration could directly lead to a number of applications in biodetections. Theoretically, any target or biological event that releases ATP or dATP could be combined with this bienzyme system to construct a smell-generating biosensor. In some occasions that people are not capable to smell, the smell signal of indole could be easily turned into a reddish color signal by adding *p*-dimethylaminobenzaldehyde. [10] Moreover, smell signal could be sensed by human nose, or detected by electronic nose which usually has the function of giving alarm on excessive odor. Hence, this smell-generating biosensor could easily provide multi-signals, including smell signal, acoustic signal and colorimetric signal. As the first enzymatic smell-generating system, it is expected to have high potential in the following research on constructing smell-generating mouth mask upon detection of virus.

Experimental Section

Solvents and reagents were purchased from Sigma-Aldrich Co. and Pierce Chemical Co. All chemicals were of reagent grade. The bienzyme reaction took place in 0.2M potassium phosphate buffer (PPB, pH 7.8), containing 6.7 mM ammonium sulphate.

Measurement of indole concentration in solution was made as described earlier by adding p-dimethylaminobenzaldehyde and measuring the absorbance at 570 nm. [10] Then the concentration of indole in the headspace of the 40 mL glass bottle is calculated by using Henry's law and Ideal gas law. Methyl mercaptan in the headspace was measured directly by using ToxiRAE PID gas detector. (See supporting Information for details)

Experiments showed that the commercial apotryptophanase had not been adequately purified as it was found to still be associated with its cofactor PLP (data not shown here). It has been reported that cooling under 4 ºC for 20hour lead to the cleavage of PLP from Tpase [14], and following this with dialysis in L-alanine[15], EDTA[16] or L-cysteine[16] could purify Tpase and eliminate PLP. TPase (5mg/mL in KDP buffer) was stored at 4ºC for approximately 20 hour prior to dialysis. The samples were then exposed to dialysis buffer containing 0.5 mM L-cysteine and β-mercaptoethanol in 10 mM PBS buffer for 4hour on ice. The dialysis buffer was then changed and replaced with PPB buffer and allowed to sit on ice for 3hour. The PPB dialysis buffer was then changed again and the dialysis tube and buffer were put in fridge (4ºC) overnight. The samples were then removed from the dialysis tubing and transferred into glass vials.

Pyridoxal kinase was purified by the following methods, taken from the literature. [17] The *E. coli* cells transformed with a pET22b vector carrying the human pdxK gene (pET22-hPLK) were grown in 200mL of Luria Birtani (LB) solution and after reaching an O.D. at 600nm of 1.2 were induced with 0.5 mM IPTG. Cells were grown for an additional 7 h at 30 °C and harvested by centrifugation (1000g, 20min). The cell pellets were washed once by 20mL potassium phosphate buffer (pH 7.2) and resuspended in 20mL of this buffer. Lysozyme was added to a concentration of 1 mg/mL. The solution was stored in the fridge under 4 °C for an hour. Before sonication, the cells were incubated on ice for 10 min, then cells were ruptured by a Virtis for 20 min at 17 amplitude. The remaining pellets and cell debris were isolated by centrifugation at 12,000g, 20min, 4 °C. The supernatant was processed with Hispur purification kit purchased from Pierce to purify the His tagged pyridoxal kinase. The concentration of purified PKase was monitored by Bradford method.

Optimization of conditions for bienzyme system of TPase and PKase is shown in the Supporting information. All the bienzyme reactions were carried out under optimized conditions.

The strategy used to apply the bienzyme smell generation system to DNA detection is shown in Figure 4 c. Capture DNA was first biotinylated and immobilized on beads and the multimeric ATP aptamer obtained by rolling circular amplification (RCA) was prepared following the published method[13]. One end of capture DNA and one end of RCA product were designed to be complementary with a portion of the target DNA. In the presence of the target DNA, the capture DNA and RCA would be bound together, effectively attaching the RCA product to the beads. After washing and adding , the RCA would bind and capture ATP from solution. Then the assembly was washed with buffer twice and the complementary RCA DNA was added to the system to displace and release ATP into solution. The ATP solution collected can then be used to trigger the bienzyme system to produce a smell signal. The DNA sequence for capturing DNA, target DNA, ATP aptamer and complement DNA are shown in the Supporting information.

Received: ((will be filled in by the editorial staff))
Published online on ((will be filled in by the editorial staff))

Keywords: keyword 1 · keyword 2 · keyword 3 · keyword 4 · keyword 5

[1] a)M. Velasco-Garcia, T. Mottram, Biosystems engineering 2003, 84, 1; b)R. Hall, Microbes and Infection 2002, 4, 425; c)J. Liu, Y. Lu, J. Am. Chem. Soc 2003, 125, 6642.
[2] L. J. Ou, P. Y. Jin, X. Chu, J. H. Jiang, R. Q. Yu, Analytical Chemistry 2010, 2306.
[3] G. W. Meyer, D. P. Greenberg, Computer Graphics and Applications, IEEE 1988, 8, 28.
[4] R. Melker, D. Dennis, Vol. U.S. Patent 6,974,706 B1, University of Florida Research Foundation, Inc., Gainesville, FL (US), 2005.
[5] S. Nicklin, M. Cooper, N. D'souza, WO Patent WO/2007/083,137, 2007.
[6] H. V. Shurmer, J. W. Gardner, Sensors and Actuators B: Chemical 1992, 8, 1.
[7] M. M. Ali, Y. Li, Angewandte Chemie 2009, 121, 3564.
[8] a)C. Suelter, E. Snell, Journal of Biological Chemistry 1977, 252, 1852; b)F. Happold, A. Struyvenberg, Biochemical Journal 1954, 58, 379.
[9] W. Newton, Y. Morino, E. Snell, Journal of Biological Chemistry 1965, 240, 1211.
[10] a)T. Scott, Biochemical Journal 1961, 80, 462; b)E. McEvoy-Bowe, The Analyst 1963, 88, 893; c)A. Shimada, H. Shishido, I. Nakamura, Amino Acids 1996, 11, 83.
[11] G. L. Long, J. Winefordner, Analytical Chemistry 1983, 55, 712.
[12] a)E. E. Snell, 1975; b)B. De Crombrugghe, R. L. Perlman, H. Varmus, I. Pastan, Journal of Biological Chemistry 1969, 244, 5828.
[13] W. Zhao, M. M. Ali, M. A. Brook, Y. Li, Angewandte Chemie International Edition 2008, 47, 6330.
[14] T. Erez, G. Gdalevsky, C. Hariharan, D. Pines, E. Pines, R. Phillips, R. Cohen-Luria, A. Parola, Biochimica et Biophysica Acta (BBA)-Protein Structure and Molecular Enzymology 2002, 1594, 335.
[15] C. Metzler, R. Viswanath, D. Metzler, Journal of Biological Chemistry 1991, 266, 9374.
[16] S. Hoch, R. DeMoss, Journal of Biological Chemistry 1972, 247, 1750.
[17] M. di Salvo, S. Hunt, V. Schirch, Protein expression and purification 2004, 36, 30

Supporting information

A Generic Smell-generating Biosensor Using a Bienzyme System

*Yaqin Xu, Joanna Sauder, M. Monsur Ali, Sergio D. Aguirre, Robert Pelton, Yingfu Li, Carlos D. M. Filipe**

Experimental Methods and Results

Measurement of indole concentration in solution. Briefly, p-dimethylaminobenzaldehyde was added to indole solutions and the absorbance of reddish solutions was measured at 570 nm to determine indole concentrations. [1] 700 µL indole standard solutions containing 0 to 9 µg/mL indole were prepared, and a volume of water saturated n-butanol equal to the sample volume (700 µL) was vigorously mixed with the sample. The mixture was then centrifuged at 1,000g for 1min, and 500 µL of the upper level supernatant was taken to mix with an equal volume of Kovac's reagent containing p-dimethylaminobenzaldehyde purchased from Sigma. Five minutes later, the absorbance of the solutions was measured at 570 nm and a standard curve of absorbance vs. indole concentrations can be generated. To measure samples, 700 µL reaction mixture was measured by following the same procedure.

Calculation of indole concentration in the headspace. For an indole solution of X µg/mL, if assume that Henry's law and Ideal gas law are obeyed and indole has a Henry's law constant of 4.08×10^5, Indole in the head space of a 40 mL glass bottle is calculated to be 0.503X ppb (part per billion) as shown in the calculation shown at last of this session. [2]

The concentration of indole in the gas phase directly relates to the intensity of the smell. The odor threshold of indole for human nose is 0.02 ppb.

Measurement of methyl mercaptan in the headspace. ToxiRAE PID gas detector measures the volatile organic chemicals in the gas phase. It is calibrated firstly by using 20 ppm methyl mercaptan in nitrogen then it is connected to a glass bottle of 40 mL where smell generation was happening. Wait for 15 seconds to get a stable reading.

Optimization of Reaction Conditions. To determine the bienzyme system's detection limit for ATP, the effects of zinc or magnesium and pyridoxal concentration on the bienzyme response were first investigated. A zinc concentration of 1mM or a concentration of 0.6mM magnesium achieved the most efficient indole production as shown in Figure S1. Magnesium was able to achieve higher production of indole compared to zinc. This is consistent with previous study that with concentrations more than 40 μM ZnATP became inhibitory and MgATP was the preferred substrate. [3] Figure S2 shows that pyridoxal in the concentration range of 0.1 to 5 mg/mL obtained highest concentration of indole production, but if pyridoxal is more than 5 mg/mL, there was obvious inhibitory effect on indole production.

DNA Detection by Utilizing DNA Aptamer. The DNA sequence for capture DNA, target DNA, ATP aptamer and complementary DNA sequences are showed below. The process for doing rolling circle RCA and related DNA sequences followed published method. [4]

Capture DNA sequence: BT-TTTTTTTTTTTTTTTTTTTTGGCCACAGTGGTACG

Target DNA sequence: TCGTGGTGGCCTCGCGTACCACTGTGGCCA

Primer part of RCA: CGAGGCCACCACGATTTTTTTTTTGGAGTATTGCGGAGGAAGG

Complementary DNA sequence for ATP aptamer:
ACCTTCCTCCGCAATACTCCCCCAG

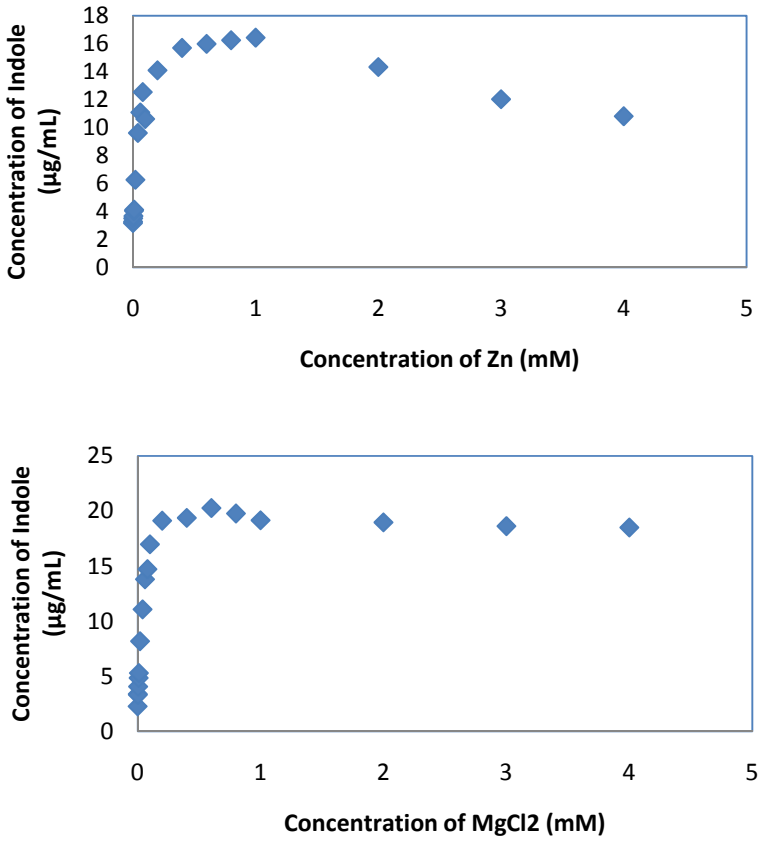

Figure S 1 Effects of Zinc and Magnesium concentration on indole production in bienzyme system containing 50 µg Pkase, 40 µg Tpase, 5 mg/mL pyridoxal, 15 mM L-tryptophan and 2 mM ATP.

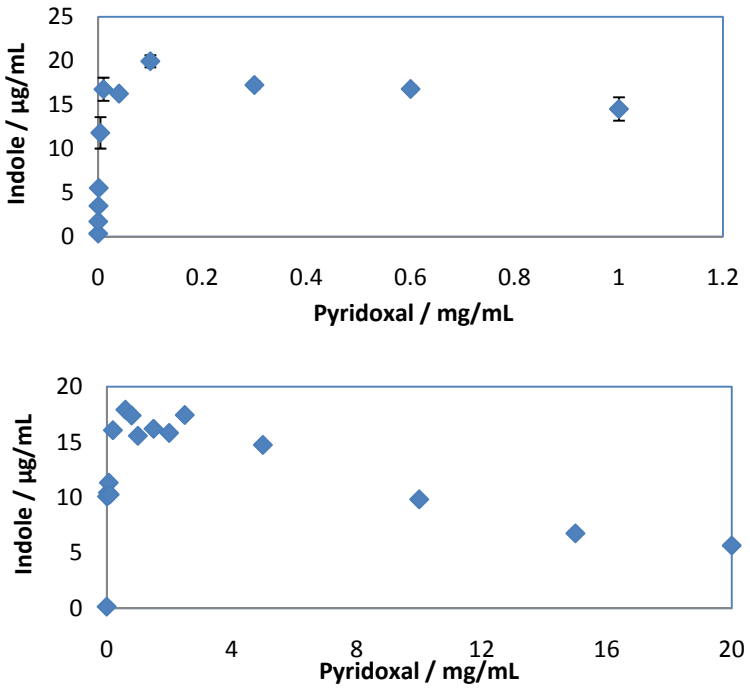

Figure S 2 Effect of pyridoxal on indole production in bienzyme system containing 50 μg Pkase, 40 μg Tpase, 0.6 mM Mg^{2+}, 15 mM L-tryptophan and 2 mM ATP. Each sample was prepared with three replicates.

Calculation:

The dimensionless form of Henry's Law constant is defined as the chemical's molar concentration in aqua c_{aq} divided by molar concentration in gas $c_{gas,}$ as shown below:

$$k_{Hcc} := \frac{c_{aq}}{c_{gas}}$$

Henry's law constant for indole (for 20°C at 1 atmosphere pressure) were reported to be 4.08 x 10^5

$$k_{Hcci} := 4.08 \cdot 100000 = 4.08 \times 10^5$$

Indole has a molecular weight M_i:

$$M_i := 117.15 \frac{gm}{mol}$$

In a 40 mL bottle filled with 0.7 mL reaction mixture

$$V_L := 0.7mL$$

$$V_G := 40mL - V_L = 0.039\ L$$

By using colorimetric method, indole concentration in liquid could be quantified. If the measurement shows that indole concentration is X μg/mL, the mole concentration of indole in liquid C_{aqi} could be calculated.

If assume that X is 1 μg/mL

$$X := 1 \cdot 10^{-3} \frac{gm}{L}$$

$$C_{aqi} := \frac{X}{M_i}$$

According to Henry's law, the mole concentration of indole in gas phase C_{gasi} is calculated to be

$$C_{gasi} := \frac{C_{aqi}}{k_{Hcci}} = 2.092 \times 10^{-8} \frac{mol}{m^3}$$

$$C_{aqi} = 8.536 \times 10^{-3} \frac{mol}{m^3}$$

If assume that all the molecules in gas phase obey Ideal Gas Law, the mole concentration of air is calculated below:

$$P := 1.01325 \cdot 10^5 Pa$$

$$T_{air} := 20\,°C$$

$$C_{air} := \frac{P}{8.314 \frac{J}{K \cdot mol} \cdot T_{air}} = 41.574 \frac{mol}{m^3}$$

Thus indole concentration in the gas phase could be converted to the value in the unit of ppb:

$$ppb := 10^{-9}$$

$$C_{ppbi} := \frac{C_{gasi}}{C_{air}} = 0.503 \cdot ppb$$

Comparing quantity of product in gas phase to liquid phase

$$V_L \cdot C_{aqi} = 5.975 \times 10^{-9} mol \qquad V_G \cdot C_{gasi} = 8.222 \times 10^{-13} mol$$

References:

[1] T. Scott, *Biochemical Journal* **1961**, *80*, 462.

[2] J. Greenman, J. Duffield, P. Spencer, M. Rosenberg, D. Corry, S. Saad, P. Lenton, G. Majerus, S. Nachnani, M. El-Maaytah, *Journal of dental research* **2004**, *83*, 81.

[3] M. di Salvo, S. Hunt, V. Schirch, *Protein expression and purification* **2004**, *36*, 300.

[4] M. Ali, S. Aguirre, Y. Xu, C. Filipe, R. Pelton, Y. Li, *Chemical communications (Cambridge, England)* **2009**, 6640.

Chapter 4 Controlling Biotinylation of Microgels and Modeling Streptavidin Uptake

The experiments involved in Chapter 4 were mainly completed by myself, including the biotinylation of microgels, characterization of microgels and streptavidin uploading. Lizanne Pharand worked as a summer student to carry out some of the experiments. Quan Wen helped prepare some of the PNIPAM-VAA microgels. Ferdinand Gonzaga, Dr. Li and Monsur Ali contributed helpful suggestions on biotinylation. I wrote the first draft and Dr. Pelton helped write the modeling of streptavidin uptake. Dr. Pelton and Dr. Filipe revised the paper draft and contributed many helpful suggestions on the experiments.

Colloid Polym Sci
DOI 10.1007/s00396-010-2305-8

ORIGINAL CONTRIBUTION

Controlling biotinylation of microgels and modeling streptavidin uptake

Yaqin Xu · Lizanne Pharand · Quan Wen · Ferdinand Gonzaga · Yingfu Li · M. Monsur Ali · Carlos D. M. Filipe · Robert Pelton

Received: 8 August 2010 / Revised: 20 September 2010 / Accepted: 20 September 2010

Abstract Compared are two approaches for the biotinylation of poly(*N*-isopropylacrylamide-*co*-vinylacetic acid) microgels, 300-nm diameter, water swollen particles with a corona of carboxyl groups. The biotinylated microgels are a platform for bioactive water-based ink. Streptavidin binding was measured as a function of biotin density, and the results were interpreted with a new model that predicts the minimum local density of biotins required to capture a streptavidin. An amino-polyethylene glycol derivative of biotin gave higher biotin contents than a biotin hydrazide. However, the streptavidin content versus biotin content results for both biotin derivatives fell on the same master curve with maximum biotin coverage of 0.11 mg of bound streptavidin per milligram of biotinylated microgel. Exclusion experiments showed that streptavidin was too big to penetrate the cross-linked microgel structure; thus, the conjugated streptavidin was restricted to the microgel surface. The colloidal stability of the microgels was preserved, and the biotinylated products showed good hydrolytic stability.

Keywords Microgel · Biotinylation · Bioconjugation · Modeling

Y. Xu · L. Pharand · Q. Wen · C. D. M. Filipe · R. Pelton (✉)
Department of Chemical Engineering, McMaster University,
Hamilton, ON, Canada L8S 4L7
e-mail: peltonrh@mcmaster.ca

F. Gonzaga · Y. Li · M. M. Ali
Department of Biochemistry and Biomedical Sciences, McMaster University,
Hamilton, ON, Canada L8S 4L7

Introduction

Since the pioneering work of Kawaguchi [1] and Pichot [2], poly(*N*-isopropylacrylamide) (PNIPAM) microgel (MG) particles [3, 4] and plastic core–PNIPAM shell nanoparticles [5] have found extensive use as support particles for drug release and biodetection [6–9]. Two key properties account for the interest in PNIPAM microgels. First, like polystyrene and some other types of support particles, PNIPAM microgels can be easily prepared as monodisperse (in diameter) suspensions that can be freeze-dried and readily redispersed in buffer. Second, PNIPAM, much like polyethylene glycol (PEG), is a benign polymer exhibiting limited nonspecific interactions with proteins and nucleic acid chains.

Most microgel applications require bioconjugation. Poly (*N*-isopropylacrylamide) is rather inert, requiring a secondary monomer suitable for bioconjugation. Carboxyl comonomers are the most commonly reported. However, aminated [10] and hydroxyl-containing microgels [11] have also been used for bioconjugation. More sophisticated approaches, such as biotinylated polymerization initiators [12] and photochemical modification [13], have also been reported.

In an effort to prepare microgel-based bioactive inks [14] for paper-supported pathogen detection [15], we have prepared biotinylated PNIPAM microgels. We chose carboxylated microgels because we can control the distribution of carboxyl groups by selecting the carboxyl monomer with appropriate reactivity ratios [16, 17]. This paper summarizes a detailed investigation of microgel biotinylation and its impact on streptavidin (SP) binding. In addition to presenting robust approaches to biotinylation, we describe a simple model that gives some physical insight into the conditions leading to streptavidin binding.

There have been other reports of microgel biotinylation. Debord and Lyon discussed the extremely high hydrolytic

Published online: 02 November 2010

stability of *N*-hydroxysulfosuccinimide (sulfo-NHS)-activated PNIPAM-*co*-acrylic acid microgels [18]. The activated microgels were nearly double the size of the parent microgels and displayed none of the temperature sensitivity expected with NIPAM copolymers. They showed that 50 °C treatment with ethanol and NaOH was required to have a complete hydrolysis. They concluded that the sulfo-NHS esters were too stable for useful bioconjugation. This work was of some concern since we employed sulfo-NHS in our work.

In our work we coupled biotin hydrazide and an amino-PEG biotin derivative to sulfo-NHS-activated carboxylated PNIPAM microgels—see the reaction scheme in Fig. 1. Biotin hydrazide is normally employed for coupling to aldehydes or ketones [19]. However, there are reports of hydrazide coupling to activated carboxyls [20–22]. Nayak and Lyon's work is the first we have found that employed biotin hydrazide for coupling to carboxylated microgels [23]. The results presented herein are the first quantitative comparison of amine versus hydrazide conjugation strategies for microgels. In addition, a new model is presented that gives insight into the factors influencing the streptavidin binding density as a function of the surface density of biotin sites.

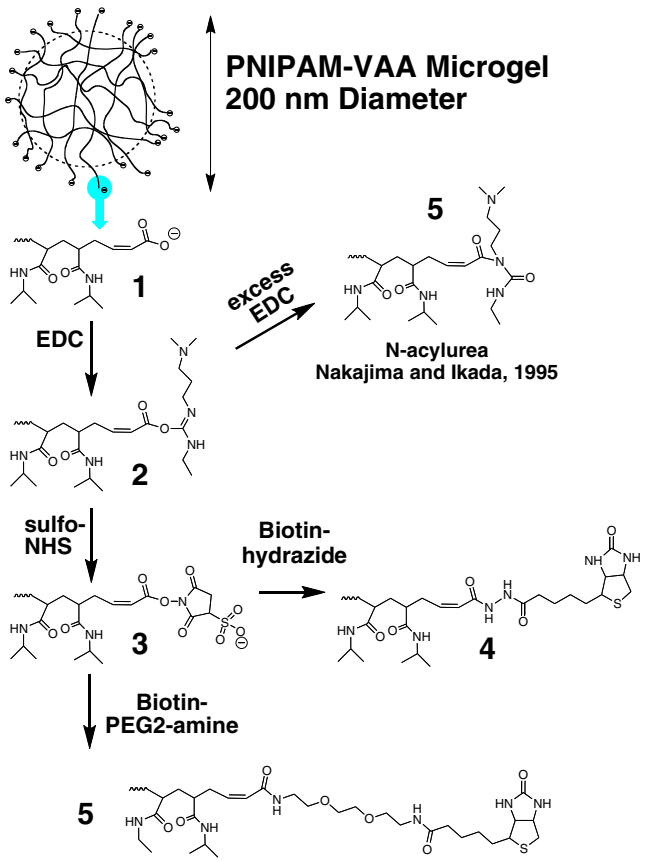

Fig. 1 Biotinylation of carboxylated microgel

Experimental procedures

Chemicals *N*-Isopropylacrylamide (NIPAM; 99%, Acros Organics) was purified by crystallization from a 60:40 toluene/hexane mixture. *N*,*N*-Methylenebisacrylamide, vinylacetic acid (97%), sodium dodecyl sulfate, 2-(*N*-morpholino)ethanesulfonic acid (MES), and ammonium persulfate (99%) were from Aldrich. *N*-(3-Dimethylaminopropyl)-*N*′-ethylcarbodiimide hydrochloride (EDC), biotin, SP, Atto 610-Streptavidin (Atto-SP), potassium periodate, ammonium molybdate, potassium iodate, potassium iodide, sodium chloroacetate, *p*-dimethylaminocinnamaldehyde, and Avidin/HABA reagent were from Sigma. Biotin hydrazide, biotin–PEG2–amine, and sulfo-NHS were from Pierce. The water used in this work was Millipore Milli-Q grade.

Microgel preparation and characterization PNIPAM-VAA microgel was prepared by the Hoare's method [24]. The polymerization was conducted in a 500-mL three-necked flask fitted with a condenser and a glass stirring rod. The reaction mixture consisted of 12.4 mmol NIPAM (1.403 g), 0.65 mmol MBA (0.100 g), 0.17 mmol sodium dodecyl sulfate (0.049 g), and 1.2 mmol vinyl acetic acid (0.10 g) in 150 mL water. After heating to 70 °C under a nitrogen blanket, 0.52 mmol (0.100 g) of ammonium persulfate initiator, dissolved in 10 mL water, was added. The mixture was stirred overnight at 250 rpm with a glass/Teflon paddle stirrer. After cooling to room temperature, the microgel dispersion was washed by several cycles of ultracentrifugation (Beckman model Optima L-80 XP, 50 min at 50,000 rpm) and redispersion in water. The microgel was considered to be clean when the supernatant conductivity was less than 5 μS/cm. Microgels were lyophilized and stored at room temperature.

The carboxyl content (from vinylacetic acid) of the microgel was determined by potentiometric titration using a Burivar-I2 automatic buret (ManTech Associates). Lyophilized microgel was suspended (1 mg/mL) in a 1 mM KCl solution. The pH was manually lowered to 3.0, and the sample was titrated with 0.1 M NaOH. A wait time of 300 s between injections was used to ensure complete ionic equilibration

Dynamic light scattering was used to measure the hydrodynamic diameter of the microgel. Measurements were made with a detection angle of 90° using a Brookhaven instrument fitted with a Melles Griot HeNe 632.8-nm laser and a BI-APD solid state detector. Microgels were dispersed in 1 mM KCl, and the pH was controlled. The scattering intensity was adjusted from 100 to 250 kcps, and the results were analyzed with the cumulant model using Brookhaven Software 9kdlsw32 ver. 3.34.

The electrophoretic mobilities of the microgel suspensions were measured using a ZetaPlus analyzer (Brookhaven Instruments Corp.), which was operating in phase analysis light scattering mode. Samples were dispersed in 1 mM KCl, and the pH was adjusted with NaOH or HCl. A total of ten runs (15 cycles each) were carried out for each sample.

Microgel biotinylation Table 1 summarizes the conditions used to biotinylate the microgel. The biotinylated microgel (BMG) series was prepared with biotin hydrazide, whereas the BaMG series was prepared with biotin–PEG–amine (see structures in Fig. 1). The preparation of BMG8 is described as an example. To 150 mg of MG in 150 mL water was added a 156-mg biotin hydrazide in 10 mL DMSO at room temperature. After 5 min, EDC and sulfo-NHS were added, and the pH was adjusted to 7.4 with NaOH (0.01 mol/L). The mixture was stirred for 10 h with pH adjusted to ~7.4 by HCl (0.01 mol/L) every 30 min. By the end of the reaction period, the pH did not drift. The microgel product, BMG8, was purified by several cycles of ultracentrifugation (50,000 rpm, 50 min), decantation, and redispersion in water. BMG1 to BMG7 were prepared on a smaller scale and included two to four replicates—see Table 1. BaMG1 and BaMG2 were also prepared on a smaller scale by adding amine–PEG2–biotin instead of biotin hydrazide.

Three methods were used to estimate the biotin content of the microgels. *Method 1* was adapted from the work of McCormick and Roth, which describes the formation of a colored adduct between biotin and *p*-dimethylaminocinnamaldehyde under anhydrous conditions [25]. Two stock solutions were prepared: A was 0.2% *p*-dimethylaminocinnamaldehyde in absolute ethanol, and B was 2% (*v*/*v*) of sulfuric acid in absolute ethanol. In preparing a calibration curve, it was necessary to account for the slight light scattering of the microgels. Ten to 100 μg of biotin and 1 mg of microgel were dissolved in 1 mL of solution B. Then 1 mL of solution A was added, and the solution was diluted with 8 mL of absolute ethanol. After an hour at room temperature, the absorbance of the reddish-orange color solution was measured at 533 nm with a UV–VIS spectrophotometer (Beckman Coulter, DU800). The reagent blank was prepared by dissolving 1 mg of microgel in 1 mL of solution B and by mixing with 1 mL of solution A and 8 mL of absolute ethanol.

For analysis of the BMG, 1 mg of dried BMG was dissolved in 1 mL of solution B, mixed with 1 mL of solution A, and diluted with 8 mL of absolute ethanol. The reagent blank was 1 mg of MG dissolved in 1 mL of solution B, mixed with 1 mL of solution A, and diluted with 8 mL of absolute ethanol.

Method 2 was adapted from the work of Ahmed and Verma [26]. In this method potassium periodate selectively oxidizes the sulfide in biotin to a sulfoxide plus iodate ion. The iodate product was converted to iodine, which was determined by titration. The following stock solutions were prepared: 80 μg/mL biotin solution, 0.01 mol/L potassium periodate solution, 3% ammonium molybdate solution, 0.1 mmol/L potassium iodate solution, 0.5 mol/L potassium iodide solution, and 0.5 mol/L sodium chloroacetate solution at pH 3 as buffer. A calibration curve was generated as follows. Into 50 mL standard flasks, 0.2, 0.4, 0.6, 0.8, and 1.0 mL of biotin solutions were mixed with 2 mL of periodate solution. The neck of the flask was washed with water to bring the volume to 5 mL. Then the mixture was shaken and left at room temperature for 20 min. Ten milliliter of molybdate solution, 5 mL of buffer solution, and 10 mL of iodide solution were added and mixed by shaking. Again the mixture was left for

Table 1 Summary of conditions for microgel biotinylation

Name	Biotin hydrazide in 3 mL DMSO (mg)	PNIPAM-VAA (mg; 1 mg/mL H_2O)	EDC (mg; 1 mg/mL H_2O)	Sulfo-NHS (mg; 1 mg/mL H_2O)	Biotin content (μg/mg MG; method 2)
BMG1	3	50	50	50	2.70
BMG2	8	50	50	50	3.75
BMG3	15.3	50	50	50	4.25
BMG4	17	50	50	50	5.82
BMG5	26	50	50	50	6.92
BMG6	38	50	50	50	12.86
BMG7	51.8	50	50	50	18.64
BMG8	156 (10 mL DMSO)	150	150	167	24.39
BMG9	50	50	50	50	21.83
BMG10	38.5	50	50	50	12.2
BaMG1	50[a]	50	50	50	42.55
BaMG2	38.5[a]	50	50	50	29.75

[a] Biotin–PEG2–amine (in milligram)

30 min. Finally, the volume was adjusted to 50 mL, and the absorbance was measured at 350 nm with a UV–VIS spectrophotometer (Beckman Coulter, DU800). For microgel analysis, 1 mL of 1 mg/mL BMG was placed into a 50-mL standard flask, followed by the steps described above. The biotin concentration was determined by the calibration curve and the results expressed as a mass fraction of the microgel. The sample blank in the spectrophotometer contained microgel to account for minor scattering effects.

In *method 3* potentiometric titration was used to measure the carboxyl content before and after biotinylation. The difference was assumed to represent the biotin content.

Atto-SP (fluorescent streptavidin) binding to BMG1 to BMG7 Fluorescently labeled streptavidin was employed to quantify binding to the microgel. Wet BMG pellets, formed by ultracentrifugation, were washed in PBS buffer (10 mmol/L). To 1.2 mL BMG suspension (1 mg/mL) in PBS buffer (10 mmol/L) was added 0.3 mL of Atto-SP solution (1 mg/mL in PBS buffer). After 4-h mixing at room temperature, the product was washed by several cycles of ultracentrifugation and redispersion in 10 mmol/L PBS buffer. The fluorescent intensity (excitation at 605 nm, measurement at 630) of 2.4-mL samples of Atto-SP–BMG suspensions (0.5 mg/mL PBS) was measured with a Cary Eclipse Fluorescence Spectrophotometer (Varian).

Streptavidin binding to BMG8, BaMG1, and BaMG2 Streptavidin solution (2.4 mL; 1 mg/mL in PBS buffer) was added to 16 mL BMG8 (1 mg/mL) in PBS buffer (10 mmol/L). The dispersion was gently mixed for 4 h at room temperature. The product, SP–BMG, was cleaned by 3 cycles of centrifugation and redispersion in 1 mM KCl.

Biotin and streptavidin penetration of microgel With the PNIPAM-*co*-vinylacetic acid microgels, most of the carboxyls are on the exterior surface of the microgel [17]. Nevertheless, we were interested in knowing whether or not the biotin and streptavidin reagents could penetrate the microgel network. To test this, 6 mg of dry MG were added to 2 mL of PBS (10 mmol/L) solutions containing either biotin (40 μg/mL) or streptavidin (8 μg/mL). The samples were equilibrated overnight at room temperature. The swollen microgels were centrifuged, and the concentrations of biotin and streptavidin in the supernatants were measured by the Avidin/HABA assay (Sigma) and by the Bradford assay (Sigma), respectively. A number of replicated experiments showed that aqueous biotin concentration after centrifugation equaled the calculated value. By contrast, streptavidin concentration in the supernatant was 10.3 μg/mL, 20% higher than the overall concentration of 8 μg/mL, indicating that streptavidin was excluded from the interior of the swollen microgel particles. Presumably, the mesh size of the cross-linked PNIPAM network was too small to pass streptavidin.

Results and discussion

The PNIPAM MG employed in this work was a copolymer of PNIPAM, methylenebisacrylamide, and vinylacetic acid [24]. The microgels are colloidal-sized spheres with narrow particle size distributions. This is a unique microgel system because the carboxyl groups are present on the exterior of the microgel on the end of short chains protruding from the microgel surface, ideal for bioconjugation [27].

Our initial attempts at microgel biotinylation involved the biotin hydrazide reaction with EDC-activated MG either in MES buffer (20 mM, pH 5.5) or water. In buffer the microgels aggregated, whereas in water the microgels were stable, but the yield was too low (7 μg biotin per milligram dried microgel) based on method 1. This corresponds to 10% conversion of microgel carboxyl groups.

In subsequent work the microgels were derivatized by EDC/sulfo-NHS/biotin hydrazide (Fig. 2). The conditions are summarized in Table 1. Microgels BMG1–BMG7 were replicated between two and four times, and the microgels were used to determine the role of biotin content on streptavidin binding. BMG8 was prepared on a larger scale. The biotin content of BMG8 was determined by three methods, and the results are compared in Table 2. Method 1 showed good agreement with method 2, whereas the result from titration was lower with more uncertainty.

The percent biotinylation of microgel carboxyl groups for all of the preparations in Table 1 is shown as functions of concentrations of biotin hydrazide or biotin–PEG2–amine in Fig. 3. Carboxyl conversion increased with concentration of biotin hydrazide. Note that in all cases the biotin reagent

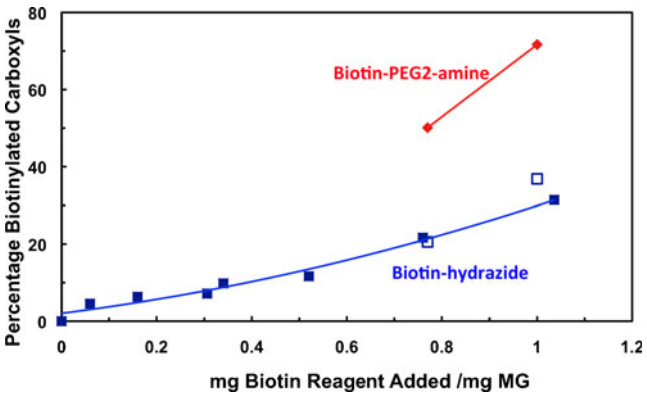

Fig. 2 Influence of concentrations of biotin hydrazide and biotin–PEG2–amine on the percent conversion of microgel carboxyls. The *open squares* denote results obtained many months after the *solid square* results

Table 2 Biotin content of BMG8 determined by three methods

	Biotin content (μg/mg)
Method 1	21.49±1.1
Method 2	24.39±1.58
Method 3	18.34±5.17

concentrations were in large excess with less than 5% being consumed by the microgels. The highest carboxyl conversions were for biotin–PEG2–amine. Although high degrees of biotinylation are not required (see below), more efficient use of the biotin reagents would be advantageous.

Dynamic light scattering and microelectrophoresis were used to measure microgel particle diameter and electrophoretic mobility as functions of pH. Particle diameter results show changes in particle swelling with pH and also can indicate the onset of colloidal aggregation. Microelectrophoresis gives a sensitive measure of the net electrical charge on the exterior of the microgel. Figure 3 shows the electrophoretic mobility and diameter of MG, the starting microgel, BMG8, the BMG, and SP–BMG obtained by exposing BMG8 to excess streptavidin.

The starting MG shows pH-dependent swelling and electrophoretic mobility reported previously [24]. MG behavior with

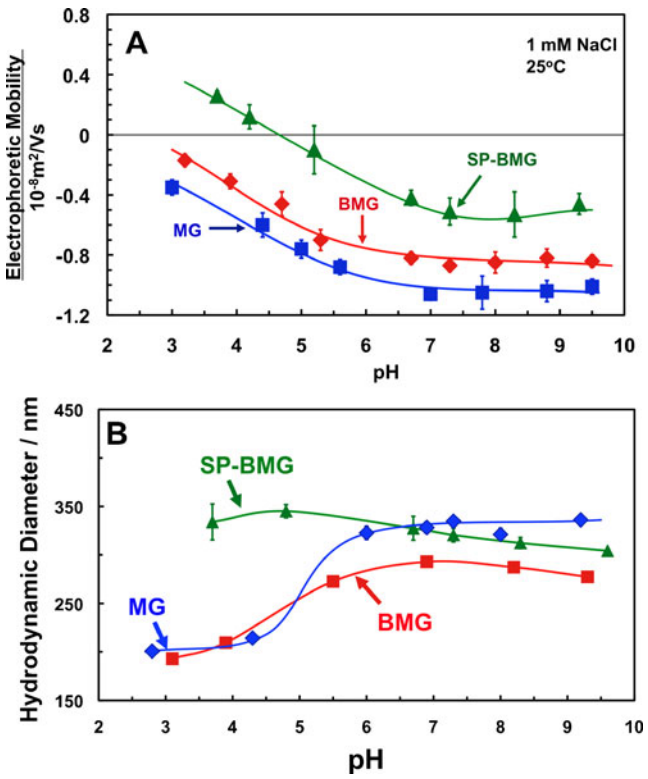

Fig. 3 Influence of pH on swelling (**b**) and electrophoretic mobility (**a**) of carboxylated microgel MG, biotinylated microgel BMG8 (24.39 μg biotin/mg MG based on method 2), and streptavidin-treated microgel SP–BMG (0.11 mg streptavidin/mg BMG)

pH reflects the dissociation of carboxyl groups isolated on the surface. The BMG is slightly less swollen and slightly less charged than MG, reflecting the replacement of about 29% of the charged carboxyls with nonionic biotins (based on method 3). Colloidal and nanoparticle support particles often have aggregation problems when undergoing surface modification. Indeed, SP–BMG results in Fig. 3, and electron micrographs indicated limited aggregation at low pH corresponding to the isoelectric point of the modified microgel.

We were also concerned about the possible presence of residual sulfo-NHS based on the work of Debord and Lyon [18]. Residual sulfonate groups from sulfo-NHS (species 3 in Fig. 1) should cause enhanced swelling and should contribute to the electrophoretic mobility. Our results did not show either of these effects, suggesting very little residual sulfo-NHS in our microgels. The carboxyl groups are on the exterior of the PNIPAM-VAA microgels, whereas the PNIPAM–AA microgels in Lyon's work would have interior carboxyls as well. Interior sulfo-NHS-activated carboxyls may be more stable.

We were also concerned that excess EDC might lead to the formation of nonreactive *N*-acylurea adducts proposed by Nakajima and Ikada—structure 5 in Fig. 1 [28]. The presence of these groups should lower swelling, lower the electrophoretic mobility, and give artificially high biotin contents, estimated by changes in the titratable carboxyl contents. Since the titration actually underestimated the biotin content (see Table 2) and since there were no unexpected effects in swelling or electrophoretic behavior (Fig. 3), we concluded that *N*-acylurea adducts were not significant in our microgels.

Streptavidin binding (SP–BMG in Fig. 3) had a large influence on microgel diameter and surface charge. The isoelectric point of streptavidin is around 7.5 [29], whereas SP–BMG had zero electrophoretic mobility around pH 4.7, suggesting a surface with more negative charge than present on pure streptavidin. Unlike MG and BMG, the SP–BMG particle size data did not decrease at low pH. Electron micrographs indicated limited aggregation at low pH corresponding to crossing the isoelectric point.

The binding of fluorescently labeled streptavidin (Atto-SP) to biotinylated microgels BMG1 through BMG7 was measured, and the results are shown in Fig. 4 as a plot of streptavidin content versus biotin content in the BMG. The maximum Atto-SP content was ~0.11 mg/mg of BMG. The area of the binding face on biotin is ~31 nm^2 [30]. Assuming close packing of biotin cubes onto a 300-nm microgel gives a mass fraction of streptavidin of 0.27 mg/mg. Thus, the experimental 0.11 mg/mg value corresponds to about one-third close packing. In the following paragraphs, a simple model is developed giving the curve in Fig. 4.

Consider a biotin attached to a surface of a sphere. We assume that a streptavidin will bind to a specific biotin

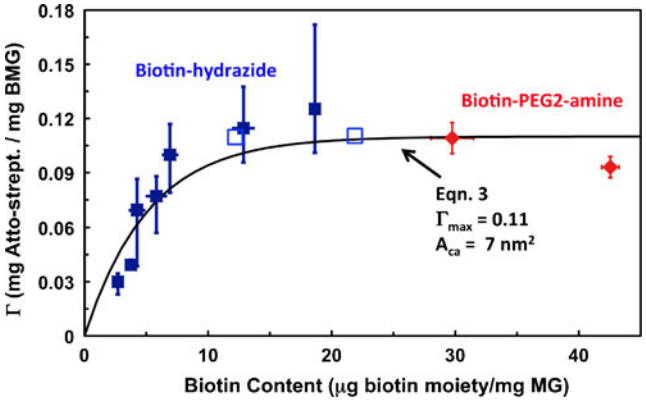

Fig. 4 Influence of the biotin content in the microgel on streptavidin uptake. The *y-axis error bars* denote the span of data; the *x-axis error bars* are standard error, and mean values are based on three to four replicates. The *curve* was calculated by Eq. 3. The *key model parameters* are on the plot; in addition, the calculation required the diameter of the deswollen microgel (200 nm), the diameter during conjugation (300 nm), and the assumed water content of the deswollen microgel (20%)

moiety if the center of the streptavidin lands within a circle surrounding the biotin that we call the capture circle or disk, having a capture area of A_{ca}.

We further assume that biotins are randomly distributed on the microgel surface. Disks associated with different bound biotin groups can overlap, so we define λ as the average number of disks at any point on the surface of the microgel sphere. λ is given by the following expression where d is the diameter of the microgel, A_{ca} is the area of the capture disk, and n_{bi} is the number of biotin molecules per microgel, which is equal to the number of disks.

$$\lambda = \frac{n_{bi} A_{ca}}{\pi d^2} \tag{1}$$

However, if the biotins are randomly distributed, λ will also vary across the microgel surface. The random distribution of disks on a surface is a Poisson process, and the probability, P_{bare}, of a point on surface being covered with zero disks (i.e., giving no binding sites for streptavidin) is given by the following:

$$p_{bare} = \exp(-\lambda) = \exp\left(-\frac{n_{bi} A_{ca}}{\pi d^2}\right) \tag{2}$$

If the maximum quantity of bound streptavidin on a completely coated microgel is Γ_{max}, the relationship between streptavidin coverage and biotin content is given by

$$\Gamma = \Gamma_{max}(1 - P_{bare}) = \Gamma_{max}(1 - \exp(-\lambda)) = \Gamma_{max}\left(1 - \exp\left(-\frac{n_{bi} A_{ca}}{\pi d^2}\right)\right) \tag{3}$$

Equation 3 was used to generate the solid line in Fig. 4, and the values of the parameters used are given either in the figure or in the caption. A_{ca}, the area of the capture disk, is the only completely adjustable parameter. An A_{ca} value of 7 nm^2 was required to fit our data. This value is about 20% of the area of a binding face on streptavidin molecule and seems reasonable. $1/A_{ca}$, the inverse of the capture area, corresponds to minimum local density of biotins that will capture a streptavidin. A_{ca}=7 nm^2 corresponds to a biotin density of about 31 μg biotin/mg of microgel, the units used in the *x*-axis of Fig. 4. Thus, from Fig. 4, we see that when the average microgel biotin content is 31 μg biotin/mg of microgel=$1/A_{ca}$, the microgel is saturated with bound streptavidin.

For our modeling we used the experimental value of Γ_{max}, the maximum bound streptavidin content. For a highly biotinylated surface, the maximum streptavidin content is dictated by the ability of the proteins to pack. Protein–protein repulsion from steric and electrostatic forces will be pH- and ionic strength-dependent. In the absence of experimental data, Γ_{max} can be estimated from molecular models.

The main advantage of applying our model (Eq. 3) to experimental data is that it gives a measure of the capture disk area and its inverse, which is the minimum local density of biotin required to capture a streptavidin. Of course, this approach could be applied to other specific binding pairs.

Biotinylated microgel is only useful if the preparation is reproducible and the product is stable. Table 3 compares the biotin contents of BMG7 and BMG8 measured over many months. The two microgels had remarkably similar characteristics, in spite of the fact that they were made from different preparations of the parent PNIPAM-VAA microgel. The biotin contents of both microgels decreased by about one-third over a year of storage. Reports in the literature suggest that derivatives of biotin hydrazide can have stability problems [31, 32].

In summary, biotinylation and streptavidin binding are widely used bioconjugation methodologies and are thus considered routine. Nevertheless, initially we had difficulties with microgel aggregation and low degrees of biotinylation. In this work we have illustrated that under the right conditions, PNIPAM-*co*-vinyl acetic acid microgels are particularly amenable to biotinylation and subse-

Table 3 The stability and reproducibility of biotinylated microgel

	BMG8	BMG7
Biotin quantified in Nov 2008 (μg/mg)	24.39	N/A
Biotin quantified in May 2009 (μg/mg)	N/A	18.64
Biotin quantified in Sep 2009 (μg/mg)	16.58	16.40
Atto-SP binding BMG (mg/mg)	~0.11	~0.11

Freeze-dried microgel was stored at 4 °C between measurements

quent streptavidin binding. Finally, we have developed a simple model to help interpret the dependency of streptavidin binding on biotin density.

Conclusions

The major conclusions from this work are the following:

1. Biotin hydrazide coupling to NHS-activated PNIPAM-carboxylated microgels can be regulated to control the streptavidin binding capacity of the microgels. The preparations were reproducible; however, the biotin content of the hydrazide derivative decreased slowly with storage time.
2. Microgel colloidal stability was maintained throughout the conjugation.
3. Microgel swelling (diameters) and electrophoretic mobility values are sensitive probes of the changes in surface properties during the stages of conjugation reactions.
4. Streptavidin was too large to penetrate our microgels, whereas biotin freely accessed the microgel core.
5. A model based on Poisson statistics gave good fits to plots of streptavidin versus biotin content. The resulting capture disk area gives a measure of the minimum local density of biotin required to capture a streptavidin.

Acknowledgments Prof. Todd Hoare is thanked for useful discussions. The authors acknowledge the SENTINEL Bioactive Paper NSERC Network for financial support. RP and YL hold Canada Research Chairs.

References

1. Kawaguchi H, Fujimoto K, Mizuhara Y (1992) Hydrogel microspheres.3. Temperature-dependent adsorption of proteins on poly-*N*-isopropylacrylamide hydrogel microspheres. Colloid Polym Sci 270(1):53–57
2. Pichot C (2004) Surface-functionalized latexes for biotechnological applications. Curr Opin Colloid Interface Sci 9(3–4):213–221
3. Pelton RH, Chibante P (1986) Preparation of aqueous latices with *N*-isopropylacrylamide. Colloids Surf 20(3):247–256
4. Pelton R (2000) Temperature-sensitive aqueous microgels. Adv Colloid Interface Sci 85(1):1–33
5. Nayak S, Lyon LA (2005) Soft nanotechnology with soft nanoparticles. Angew Chem Int Ed 44(47):7686–7708
6. Oh JK, Drumright R, Siegwart DJ, Matyjaszewski K (2008) The development of microgels/nanogels for drug delivery applications. Prog Polym Sci 33(4):448–477. doi:10.1016/j.progpolymsci.2008.01.002
7. Hoare T, Pelton R (2008) Impact of microgel morphology on functionalized microgel–drug interactions. Langmuir 24 (24):1005–1012
8. Das M, Zhang H, Kumacheva E (2006) Microgels: old materials with new applications. Annu Rev Mater Res 36:117–142
9. Kawaguchi H, Kisara K, Takahashi T, Achiha K, Yasui M, Fujimoto K (2000) Versatility of thermosensitive particles. Macromol Symp 151:591–598
10. Taniguchi T, Duracher D, Delair T, Elaissari A, Pichot C (2003) Adsorption/desorption behavior and covalent grafting of an antibody onto cationic amino-functionalized poly(styrene-*N*-isopropylacrylamide) core–shell latex particles. Colloids Surf B Biointerfaces 29(1):53–65
11. Colonne M, Chen Y, Wu K, Freiberg S, Giasson S, Zhu XX (2007) Binding of streptavidin with biotinylated thermosensitive nanospheres based on poly(*N*,*N*-diethylacrylamide-*co*-2-hydroxyethyl methacrylate). Bioconjug Chem 18 (3):999–1003
12. Hong C-Y, Pan C-Y (2006) Direct synthesis of biotinylated stimuli-responsive polymer and diblock copolymer by raft polymerization using biotinylated trithiocarbonate as raft agent. Macromolecules 39(10):3517–3524. doi:10.1021/ma052593+
13. Sirpal S, Gattas-Asfura KM, Leblanc RM (2007) A photodimerization approach to crosslink and functionalize microgels. Colloids Surf B Biointerfaces 58(2):116–120
14. Su S, Ali MM, Filipe CDM, Li Y, Pelton R (2008) Microgel-based inks for paper-supported biosensing applications. Biomacromolecules 9(3):935–941
15. Pelton R (2009) Bioactive paper—a low cost platform for diagnostics. Trends Anal Chem 28(8):925–942
16. Hoare T, McLean D (2006) Kinetic prediction of functional group distributions in thermosensitive microgels. J Phys Chem B 110 (41):20327–20336
17. Hoare T, Pelton R (2004) Functional group distributions in carboxylic acid containing poly(*N*-isopropylacrylamide) microgels. Langmuir 20(6):2123–2133
18. Debord JD, Lyon LA (2007) On the unusual stability of succinimidyl esters in pNIPAm-AAc microgels. Bioconjug Chem 18(2):601–604
19. Hermanson GT (1996) Bioconjugate techniques. Academic, San Diego
20. Prestwich G, Marecak D, Marecek J, Vercruysse K, Ziebell M (1998) Controlled chemical modification of hyaluronic acid: synthesis, applications, and biodegradation of hydrazide derivatives. J Control Release 53(1–3):93–103
21. Kremsky J, Wooters J, Dougherty J, Meyers R, Collins M, Brown E (1987) Immobilization of DNA via oligonucleotides containing an aldehyde or carboxylic acid group at the 5′ terminus. Nucleic Acids Res 15(7):2891
22. Yang M, Teeuwen RLM, Giesbers M, Baggerman J, Arafat A, de Wolf FA, van Hest JCM, Zuilhof H (2008) One-step photochemical attachment of NHS-terminated monolayers onto silicon surfaces and subsequent functionalization. Langmuir 24(15):7931–7938. doi:10.1021/la800462u
23. Nayak S, Lyon LA (2004) Ligand-functionalized core/shell microgels with permselective shells. Angew Chem Int Ed 43 (48):6706–6709
24. Hoare T, Pelton R (2004) Highly pH and temperature responsive microgels functionalized with vinylacetic acid. Macromolecules 37(7):2544–2550
25. McCormick D, Roth J (1970) Specificity, stereochemistry, and mechanism of the color reaction between *p*-dimethylaminocinnamaldehyde and biotin analogs. Anal Biochem 34(1):226–236
26. Ahmed J, Verma K (1979) Determination of *d*-biotin at the microgram level. Talanta 26(11):1025
27. Hoare T, Pelton R (2006) Dimensionless plot analysis: a new way to analyze functionalized microgels. J Colloid Interface Sci 303 (1):109–116
28. Nakajima N, Ikada Y (1995) Mechanism of amide formation by carbodiimide for bioconjugation in aqueous-media. Bioconjug Chem 6(1):123–130

29. Kurzban GP, Bayer EA, Wilchek M, Horowitz PM (1991) The quaternary structure of streptavidin in urea. J Biol Chem 266 (22):14470–14477
30. Ren CL, Carvajal D, Shull KR, Szleifer I (2009) Streptavidin–biotin binding in the presence of a polymer spacer. A theoretical description. Langmuir 25(20):12283–12292. doi:10.1021/la901735d
31. Bogusiewicz A, Mock NI, Mock DM (2004) Instability of the biotin–protein bond in human plasma. Anal Biochem 327(2):156–161. doi:10.1016/j.ab.2004.01.011
32. Bogusiewcz A, Mock NI, Mock DM (2004) Release of biotin from biotinylated proteins occurs enzymatically and nonenzymatically in human plasma. Anal Biochem 331(2):260–266. doi:10.1016/j.ab.2004.05.020

Supporting Infomation

Title: Controlling Biotinylation of Microgels and modeling streptavidin uptake

Department of Chemical Engineering
JHE-136, McMaster University
Hamilton, Ontario, Canada, L8S 4L7
(905) 529 7070 ext. 27045
FAX (905) 528 5114 Email peltonrh@mcmaster.ca

Figures

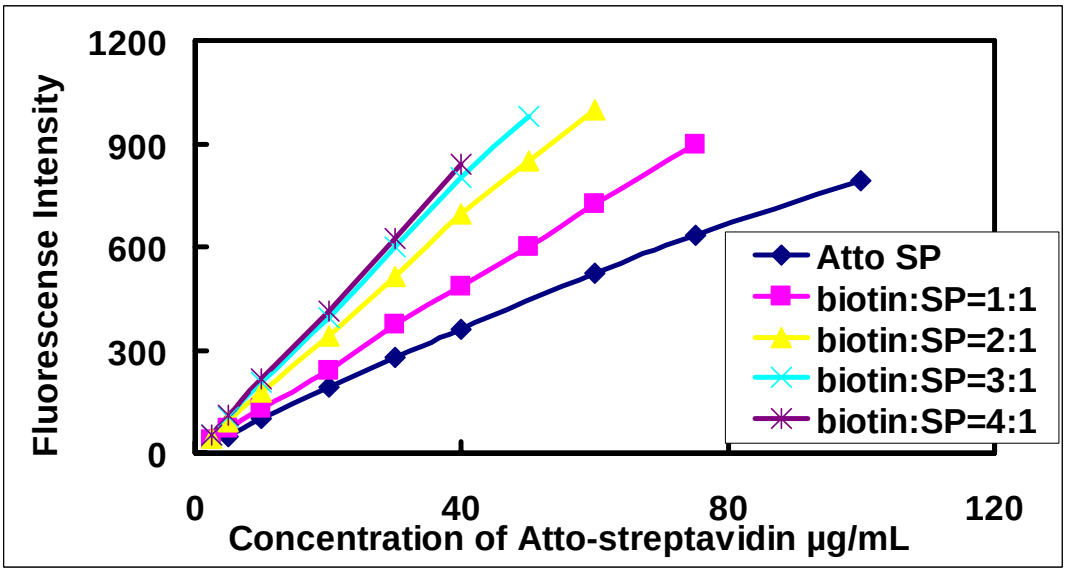

Figure S 1. Standard curves of fluorescence intensity vs. Atto-SP concentration under different mole ratio of biotin to Atto-SP. Biotin binding induces fluorescence enhancement of Atto-SP labelled streptavidin. The standard curves corresponds to literature. (Al-Hakiem, Landon et al. 1981)

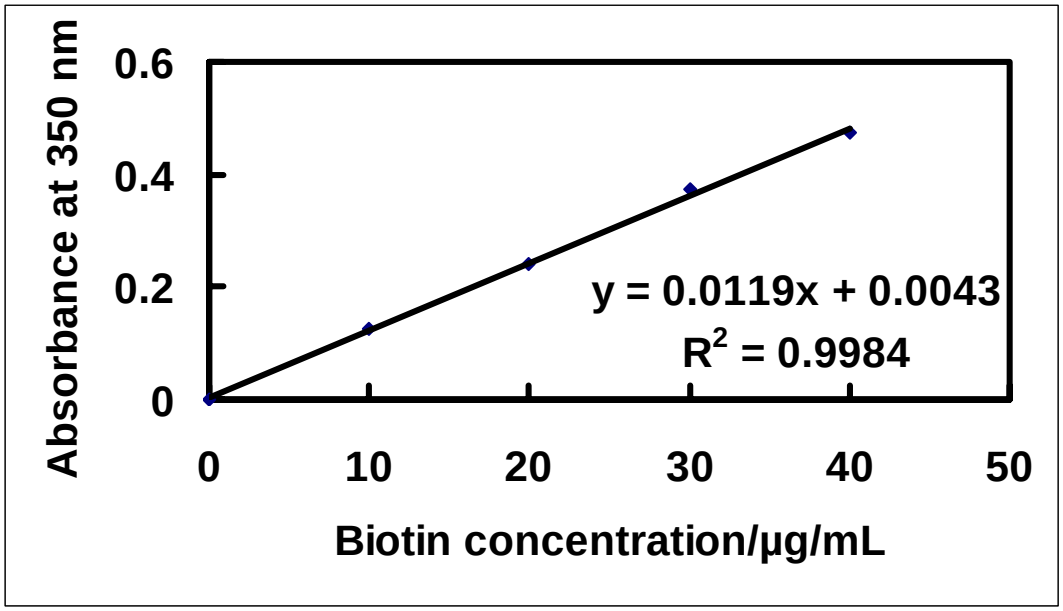

Figure S 2. Standard curve of absorbance at 533nm vs. biotin concentration by method I.

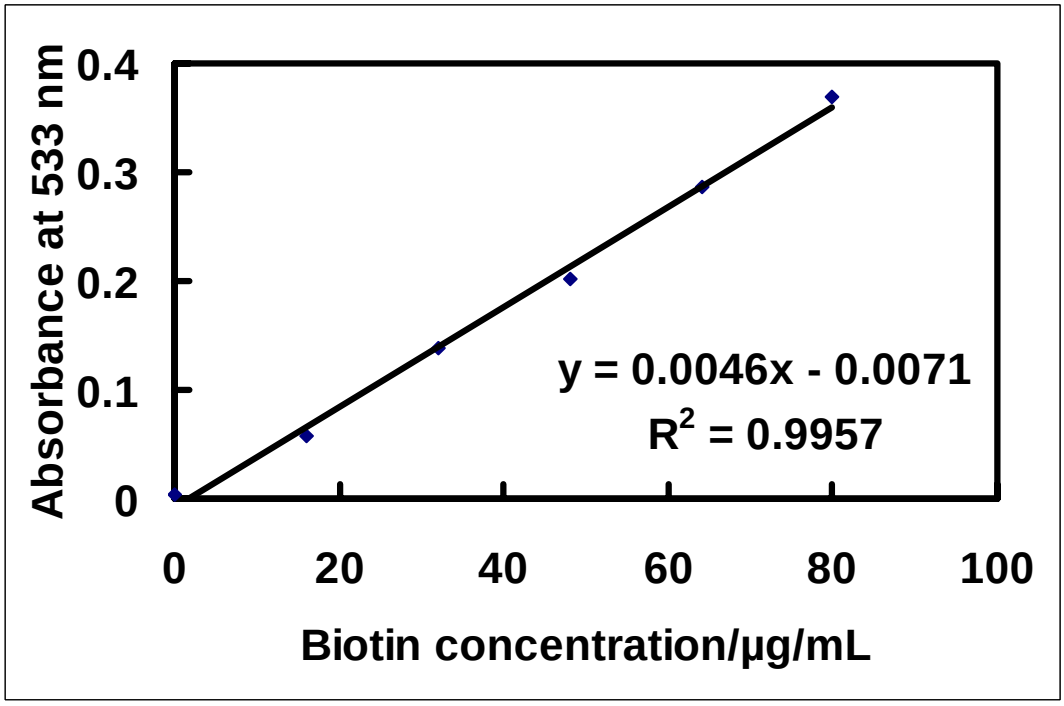

Figure S 3. The standard curve of absorbance at 350nm vs. biotin concentration by Method II

Schemes

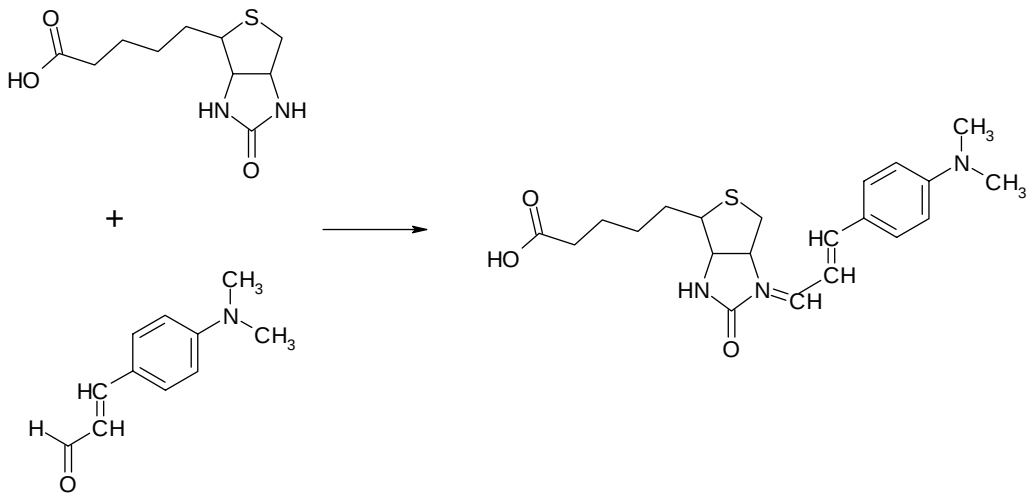

Scheme S 1. Mechanism for Mehod I, biotin and p-dimethylaminocinnamaldehyde react under anhydrous conditions to form a product that has maximal absorbance at 533 nm (McCORMICK and Roth 1970).

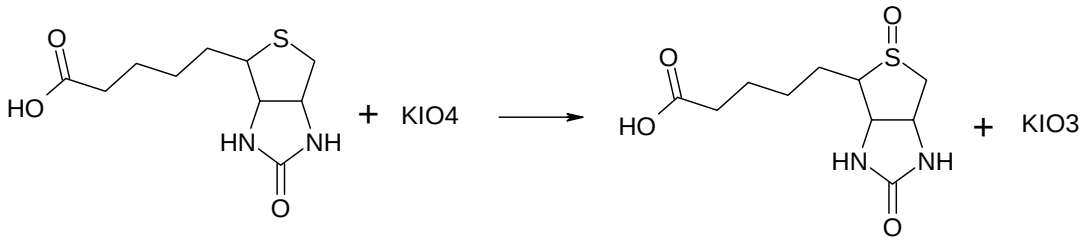

Scheme S 2. Mechanism for Method II, biotin reacts with periodate to form a sulphoxide and an iodate (Ahmed and Verma 1979).

Reference

Ahmed, J. and K. Verma (1979). "Determination of d-biotin at the microgram level." Talanta **26**(11): 1025.

Al-Hakiem, M., J. Landon, et al. (1981). "Fluorimetric assays for avidin and biotin based on biotin-induced fluorescence enhancement of fluorescein-labeled avidin." Analytical Biochemistry **116**(2): 264-267.

Hoare, T. and R. Pelton (2008). "Characterizing charge and crosslinker distributions in polyelectrolyte microgels." Current Opinion in Colloid & Interface Science **13**(6): 413-428.

McCORMICK, D. and J. Roth (1970). "Specificity, stereochemistry, and mechanism of the color reaction between p-dimethylaminocinnamaldehyde and biotin analogs." Analytical Biochemistry **34**(1): 226-236.

Chapter 5 Immobilization of a Bienzymatic Smell Generating System on Paper Using Microgels

Abstract

In the pevious chapters, a new smell generating biosensor was invented by using a bienzymatic system consisting of pyridoxal kinase and tryptophanase. In this Chapter, it is shown that the bienzyme system can be immobilized onto microgel particles and these particles can be added to paper – leading to the creation, for the first time, of a paper based smell-generating biosensor. Poly(N-isopropylacrylamide-co-vinylacetic acid) (PNIPAM-VAA) microgels were biotinylated first and biotinylation of the enzymes was done using either Sulfo-NHS-biotin or amino biotin, without significant loss of enzyme activity. Biotinylated pyridoxal kinase and tryptophanase were attached to PNIPAM-VAA microgels using avidin. The enzyme loaded microgels were spotted on paper and the enzyme activity remaining on paper was compared with and without the use of microgels. The results obtained clearly show that the bienzyme system works on paper, leading to smell generation on paper in the presence of the target. The results also show that the process of biotinylation and uploading of bienzyme on microgel particles leads to a similar activity of the biosensor after washing the paper with buffer. The work in this Chapter is the first function demonstration of a paper sensor that reports the presence of a target by generating a smell.

5.1 Introduction

Bioactive paper has been gaining a great deal of interest, mainly in the last decade. Bioactive paper was defined as "paper-like products, cardboard, fabrics and their combinations, etc., with active recognition and/or functional material capabilities" by a Finnish research organization. [1] Two key properties account for the interest in bioactive paper. First, paper is easily accessible, cheap, environmentally friendly and commonly used as typical filter material or packing material. Second, cellulose is biomolecule friendly [2] and porous structures in paper enable efficiency in trapping biomolecules. [3]

There are several major bioactive-paper research initiatives in the world currently, including SENTINEL bioactive paper network in Canada, Whiteside's group at Harvard, and other groups in Australia and Japan. [3] The main efforts have been directed towards building cheap and efficient paper chips for diagnostic applications [4], environmental control [5], food safety control [6] and virus/DNA detections.[7] Usually, a visual signal is utilized to report the detection because it is a direct signal to the human eye. These visual signals include color [8], illuminance [9] and fluorescence [7].

In Chapter 3 of this thesis a new generic smell-generating biosensor was reported. This biosensor could detect adenosine-5'-triphosphate (ATP) and generate a smell through the production of indole or methyl mercaptan. Since ATP that exists in virtually any biological system, this biosensor could be applied to a large number of biological events. Because a smell signal is also a direct signal to the human nose, and because it can be detected under any light conditions, the smell-generating biosensor has high potential for various applications. However, solution based systems are not ideal for practical use, especially when multiple steps and sample manipulation are required for analysis. Herein we report on the immobilization of the bienzyme system described in Chapter 3, which consists of pyridoxal kinase and tryptophanase, onto PNIPAM-VAA microgels through biotin-avidin linkage. It was found that the bienzyme system does not loose its activity after being immobilized on the particles. It was also found that using these particles, it is possible to immobilize the bi-enzymatic system on paper, which is a first (but important step) in the creation of a smell generation bioink.

5.2 Experimental

5.2.1 Chemicals.

N-(3-Dimethylaminopropyl)-N'-ethylcarbodiimide hydrochloride (EDC), avidin from egg white, streptavidin, Isopropyl β-D-1-thiogalactopyranoside (IPTG), Kovac's reagent, Bradford reagent and Avidin/HABA reagent were from Sigma. Biotin hydrazide, biotin-PEG2-amine, N-hydroxysulfosuccinimide (NHS) and EZ-Link Sulfo-NHS-biotin reagent were from Pierce. The water used in this work was Millipore Milli-Q grade. KDP buffer

consisted of 0.2 M potassium phosphate (pH 7.8), 2mM dithiothreitol and 6.7 mM ammonium sulfate.

5.2.2Preparation of Biotinylated and Avidin Uploaded Microgels.

Poly(N-isopropylacrylamide-co-vinylacetic acid) (PNIPAM-VAA) microgel was prepared by Hoare's method. [10] Then the microgel was biotinylated according to the procedure for preparing "BMG1" described before in chapter 4. To 50 mg of microgels in 50 mL water was added a 50 mg biotin hydrazide in 3 mL DMSO at room temperature. After 5 min, EDC and sulfo-NHS were added, and the pH was adjusted to 7.4 with NaOH (0.01 mol/L). The mixture was stirred for 10 h with the pH adjusted to ~7.4 by HCl (0.01 mol/L) every 30 min. Then the MG was washed by several cycles of ultracentrifugation (50,000 rpm, 50 min), decantation, and redispersion in water and stored in fridge.

Avidin and streptavidin uploading on biotinylated microgel (BMG) were compared by adding 450 μg avidin or streptavidin to 3 mL 1 mg/mL BMG in PBS buffer (10mM, pH 7.4). The mixture was stirred at room temperature for 4 hours and then the microgels were collected and washed three times by ultracentrifugation in PBS buffer. The cleaned microgels were resuspended in 3 mL PBS buffer. Each sample was done in triplicates. A set of control samples was created by only adding PBS buffer to BMG. Then 50 μL of each sample was taken out and diluted to 200 μL and a Bradford microassay was used to determine protein concentration.

5.2.3 Preparation of Biotinylated Enzyme.

As described in Chapter 2, TPase was effectively biotinylated by Sulfo-NHS-biotin with the presence of L-tryptophan. Briefly, three samples of TPase were prepared at 4 mg/mL concentrations. 500 μL of each sample was added to L-tryptophan with a final concentration of 10 mM and 200 μg of Sulfo-NHS-biotin was added to each. The samples were left at room temperature for 2 h, after which another 200 μg of biotin were added to each and the samples were placed on ice for four hours. Another 200 μg of biotin was added after the four hours and the samples were placed in the fridge overnight. The following day, the solutions were transferred into dialysis tubes and dialyzed in potassium phosphate buffer (20 mM, pH 7.8) for 8 hours. The dilution buffer was changed 2 h, 5 h and 8h. The beaker containing the dialysis buffer and tubes was placed in the fridge (4 °C) overnight. The next day, the dialyzed solution was transferred to glass vials and the protein concentration of biotinylated TPase (BTPase) samples were determined by a Bradford assay and the biotin content on TPase was determined by using Avidin/HABA reagent.

Pyridoxal kinase was purified by following published materials and the procedure described in Chapter 3. [11] Biotinylation of PKase followed a similar procedure to the biotinylation of TPase. PKase was biotinylated in the presence of 0.1 mg/mL pyridoxal, using sulfo-NHS biotin and amine-PEG2-biotin. To 1.4 mL PKase (0.3mg/mL) solution,

200 μg Sulfo-NHS-biotin or biotin-PEG2-amine was added first and the mixture was left to sit at room temperature for 2 hours. Then another 200 μg biotin reagent was added and the mixture was placed on the ice for 4 hours. Following this another 200 μg biotin reagent was added and the mixture was placed in the fridge (4°C) overnight. The next day, the mixture was transferred to a dialysis tube and dialyzed against potassium phosphate buffer (20 mM, pH 7.8) for 8 hours. The dilution buffer was changed after 2 hours, 5 hours and 8 hours. The beaker containing the dialysis buffer and tube was placed in the fridge (4°C) overnight. The following day, the dialyzed solution was transferred to a glass bottle from dialysis tube. The concentration of biotinylated PKase (BPKase) was measured by using Bradford reagent. The amount of biotin on BPkase was measured by Avidin/HABA method.

5.2.4 Immobilization of Enzyme on Microgels.

To 1 mL of ABMG (avidin immobilized biotinylated microgels, avidin-BMG), 400 μg BTpase or BPKase was added and the mixture was left in fridge (4°C) overnight. The following day, all the samples were ultracentrifuged and the supernatants were kept. The samples were then washed two times with potassium phosphate buffer (200 mM, pH 7.8), and the cleaned pellets were resuspended in the same buffer. The protein concentration in the supernatant was measured by the Bradford method. The amount of immobilized enzyme was determined indirectly from the difference between the amount of protein introduced into the reaction mixture and the amount of protein present in the washing solutions after immobilization. Each sample was prepared in triplicate.

5.2.5 Assay of Enzyme Activity.

TPase activity was determined by measuring the product produced using two different substrates, L-tryptophan or S-methyl-L-cysteine (SMLC). If L-tryptophan was used, the indole produced was measured with a spectrophotometer, following the procedure described before in Chapter 3 using Kovac's reagent and measuring absorbance under 570 nm. The 700 μL reaction mixture contained 15 mM L-tryptophan or SMLC and 0.1 mM pyridoxal phosphate (PLP). If SMLC was used as the substrate, the concentration of methyl mercaptan produced in a 40 mL glass vial was quantified using an electronic nose, ToxiRAE PID detector. The activity of PKase was measured by following the published method. [12] 10 μg of each pyridoxal kinase sample was used to create a 700 μL solution, which also contained pyridoxal (0.05 mg/mL), magnesium chloride (0.6 mM), ATP (2 mM), and KDP buffer was to adjust the final volume. These samples were left at room temperature for one hour, and then placed on ice for 10 minutes. To each sample, 92.1 μL of H_2SO_4 and 0.67 μL of phenylhydrazine were added and the samples were left for 30 minutes on ice before being transferred to cuvettes and read with the UV spectrophotometer at 410 nm. These readings were compared against a standard curve for PLP concentration and the amount of PLP produced in each sample was determined.

5.2.6 Comparison of Single Enzyme Activity on Paper with and without MG.

Preliminary experiments showed that spotting the enzymes on paper does reduce enzyme activity (data not shown here). To compare the activity of TPase on paper with the activity of TPase-MG (tryptophanase immobilized on microgels) on paper, 25 μg of TPase solution or TPase-MG solution containing 50 μg of TPase was spotted on paper strips (No. 1 Watman filter paper, 1×0.5 cm) and the strips were left to dry at room temperature for 1 hour. Then the paper strips were totally submerged into 700 μL of reaction mixture to test the enzyme activity. A similar procedure was done to compare the percentage of PKase activity enzyme activity retained on paper with or without and immobilizing trhe enzyme on the microgels. PKase solution containing 25 μg of Pkase or PKase-MG (pyridoxal kinase immobilized on microgels) solution containing 50 μg of PKase were used. The percentage of enzyme activity retained on paper is calculated as the amount of product generated by enzyme on paper divided by the amount of produce generated by free enzyme in solution.

Washing experiments on enzyme immobilized paper strips were carried out after drying the paper strips at room temperature for 1 hour. The paper strips were flushed using 10 mL of 20 mM potassium phosphate buffer (pH 7.4) for 5 mins as shown below in Figure 1. Then the paper strips were totally submerged into 700 μL of reaction mixture to test the amount of the product generated by the enzyme on paper.

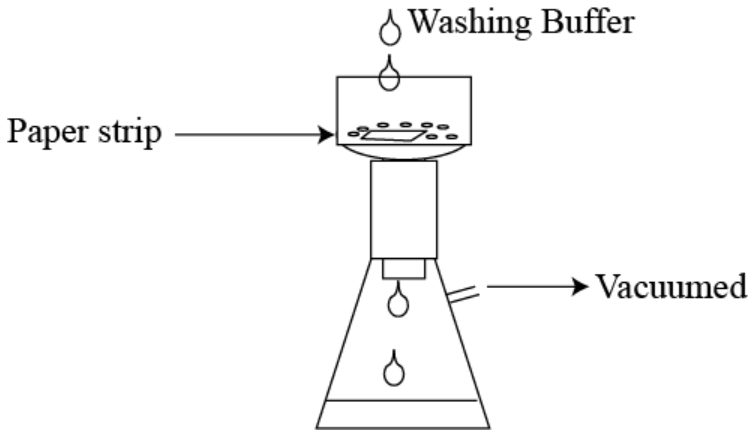

Figure 1 Device for washing experiments on paper strips.

5.2.7 Immobilized Bienzyme for Detection of ATP.

After investigating the immobilization of single enzyme on paper, the immobilized bienzyme system on paper was used for detection of ATP. TPase-MG solution containing 100 μg of TPase and PKase-MG solution containing 100 μg of PKase were

mixed and spotted on paper strips (No. 1 Whatman filter paper, 1×0.5 cm) and the strips were left to dry at room temperature for 1 hour. The solution containing 25 μg of TPase and 25 μg of PKase was mixed and the volume was adjusted by adding KDP buffer to be the same as the sample volume with microgels. Then the solution was spotted on paper strips. Every sample was done in triplicates. After drying, the paper strips were totally submerged into 700 μL of reaction mixture separately for the detection of ATP. The reaction mixture contains 0.1 mg/mL pyridoxal, 0.1 mM Mg^{2+}, 0.2 mM ATP and 15 mM L-tryptophan. The amount of indole generated on these paper strips were quantified by colorimetric method, and the activity of the bienzyme system on paper with or without microgels were compared.

Similar to the washing experiments above, bienzyme immobilized paper strips were dried at room temperature for 1 hour and washed on the filter on the top of a vacuumed filter flask by 10 mL of 20 mM potassium phosphate buffer (pH 7.4) for 5 mins. Then the paper strips were totally submerged into 700 μL of reaction mixture to test the amount of indole generated by the bienzyme on paper.

5.3 Results and Discussion

The PNIPAM microgel (MG) employed in this work was a copolymer of PNIPAM, methylenebisacrylamide, and vinylacetic acid. [10] This MG has carboxyl groups present on the exterior of the microgel surface which is ideal for bioconjugation. Previous work in our group directly coupled streptavidin to microgel to build a platform for the immobilization of biomolecules, such as DNA aptamers and antibodies. [13] However, the streptavidin coverage was very low (around 7.5 μg per mg MG). [13] Our work in Chapter 4 showed that biotinylation of microgel achieved higher streptavidin loading of 120 μg per mg BMG. [14] This provides a platform for highly efficient biomolecule immobilization on microgel.

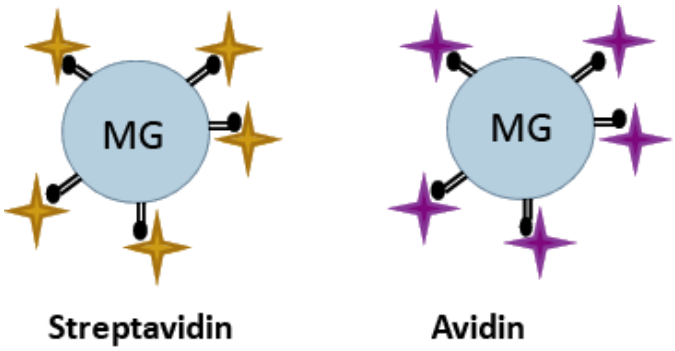

Figure 2. Streptavidin binding on biotinlyated microgels (BMG) vs. Avidin binding on BMG

Streptavidin is very expensive compared to avidin. Avidin and streptavidin have almost identical three dimensional structures and both have four binding sites for biotin, but they

have different molecular weight and different amino acid sequences. Avidin has higher affinity for biotin, which is given by a K_d of 10^{-15} M, while streptavidin has lower affinity of K_d around 10^{-13} M, but streptavidin has higher specificity for biotin. [15] Figure 2 shows the binding of streptavidin vs. avidin on BMG. Quantification of streptavidin and avidin uploading on 1 mg of BMG showed that 84.132±3.954 μg of streptavidin and 82.932±4.308 μg of avidin were uploaded on 1 mg of BMG separately, and the control sample showed no uploading of protein. The amount of avidin and streptavidin immobilized on BMG are actually similar with a difference less than 3% as shown in Table 1. Since avidin is much cheaper, avidin covered BMG particles were used for immobilizing the enzymes in the following experiments.

Table 1 Comparing the amounts of streptavidin and avidin loaded on biotinylated microgels

Samples	Streptavidin on BMG-SA μg/mL	Avidin on BMG-A μg/mL
1	80.985	78.028
2	79.423	91.520
3	91.989	79.250
Average	84.132 ± 3.954	82.932 ± 4.308

Biotinylation of TPase was achieved by following the procedure described in Chapter 2. Previous research found that the presence of substrate L-tryptophan helps retain enzyme activity. After biotinylation, every biotinylated TPase (BTPase) molecule was calculated to have 1.86 ±0.12 biotin molecules attached. The enzyme activity after biotinylation was found to be around 70% of actvity before biotinylation.

Biotinylation of PKase done by using either Sulfo-NHS-Biotin orAmine-PEG2-Biotin. Sulfo-NHS-Biotin reacts with amine groups on the protein, while Amine-PEG2-Biotin reacts with carboxylic groups on the protein. It is not clear if the active site of pyridoxal kinase contains more amine groups or more carboxylic group, hence the two different biotin reagents were used to compare the effect of biotinylation. The results present in Table 2 shows that biotinylation of PKase using Sulfo-NHS-Biotin resulted in 1.435±0.186 biotin per molecule of PKase and biotinylation using amine-PEG2-Biotin reulted in the presence of 1.184±0.07 biotin per molecule of PKase. The enzyme activity using the two biotinylation approaches was found to be similar: 0.1918±0.0134 mg/mL PLP were produced by 50 μg of BPKase biotinylated using Sulfo-NHS-Biotin and 0.2011±0.0101 mg/mL PLP were produced by 50 μg of BPKase biotinylated by amine-PEG2-Biotin. The control sample did not show any biotin attachment. In the following experiments, biotinylation of PKase was done using Sulfo-NHS-Biotin.

As a commonly used ligand in biomolecule linking, biotin-avidin was used to link the biotinylated enzymes to microgel surface. By adding 400 μg BTpase or BPKase to 1 mL of ABMG, the amount of enzyme immobilized on the microgel was found to be as shown in Table 2. It has been reported before that microgels can be physically trapped in the

porous structure of paper [13], so washing experiments (10 mL of 20 mM potassium phosphate buffer for 5 mins) were carried out to compare how much of the enzyme activity was maintained on paper strips with and without using microgels for enzyme immobilization.

Table 2 The mass of biotinylated enzyme loaded onto ABMG*

Sample	Protein in Supernatant (mg/mL)	Mass of Immobilized Enzyme in 1mL of microgel (μg)	Average Mass of Immobilized Enzyme in 1 mL of microgel (μg)
BTPase 1	0.1552	244.8	248.83 ± 12.95
BTPase 2	0.1713	228.7	
BTPase 3	0.1270	273	
BPKase 1	0.2051	194.9	201.67 ± 10.79
BPKase 2	0.1772	222.8	
BPKase 3	0.2127	187.3	

* ABMG: avidin-BMG

To investigate the effect of microgels as supporter for retaining enzyme activity on paper, PKase, PKase-MG, TPase and TPase-MG were spotted and dried on paper strips. The results are shown in Table3, Table 4 and Figure 3. The TPase-MG on paper retained 60.18±6.75% of the initial enzyme activity in TPase-MG solution, while Tpase on paper only retained 50.95±1.26% of original activity in TPase solution. The PKase-MG on paper retained 73.17±3.53% of the activity, while PKase on paper only remained 61.61% ± 2.11% of the original enzyme activity. The reduced enzyme activity could be due to drying enzyme on the paper which results in damage of protein structure and interactions of the enzyme with the paper surface. Biotinylation of the enzyme usually causes 40% loss of enzyme activity as described in the previous chapters. The results show that spotting enzyme directly on paper has similar enzyme activity compared to biotinylation and immobilization of enzyme on microgel and then paper. However, microgel particles do help remain a higher percent of activity than spotting free enzyme solution on paper. Previous research in our group showed that microgel would help keep biomolecules on a specific region on paper, and this could be an advantage of using microgels as supporter. [13]

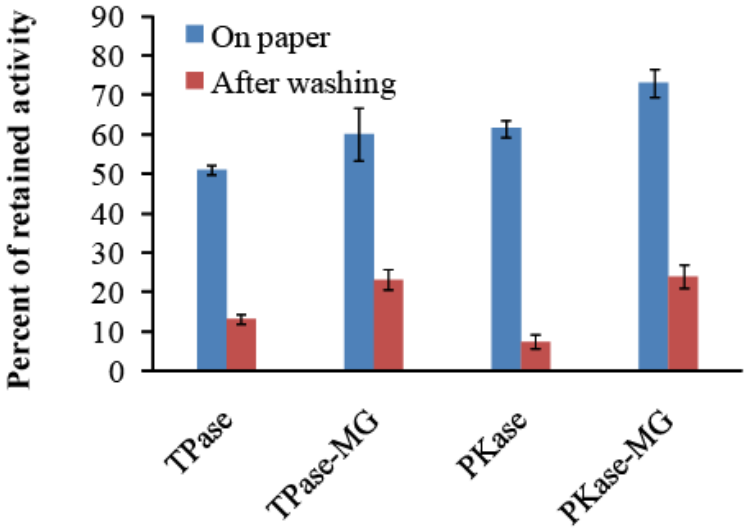

Figure 3 Monitoring the percentage of the initial enzyme activity that is preserved after spotting it on paper, either as a free solution or loaded onto microgel particles and the effect of washing on the percentage of initial activity retained. Error bars represent standard error of three samples.

Table 3 Indole generation by TPase or TPase-MG in solution, on paper and after washing.

Samples	TPase	1	2	3	TPase-MG	1	2	3
Indole generated in 700 µL reaction mixture (µg/mL)	Original TPase solution	9.4859	8.8131	8.9367	Original TPase-MG solution	4.0461	5.8256	4.6683
	TPase on paper	4.677	4.4183	4.774	TPase-MG on paper	2.2116	3.4361	1.7225
	Tpase on paper after washing	1.0331	1.2217	1.314	TPase-MG on paper After washing	1.1422	1.1924	0.9721

* TPase-MG: biotinylated tryptophanase immobilized on BMG by avidin (BTPase-A-BMG)

Table 4 PLP produced by Pkase or Pkase-MG in solution, on paper and after washing.

Samples	PKase	1	2	3	PKase-MG	1	2	3
PLP concentration (mM)	Original PKase solution	0.2043	0.2234	0.2506	Original PKase-MG solution	0.0928	0.0892	0.085
	PKase On paper	0.1336	0.1298	0.1537	PKase-MG On paper	0.0614	0.069	0.0646
	PKase on paper after washing	0.0102	0.014	0.0274	PKase-MG on paper after washing	0.0286	0.0178	0.0188

* PKase-MG: biotinylated pyridoxal kinase immobilized on BMG by avidin (BPKase-A-BMG)

Similar to the single enzyme activity test, bienzyme or bienzyme-MG were dried on paper under room temperature for 1 hour, and then the amount of indole generated by these paper strips in reaction mixture containing 0.2 mM of ATP was quantified by colorimetric method. Table 5 and Figure 4 shows: 1) without using microgel as supporter, bienzyme can still detect ATP and generate indole signal though the signal is weak that the amount of indole generated is only 17.37±1.66% of the amount generated using the bienzyme system in solution; 2) with microgel the amount of indole generated by the bienzyme system on microgels is 29.32±3.53% of the original activity of bienzyme-MG in solution; 3) after washing experiment, the bienzyme paper strips only produced less than 5% of indole compared to the original bienzyme solution; 4) after washing experiment, bienzyme-MG paper strips produced more than 10% of indole compared to the original bienzyme-MG solution.

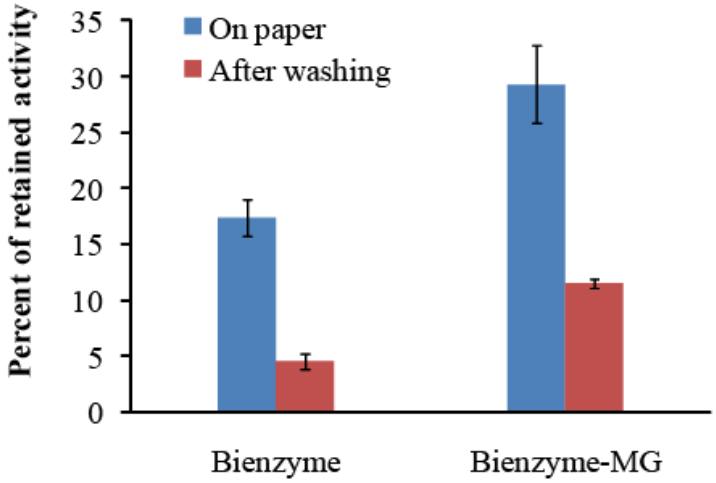

Figure 4 Monitoring the percentage of the initial bienzyme activity that is preserved after spotting it on paper, either as a free solution or loaded onto microgel particles and the effect of washing on the percentage of initial activity retained. Bars represent the standard error of triplicate samples.

Table 5 Indole generation by bienzyme or bienzyme-MG in solution, on paper and after washing at the presence of 0.2 mM ATP.

	Bienzyme	1	2	3	Bienzyme-MG	1	2	3
Indole generated in 700 µL reaction mixture (µg/mL)	Original bienzyme solution	8.9673	9.3212	8.6739	Original bienzyme-MG solution	8.2122	7.9387	8.1377
	Bienzyme On paper	1.2693	1.6999	1.7108	Bienzyme-MG on paper	2.2109	2.8796	2.0143
	Bienzyme on paper after washing	0.3478	0.3589	0.5162	Bienzyme-MG on paper After washing	1.0135	0.8763	0.9111

* bienzyme-MG: mixture of TPase-MG and PKase-MG

5.4 Conclusions

The major conclusions from this work are:

1. The amount of avidin and streptavidin that was loaded per mg of BMG were similar.
2. Using avidin as a linking agent, 249 μg BTPase and 202 μg BPKase were immobilized on per mg of BMG.
3. Microgels help retain the activity of TPase and PKase on paper after drying at room temperature.
4. Washing experiments showed that enzyme immobilized on microgels sustained washing steps and remained on paper, while the enzyme on paper without microgels was easily flushed away from the paper.
5. Loading the bienzyme system on microgels and spotting it on paper, resulted in similar indole production in the presence of ATP, after drying and washing on the paper. However, microgels do help retain more amount of enzyme on paper and help keep enzyme immobilized in certain area of the paper strips.
6. This is the first function demonstration of a paper sensor that reports the presence of a target by generating a smell.

REFERENCES

[1] S. Aikio, S. Gronqvist, L. Hakola, E. Hurme, S. Jussila, **2007**.
[2] U. Bora, K. Kannan, P. Nahar, *Journal of membrane science* **2005**, *250*, 215.
[3] R. Pelton, *TrAC Trends in Analytical Chemistry* **2009**, *28*, 925.
[4] A. W. Martinez, S. T. Phillips, M. J. Butte, G. M. Whitesides, *Angewandte Chemie International Edition* **2007**, *46*, 1318.
[5] S. M. Z. Hossain, R. E. Luckham, A. M. Smith, J. M. Lebert, L. M. Davies, R. H. Pelton, C. D. M. Filipe, J. D. Brennan, *Analytical Chemistry* **2009**, *81*, 5474.
[6] R. E. Luckham, J. D. Brennan, *Analyst* **2010**, *135*, 2028.
[7] M. Ali, S. Aguirre, Y. Xu, C. Filipe, R. Pelton, Y. Li, *Chemical communications (Cambridge, England)* **2009**, 6640.
[8] W. Zhao, M. A. Brook, Y. Li, *ChemBioChem* **2008**, *9*, 2363.
[9] O. Minikh, M. Tolba, L. Brovko, M. Griffiths, *Journal of microbiological methods* **2010**, *82*, 177.
[10] T. Hoare, R. Pelton, *Macromolecules* **2004**, *37*, 2544.
[11] M. di Salvo, S. Hunt, V. Schirch, *Protein expression and purification* **2004**, *36*, 300.
[12] H. Wada, E. E. Snell, *The Journal of biological chemistry* **1961**, *236*, 2089.
[13] S. Su, M. Ali, C. Filipe, Y. Li, R. Pelton, *Biomacromolecules* **2008**, *9*, 935.
[14] Y. Xu, L. Pharand, Q. Wen, F. Gonzaga, Y. Li, M. Ali, C. Filipe, R. Pelton, *Colloid & Polymer Science* **2010**, 1.
[15] O. Livnah, E. A. Bayer, M. WiLCHEK, J. L. Sussman, *Proceedings of the National Academy of Sciences of the United States of America* **1993**, *90*, 5076.

Chapter 6 Concluding Remarks

6.1 Conclusions

The research objectives proposed in Chapter 1 were fulfilled and the major contributions of this work are listed as follows:

1. To the best of my knowledge, this is the first time that an enzyme based system has been demonstrated for smell-generating biosensing. The enzyme tryptophanase (TPase), which catalyzes the formation of indole or methyl mercaptan, was used as a reporter molecule. Proof-of-principle was obtained by performing an ELISA-like assay where the presence of a specific antibody was reported through the generation of a smell.

2. To facilitate general use of TPase as a reporter, the enzyme was biotinylated, so that it can be linked to other biotin labeled molecules, using streptavidin or avidin as the linker. Minimal loss of activity during biotinylation was observed when the coupling reaction was done in the presence of L-tryptophan (the substrate used by TPase).

3. Combined use of pyridoxal kinase (PKase) and TPase allow specific detection of ATP and reporting its presence through the generation of a smell. This bienzyme system was then optimized to determine the set of experimental conditions that provide the lowest detection limits possible for ATP which are 0.1 μM through indole production and 1 μM through methyl mercaptan production.

4. The potential of the bi-enzymatic system was further demonstrated by using it to detect the presence of a target molecule of DNA (with a specific sequence) and to detect the presence of bacteria cells:
   i. A system was designed to capture a target molecule of DNA and reporting this capture through utilizing a repeat sequence of ATP aptamers pre-loaded with ATP and to use this ATP to trigger the bi-enzyme system to generate smell signals.
   ii. *E. coli*, *L. planturum* and *B. subtilis* cells were cultured, harvested and washed before adding to the bienzyme system. Since all living cells contain ATP, their presence resulted in the activation of the bienzyme system and a strong smell was rapidly produced.

5. The bienzyme system can be used to produce either of two different molecules (depending on the substrate used) that have strong and different smells: indole or methyl mercaptan. Indole can also be quantified using a colorimetric method through the formation of a reddish color. This means that the bienzyme system is

in fact a multi-sensory reporting biosensor. Methyl mercaptan can also be detected through the use of a photoionization detector (PID, electronic nose). The PID can give alarm signal if the methyl mercaptan concentration becomes too high, yet another way of having multi-sensory reporting.

6. An efficient recipe for biotinylation of PNIPAM-VAA microgels and uploading of streptavidin on the microgels was developed. This provides a platform for the following immobilization of biomolecules on microgels and application of modified microgels in constructing biosensors.

7. The bienzyme system was immobilized in the biotin labeled microgel particles and it was found that these particles could be immobilized effectively on paper with comparable enzymatic activity retained. This is the first account of the creation of printable smell-reporting bio-inks.

6.2 Proposed Work

6.2.1 Achieve lower detection limit for ATP

In this work, a volume of 700 μL reaction mixture was prepared for tryptophanase or the bienzyme reaction. All the optimized conditions were based on this volume. If the total volume could be reduced to 70 μL, then the detection limit of this system for ATP could be lowered. There is one important step for minimizing the volume that purified pyridoxal kinase from recombinant cells needs to be concentrated. Freeze dry of purified pyridoxal kinase was performed once and we found that part of the enzyme activity lost during the process. Thus an effective and efficient method for producing concentrated pure pyridoxal kinase needs to be explored to minimize the reaction volume and increase sensitivity of the system for ATP.

In Chapter 3, ATP is transformed into ADP in the bienzyme reaction by pyridoxal kinase while pyridoxal is transformed into pyridoxal phosphate. If ADP could be regenerated into ATP by a third enzyme, the detection limit for ATP might be much lower. Pyruvate kinase is an important enzyme for regenerating of ATP in vivo. The reaction catalyzed by pyruvate kinase is shown below in Figure 1. By adding phosphoenol pyruvate and pyruvate kinase to the bienzyme system, a tri-enzymatic system is formed and the reactions are illustrated in Figure 2.

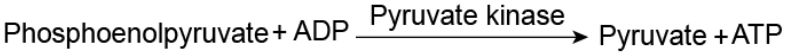

Figure 1 Generation of ATP from ADP by pyruvate kinase.

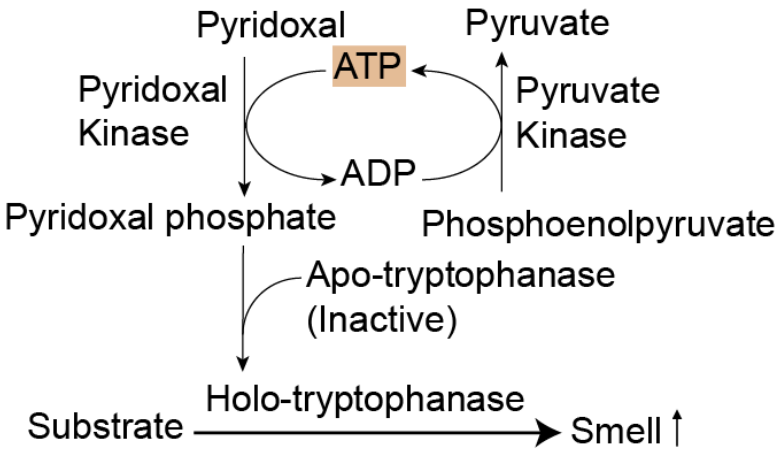

Figure 2 Tri-enzymatic system for lower ATP detection limit through regeneration of ATP by the third enzyme pyruvate kinase.

6.2.2 Application of bienzyme-immobilized filter paper in bacteria cell detections

In chapter 3, it is demonstrated that bacteria cells, such as *E. coli* could be detected by the bienzyme system in solution. Commercial available filter paper, Whatman No. 602, has a pore size of 5μm which is similar to the size of *E. coli* cells, so the filter paper may retain bacteria cells on the paper. It is proposed here that bienzyme-immobilized filter paper might be used for concentration of bacterial cells from diluted solution for producing strong signals and achieving lower detection limit for bacteria cells.

6.2.3 Bienzyme-microgels on paper

As shown in chapter 5, microgels help retain bienzyme activity on paper and protect bienzyme against washing away from the paper surface. Previous work in our group also shown that microgels could be inkjet-printed on paper, so the bienzyme loaded microgels could probably be printed on a piece of filter paper in high concentration and in the form of some patterns. In chapter 5, the filter paper shows absorption of TPase or PKase which could result in high background interference for subsequent biodetections. So if some efforts could be made to block the paper surface for absorption of enzyme solution by using reagents such as milk, bovine serum albumin or some polymer solutions, better results may be obtained.

6.2.4 Modeling of smell generation and distribution around a smell-generating mouth mask

The final goal for this work might be the construction of a smell-generating mask which

can detect certain bacterial cells and viruses and report their presence by generating a smell to be quickly sensed by the person who wears the mask. The rate at which the smell molecule is generated and how that molecule is distributed are critical factors for estimating how easily the smell signal can be detected. The rate for indole or methyl mercaptan generation could be theoretically calculated by using kinetic constants of enzyme pyridoxal kinase and tryptophanase which are provided in literatures. Then a model could be set up to predict the production and distribution of the smell chemical in and around the mask during inhalation and exhalation. Furthermore, the time needed for the human nose to detect the smell could be predicted, since thresholds of indole and methyl mercaptan for human nose are provided.